Peninsula Technikon

Department of Mechanical Engineering

Centre for Research in Applied Technology (CRATECH)

Thermal Buckling of Laminated Composite Plates

Philemon Sphiwe Simelane

NDipME, BTechME (Peninsula Technikon, South Africa)

A Thesis Submitted towards the Degree of
Master of Technology (MTech)

Supervisor: B. Sun, BSc. (Eng.), MSc. (Eng.), PhD

CAPE TOWN, 1998

Acknowledgements

The following have made possible the commencement, pursuance, compilation, and the final release of this work and their assistance is highly acknowledged and appreciated.

Dr. B. Sun, my supervisor, who laid the foundation and guided me through. His role, the biggest in terms of the study material and the need to maintain high international research standards, enabled me to feel confident as this study developed.

Dr. Nawaz Mahomed, the Head of Research, who started the postgraduate programme, and took care of my other very important research needs. These include the acquisition of funds, the computer software and hardware, and the climate conducive to this sort of work. He created and maintained the "learning" environment and pointed out the importance of keeping the research culture and by so doing I could pursue my project with zeal.

Mr. Keith Jacobs, the Head of Department (Mechanical Engineering), for allowing me to take part in other academic activities such as lecturing, and this improved my ability to present my work both verbally and in writing.

Mr. Graeme Oliver, for his assistance in computer related matters, especially the use of the state of the art computer hardware and the ABAQUS Finite Element package.

Enoch and Constance Simelane, my parents, for believing in me and giving me all the love, courage and determination.

My fiancée and wife-to-be Sandra Mokgatla, for taking care of our daughter, Nomthandazo for the past five years, while I was selfishly "improving" my qualifications far away in Cape Town.

My friends and colleagues, Marino Kekana, Oscar Philander, Mark Ludick, Mornay Riddles, Brian Hendricks, Bart Riedstra, with whom we started the postgraduate projects, and Abed Mennad, Da Huang and Xun Li, who joined us latter. Without all these guys Cape Town, Peninsula Technikon and my studies would have been unbearably lonesome.

I wish to thank Prof.Dr.-Ing. H. Stumpf for his willingness to peruse the project and make valuable comments.

My gratitude goes to the Foundation for Research Development (FRD) who recognised and fulfilled my financial needs, and Peninsula Technikon for providing the infrastructure to pursue my studies.

Finally I would like to express my gratitude to everyone who, directly or indirectly, contributed to making this project a success.

Summary

A thermal buckling analysis of laminated composite plates is studied using plates with rectangular geometry and antisymmetric lamination with respect to the middle plane. A Duhamel-Neumann type constitutive model is used. The effects of transverse shear deformation are accounted for by the use of the Mindlin first-order shear deformation (FSDT) plate theory. An angle-ply laminated construction was used to generalise the formulation. Since buckling is essentially a non-linear behaviour, the intermediate class of deformation was employed. The buckling analysis was carried out in a series of steps; the derivation of the equilibrium equation, nonlinear prebuckling and linearized buckling analysis, and the evaluation of the critical temperature by solving the resulting eigenproblem. The first variation of the total potential energy establishes the equilibrium equation and the second variation analyses the stability of the laminated composite. A displacement-based finite element with five degrees of freedom in each node was used. The effects of lamination angle, modulus ratio, plate aspect ratio, and boundary constrains upon the critical buckling temperature were investigated and found to be quite significant.

In this study several tools are used to analyse the behaviour of composite plates that are subjected to temperature variations on a macro-level. The study can be divided into three different parts: formulation of finite elements, constitutive modelling, and application to specific problems using ABAQUS computer package. The present analysis will be limited to the prediction of the non-linear structural behaviour of composites in the prebuckling and buckling regime, with postbuckling being outside the scope of this study. With respect to the description of structural failure a distinction is made between discrete and continuous modelling of buckling and this study will be based on the latter, again with the former being beyond the scope of this work. For the structural analysis on a macro-level, layered plate elements will be used to model the laminated thin wall structure. Loss of structural stability on a global level is an important cause for structural collapse and therefore an investigation into problems involving structural stability is carried out.

Although a great deal of work has been done on thermal problems of plates, an opportunity exists to make use of the modern computer software to simulate the process of thermal loading. The results can then be compared to those in real life applications and those found in published work. Either way, the need for improved, cost-effective and more accurate method of analysis warrants a research of this nature. The advent of digital computer and the accompanying development of the Finite Element Method has put a challenge to the traditional ways of solving problems, where exact solutions are not only difficult to find, but more expensive as well. That the approximate answers to complicated problems are satisfactory can, perhaps be shown in this project.

A considerable amount of work has been done on buckling of laminated composite plates, but most of the studies have been confined to in-plane mechanical loading. Zeggane and Sridharan (1991) studied the stability of deformable laminated composite plates under combined loading using 'infinite' strips. Walker *et al.* (1995) examined the optimal fibre angles for four layer rectangular laminates with central cut-outs subjected to biaxial buckling loads. They concluded that the effect of the cut-out is greatest when the aspect ratio of the plate is small and the buckling load capacity of the laminates containing holes is lower than those without holes.

However, studies were also conducted for the buckling of composite laminates involving temperature distribution. Chen and Chen (1991) studied thermal buckling of laminated plates under uniform and nonuniform temperature distribution using the eight-node Serendipity finite element. Mathew, Singh and Rao (1992) investigated thermal buckling of antisymmetric cross-ply composite laminates with a one-dimensional finite element having two nodes and six degrees of freedom. Chandrashekhara (1992) accounted for transverse shear flexibility by using the thermo-elastic version of the first-order shear deformation theory. This will also be the case in this report. Literature on buckling and laminated composites abounds. Brush and Almroth (1975) published a book on Buckling of Bars, Plates, and Shells, while Bushnell (1985) surveyed the Methods and Modes of Behaviour in Static Collapse. The foundation for the study of composite materials was based on the references [8], [10], [15] and [18]. The use of the Finite Element Method to analyse the buckling behaviour of laminated structures comes from references [1], [4], [12], [16], [24] and [32]. Reference [14] provided the basis for the formulation of the variation of the governing equations. Most of the ideas in this report are based on these publications and references.

Chapter 1 of this report introduces the concept of a composite, the formation of a composite and a brief overview of the elements of a composite material. This chapter also presents the concept of buckling that will form the basis of the development of this project. At the end of this chapter the choice of the element that is used in this study is justified. Chapter 2 provides the fundamentals of elasticity that relate to the deformation of a loaded body. In this Chapter the stresses and strains are defined and the temperature terms are introduced. In Chapter 3 the Mindlin plate theory is presented with a view to laying the foundation for the analysis of laminated plates, and as a starting point in the formulation of thermal buckling behaviour of laminated plates. In Chapter 4 the elements of a composite material are discussed and the constitutive equations of a laminated composite plate are built. Also the idea of lamination is introduced and the various simplifications that can be introduced as a result of lamination are discussed. The non-linear equilibrium equations and the stability analysis of a composite plate are formulated in Chapter 5 using the conventional analytical method. The resulting equations justify the use of the Finite Element Method as introduced in Chapter 6 and it is the method by which the governing equations will be solved in ABAQUS computer analysis. The results for various computer runs are presented for a normal plate, a plate with a square hole, and the plate with a circular cut-out in Chapter 7. Also in chapter 7 a comparison is made between the laminate with a central hole and a normal plate to study the effect of a cut-out on a critical buckling temperature. Appendices A deals the transverse shear in plates, and Appendix B deals with the transformation of the laminate elastic constants form the principal material direction to the general Cartesian co-ordinates. Also in Appendix B the laminate stiffness matrices and these matrices are briefly evaluated analytically. Appendix C is about the governing equations of laminated composites, while Appendix D gives a full representation of the abbreviated finite element equations of Chapter 6. Appendix E presents the list of ABAQUS input files that were used in the computer simulation of Chapter 7.

Contents

List of Figures

List of Tables

Chapter 1

On Composites and Buckling

1.1 Introduction

The advent of new stiff, strong and lightweight composites consisting of high performance fibers offers aerospace engineers a lucrative choice in designing composite structures which have high potential in replacing metallic structures for most of the structural applications. The analysis of composite laminates is a complex task because composites are generally anisotropic and are characterized by bending extension coupling. Structures such as beams, plates, shells, and so on are often subjected to severe thermal environments during launching and re-entry, and so their stability study under thermal loads is of utmost importance to aerospace engineers. Aircraft and space vehicles are examples of applications that are weight-sensitive. As a result thermal-buckling analysis of composite laminates is very important, especially in thin-walled members, since structural components of these high-speed machines are usually subjected to nonuniform temperature distribution due to aerodynamic and solar radiation heating.

1.2 Background on Composites

Among the most important developments in materials in recent years are **composite materials**. These are defined as a combination of two or more chemically distinct and insoluble phases whose properties and structural performance is superior to those of the constituents acting independently. Plastics, for example, possess mechanical properties (particularly strength, stiffness, and creep resistance) that are generally inferior to those of metals and alloys. These properties can be improved by embedding reinforced plastics. Reinforcements improve the strength, stiffness, and creep-resistance of plastics - and their strength-to-weight and stiffness-to-weight ratios. Composite materials have found increasingly wider applications in aircraft, automobiles, boats, ladders, and sporting goods. Metals and ceramics also can be embedded with fibers or particles to improve their properties. Reinforced plastics consist of *fibers* (the discontinuous or dispersed phase) in a plastic *matrix* (the continuous phase). Commonly used fibers are glass, graphite, aramids, and boron. These fibers are strong and stiff, and have high specific strength (strength-to-weight ratio) and specific modulus (stiffness-to-weight ratio). However, they are generally brittle and abrasive and lack toughness. Thus fibers, by themselves, have little structural value. The plastic matrix is less strong and less stiff but tougher than the fibers. Thus reinforced plastics combine the advantages of each of the two constituents. When more than one type of fiber is used in a reinforced plastic, the composite is called a *hybrid*, which generally has better properties yet. In addition to high specific strength and specific modulus, reinforced plastic structures have improved fatigue resistance, greater toughness, and higher creep-resistance than unreinforced plastics. These structures are relatively easy to design, fabricate, and repair. The

percentage of fibers (by volume) in reinforced plastics usually ranges between 10 percent and 60 percent. Practically, the average distances between adjacent fibers or particles limit the percentage of fiber in a matrix. The highest practical fiber content is 65 percent; higher percentages generally result in diminished structural properties.

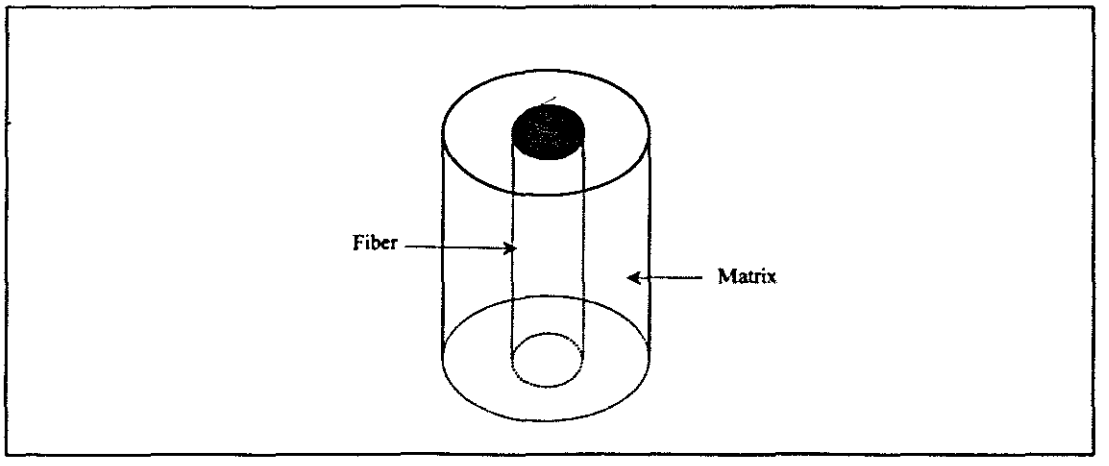

Figure 1.1 A single fiber surrounded by its matrix shell

The properties of reinforced plastics depend on the kind, shape, and orientation of the reinforcing material, the length of the fibers, and the volume fraction (percentage) of the reinforcing material. Short fibers are less effective than long fibers, and their properties are strongly influenced by time and temperature. Long fibers transmit the load through the matrix better and thus are commonly used in critical applications, particularly at elevated temperatures. Fiber reinforcement also affects the physical and other properties of composites. These include thermal conductivity and thermal expansion, electrical resistance, creep resistance and wear resistance, as well as endurance limit. A critical factor in reinforced plastics is the strength of the bond between the fiber and the polymer matrix, since the load is transmitted through the fiber-matrix interface. Weak bonding causes fiber pullout and delamination of the structure, particularly under adverse environmental conditions. Poor bonding in composites is analogous to a brick structure with poor bonding between the bricks and the mortar. Bonding can be improved by special surface treatments for better adhesion at the interface, such as coatings and the use of coupling agents. Generally, the greatest stiffness and strength in reinforced plastics is obtained when the fibers are aligned in the direction of the tension force. This composite, of course, is highly anisotropic. As a result, other properties of the composite, such as stiffness, creep resistance, thermal and electrical conductivity, and thermal expansion, are also anisotropic. The transverse properties of such a unidirectionally reinforced structure are much lower than the longitudinal. This is evident when one can easily split a fiber-reinforced packaging tape but finds it difficult to pull on it (tension). For a specific service condition (for example in thin-walled, pressurized vessels), a reinforced plastic part can be given an optimal configuration by crisscrossing the fibers in the matrix. Reinforced plastics may also be made with various other materials and shapes of the polymer matrix in order to impart specific properties, such as permeability and dimensional stability, as well as making processing easier and reducing costs.

1.2.1 A Brief Overview of Composites

In recent years there has been a rapid growth in the use of fiber-reinforced composites. As it is becoming increasingly likely that engineers and designers will at some stage have to become involved in the design of components made from fiber composites it is important that they should have an appreciation of the stages in the design process. The major advantages of such materials are that high strength and stiffness can be achieved at low weight. Products that have benefited from the use of composites include aircraft, ships, automobiles, chemical vessels and sporting goods. In these industries the base material is usually metal or plastic and the fiber used include glass, carbon, aramid ("Kevlar'), boron and asbestos. In some cases short ("chopped") fibers are used and this provides a significant property enhancement over base resin. However, by far the greatest improvement in properties is observed if the fibers are continuous, for example, if unidirectional (same direction) carbon fibers are added to epoxy resin. The modulus of the resulting composite is improved by a factor of about 60 and the strength by a factor of about 30 compared with the unreinforced base resin. However, the composite is markedly anisotropic in that in the direction perpendicular to the fiber axis the modulus is only improved by a factor of about 2 and the strength is likely to be reduced. Therefore, in the aircraft industry, for example, in order to get property enhancement in all the required directions within the component, it is normal practice to build up a laminate structure where each layer has fibers arranged in the desired direction. There are various forms of fiber arrangement in composites; (a) a square fiber arrays, hexagonal fiber arrays, random fiber arrays, and so on. A square array, for example, will have symmetry plane parallel to the fibers as well as perpendicular to them. Such a material is an orthotropic material (three mutually perpendicular planes of symmetry) and possesses nine independent elastic constants. Hexagonal and random arrays of aligned fibers are transversely isotropic and have five independent elastic constants. There are two Poisson ratios: one gives the transverse strain caused by an axially applied stress and the other gives the axial strain caused by a transversely applied stress. The two are not independent but are related. Thus, the number of independent elastic constants for a transversely isotropic composite is five.

1.2.2 Reinforcing fiber

Fibers are classified as short or long; both also called *chopped fibers*. Short fibers generally have an aspect ratio between 20 and 60 and long fibers between 200 and 500. In addition to the discrete fibers, reinforcements in composites may be in the form of continuous *roving* (slightly twisted strand of fibers), *yarn* (twisted strand), *woven* fabric (similar to cloth), and *mats* of various combinations. Reinforcing elements may also be in the form of particles and flakes. Some of the more common fibers are;

Glass: Glass fibers are the most widely used and least expensive of all fibers. The composite material is called *glass-fiber reinforced plastic* (GFRP) and may contain between 30 percent and 60 percent glass fibers by volume. There are two principal types of glass fibers: (1) the E type, a borosilicate glass, which is used most; and (2) the S type, a magnesia-alumina-silicate glass, which has higher strength and stiffness and is more expensive.

Graphite: Although more expensive than glass, graphite fibers have a combination of low density, high strength, and high stiffness. The product is called

carbon fiber reinforced plastic (CFRP). All graphite fibers are made by pyrolysis of organic precursors, commonly polyacrylonitrile (PAN) because of its low cost. Rayon and pitch (the residue from catalytic crackers in petroleum refining) can also be used as precursors. *Pyrolysis* is the term for inducing chemical changes by heat, such as burning a length of yarn, which becomes carbon and black in colour. The temperatures for carbonizing range up to about 3000°C. The difference between carbon and graphite, although the words are often used interchangeably, depends on the temperature of pyrolysis and the purity of the material. Carbon fibers are generally 93-95 percent carbon, and graphite fibers are usually more than 99 percent carbon.

Aramids: Marketed under the trade name *Kevlar*, aramids are the toughest fibers available and have the highest specific strength of any fiber. They can undergo some plastic deformation before fracture and thus have higher toughness than brittle fibers. However, aramids absorb moisture, which reduces their properties and complicates their application.

Boron: Boron fibers consist of boron deposited (by chemical vapour-deposition techniques) on tungsten fibers, although boron can also be deposited on carbon fibers. These fibers have favourable properties, such as high strength and stiffness in tension and compression and resistance to high temperatures. However, because of the use of tungsten, they have high density and are expensive, thus increasing the cost and weight of the reinforced plastic component.

Other fibers: Other fibers that are being used are nylon, silicon carbide, silicon nitride, aluminum oxide, sapphire, steel, tungsten, molybdenum, boron carbide, boron nitride, and tantalum. Whiskers are also used as reinforcing fibers. They are tiny needlelike single crystals that grow to 1μm to 10μm in diameter and have aspect ratios (length to diameter) ranging from 100 to 15 000. Because of their small size, either they are free of imperfections or the imperfections they contain do not significantly affect their strength, which approaches the theoretical strength of the material. The mean diameter of fibers used in reinforced plastics is usually less than 0.01mm. The fibers are very strong and rigid in tension. The reason is that the molecules are oriented in the longitudinal direction, and their cross-sections are so small that the probability is low that any defects exist in the fiber. Glass fibers, for example, can have tensile strengths as high as 4600MPa, whereas the strength of glass in bulk form is much lower. So glass fibers are stronger than steel.

1.2.3 Matrix material

The matrix in reinforced plastics has three functions:

- Support and transfer the stresses to the fibers, which carry most of the load.
- Protect the fiber against physical damage and the environment
- Prevents propagation of cracks in the composite by virtue of the ductility and toughness of the matrix

Matrix materials are usually epoxy, polyester, phenolic, fluorocarbon, polyethersulfone, and silicon. The most used are epoxies (80 percent of all reinforced plastics) and polyesters, which are less expensive than epoxies. Polyimides, which resist exposure to temperatures in excess of 300° C, are being developed for use with graphite fibers. Some thermoplastics, such as polyetheretherketone, are also being developed as matrix

materials. They generally have higher toughness than thermosets, but their resistance to temperature is low, being limited to 100-200° C.

1.2.4 Other composites

New developments in composite materials are continually taking place, with a wide range and form of polymeric, metallic, and ceramic materials being used both as fibers and as matrix materials. Research and development activities in this area are concerned with improving strength, toughness, stiffness, resistance to high temperatures, and reliability in service.

Metal-matrix composites The advantage of a metal matrix over a polymer matrix is its higher resistance to elevated temperatures and higher ductility and toughness. The limitations are higher density and greater difficulty in processing components. Matrix materials in these composites are usually aluminum, aluminum-lithium, magnesium, and titanium, although other metals are also being investigated. Fiber materials are graphite, aluminum oxide, silicon carbide, and boron, with beryllium and tungsten as other possibilities. Metal-matrix composites are used for structural tubular supports in the space shutters. Other applications include bicycle frames and sporting goods.

Ceramic-matrix composite Ceramic-matrix composites are another important development in engineering materials because of their resistance to high temperatures and corrosive environments. Ceramics are strong and stiff, resist high temperatures, but lack toughness. New matrix materials that retain their strength to 1700°C are silicon carbide, silicon nitride, aluminum oxide, and mullite (a compound of aluminum, silicon, and oxygen). Present applications for ceramic-matrix composites are in jet and automotive engines, deep-sea mining equipment, pressure vessels, and various structural components. Composites may also consist of coatings of various kinds of base metals or substrates. Examples are plating of aluminum and other metals over plastics for decorative purposes and enamels. Composites are also made into cutting tools and dies, such as cemented carbides, usually tungsten carbide and titanium carbide, with cobalt and nickel, respectively as a binder. Yet other composites are grinding wheels made of aluminum oxide, silicon carbide, diamond, or cubic boron nitride abrasive particles, held together with various organic, inorganic, or metallic binders.

Honeycomb structure and similar sandwich, or laminate, structures are another form of composites having high strength and specific stiffness. The structure consists basically of a core of honeycomb or other corrugated shapes bonded to two thin outer skins. The simplest example is the corrugated cardboard, which has a high stiffness-to-weight ratio and is used extensively in packaging for consumer and industrial goods. Because of their lightweight and high resistance to bending forces, honeycombs structures are used for aircraft and aerospace components, as well as in buildings and transportation equipment. The core in the honeycomb can be filled with fiberglass, or similar batting materials, which serve as sound- and vibration-absorbing media, thus reducing engine noise levels in the fuselage.

1.3 Background on Buckling

If an axially loaded column is purposely bent and the compressive load is then gradually decreased until the column becomes perfectly straight, the load at this point is the limiting load that the column can carry without buckling. This load is known as the *critical load, crippling load, buckling load* or *failing load.* Also, a short and stocky column that is axially loaded does not tend to bend sideways, while a long and slender column will buckle and collapse under an axial compressive load less than that which will cause crushing in a short column of the same material and cross-sectional area. This could be due to the fact that the column is not straight prior to loading, the load is applied eccentrically, and that the material of the column is not homogeneous. These are termed imperfections. Buckling analysis follows three general procedures. The first one is the determination of nonlinear equilibrium equation. The second one is the stability analysis to determine the existence of the bifurcation point on the equilibrium paths. The third procedure studies the post-buckling behaviour of the structure under consideration. The formulation for the equilibrium equations will be done using the Stationary Potential Energy criterion and the stability analysis will be done using the Minimum Potential Energy criterion.

1.3.1 Buckling of Structures

For thin wall structures the membrane stiffness is generally several orders of magnitude greater than the bending stiffness. A thin wall structure can absorb a great deal of membrane strain energy without deforming too much. It must deform much more in order to absorb an equivalent amount of bending strain energy. If the structure is loaded in such a way that most of its strain energy is in the form of membrane compression, and if there is a way that this stored-up membrane energy can be converted into bending energy, the plate may fail rather dramatically in a process called "buckling", as it exchanges its membrane energy for bending energy. The way in which buckling occurs depends on how the structure is loaded and on its geometrical and material properties. The prebuckling process is often non-linear if there is a reasonably large percentage of bending energy being stored in the structure throughout the loading history. According to the percentage of bending energy, the two basic ways in which a conservative elastic system may lose its stability are non-linear collapse (snap-through) and bifurcation buckling. Non-linear collapse is predicted by means of a non-linear analysis. The stiffness of the structure or slope of the load-deflection curve decreases with increasing load. At the collapse load the load-deflection curve has zero slope and, if the load is maintained as the structure deforms, failure is often called snap-through, a term derived from the many early tests and theoretical models of shallow arches, caps and cones [28]. These very non-linear systems initially deform slowly with increasing load. As the load approaches the maximum value, the rate of deformation increases until, reaching a status of neutral equilibrium in which the average curvature is almost zero, these shallow structures subsequently "snap-through" to a post buckled state which resembles the original structure in an inverted form. On the other hand "bifurcation buckling" refers to a different kind of failure, the onset of which is predicted by means of an eigenvalue analysis. At the buckling load, or bifurcation point on the load-deflection path, the deformation begins to grow in a new pattern that is quite different from the prebuckling pattern. Failure, or unbounded growth of this new deflection mode, occurs if the post-bifurcation load-deflection curve has a negative slope and the

applied load is independent of the deformation amplitude. In this study, the discussion is restricted to those structures that lose their stability through bifurcation.

1.3.2 Classical Buckling Analysis

Buckling analysis is fundamentally a subtopic of nonlinear rather than linear mechanics [6]. Also, this analysis is essentially an eigenvalue analysis where the central question is, "Assuming that the steady-state solution of the system is known, is there another solution into which the system could bifurcate if it were slightly perturbed from its equilibrium position?" (Bath, 1996). The essence of buckling is a disproportionate increase in displacement resulting from small increase in load. The treatment in this work considers the geometric nonlinearity where the nonlinearity enters the theory in expressions representing the influence of rotation of structural elements on the behaviour of the structure. The stresses and strains are assumed to obey Hooke's law.

Classical eigenvalue buckling analysis is often used to estimate the critical (buckling) load of "stiff structures. "Stiff" structures are those that carry design loads primarily by axial or membrane action, rather than by bending action. Their response usually involves very little deformation prior to buckling. In the finite element context, the classical eigenvalue-buckling problem may be stated as follows; Given a structure with an elastic stiffness matrix, K, a loading pattern defined by the vector $\{N\}$, and an initial stress and loading stiffness matrix, K_g, find load multipliers (eigenvalues), λ, and buckling modes shapes (eigenvectors), a, which satisfy $[K + \lambda K_g]\{a\} = 0$. The critical buckling loads are then given by λN. Usually only the smallest load multiplier and its associated mode shape are of interest.

In static analysis of structures, two phenomena are generally investigated in connection with buckling; these are *collapse* at the maximum point in a load versus deflection curve and *bifurcation buckling*. Fig. 1.3.1 illustrates an axially compressed cylinder that deformed approximately axisymmetrically along the path OA until a maximum or limit load λ_L is reached at point A. The reduction in axial stiffness may relieve the axial load λ. If this does not happen, the perfect cylinder will fail at this limit load, following either the path ABC along which it continues to deform axisymmetrically, or some other path ABD along which it first deforms axisymmetrically from A to B and then nonaxisymmetrically form B to D. Snapthrough or limit point buckling occurs at point A, and bifurcation buckling at point B. The equilibrium path OABC corresponding to the axisymmetrical mode of deformation is called *fundamental path*, and the postbifurcation equilibrium path BD, corresponding to the nonaxisymmetrical mode of deformation, is called the *secondary path*. Buckling of either type may occur at loads for which some or all of the structural material has been stressed beyond its proportional limit. The example in Fig.1.3.1 is somewhat unusual in that the bifurcation point B is shown to occur after the collapse point has been reached. In this particular case, therefore, bifurcation buckling is of less engineering significance than axisymmetric collapse.

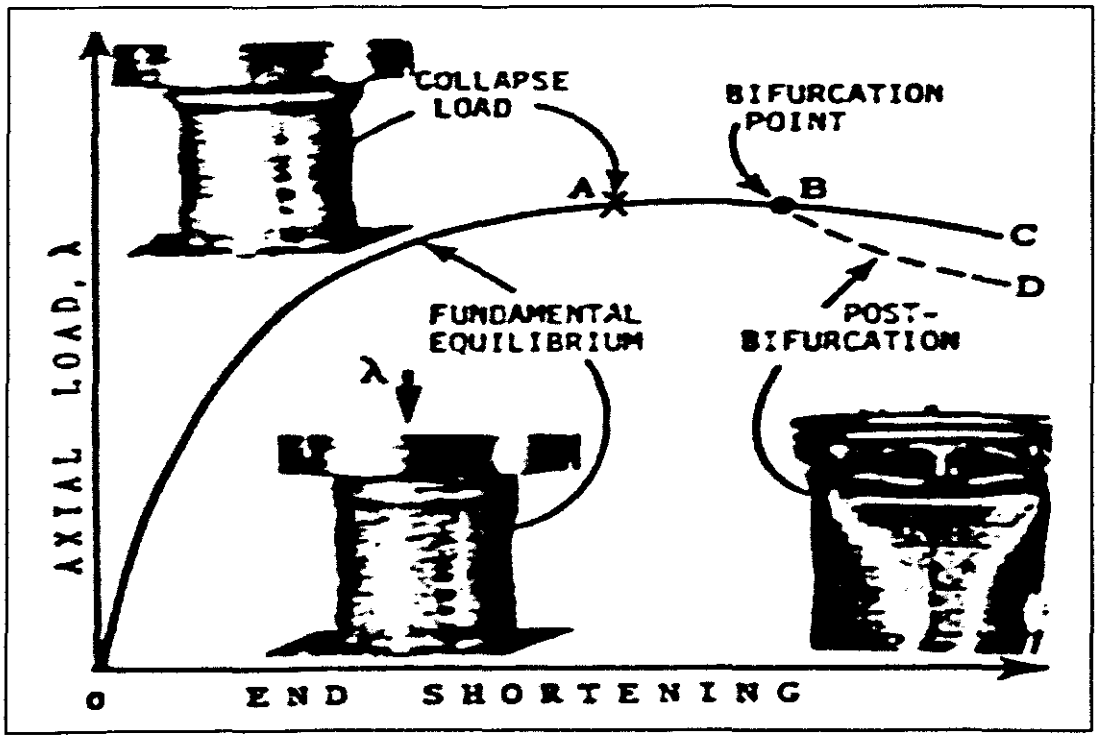

Figure 1.3.1 Load/end-shortening curves with collapse load A, bifurcation point B and postbifurcation equilibrium path BD [7].

Fig 1.3.2(a) illustrates a more commonly occurring situation where the bifurcation point B is between O and A. If the fundamental path OAC corresponds to axisymmetrical deformation and BD to nonaxisymmetrical deformation, then initial failure of the structure would generally be characterised by rapidly growing nonaxisymmetrical deformations. In this case, the collapse load of the perfect structure λ_L is of less engineering significance than the bifurcation point, λ_C. In the case of real structures that contain unavoidable imperfections, there is no such thing as bifurcation buckling. The actual structure will follow a fundamental path OEF, with the failure corresponding to 'snapthrough' at point E at the collapse load λ_S. However, the bifurcation buckling analytical model is valid in that it is convenient and often leads to a good approximation of the actual failure and mode, particularly in cases involving much prebifurcation symmetry. Fig. 1.3.2(a) thus illustrates the general non-linear approach in which the computations involve essentially a 'prebuckling' analysis, or a determination of the unique equilibrium states along the fundamental path OEF. On the other hand Fig. 1.3.2(b) depicts the asymptotic approach in which the prebuckling state is usually statically determinate.

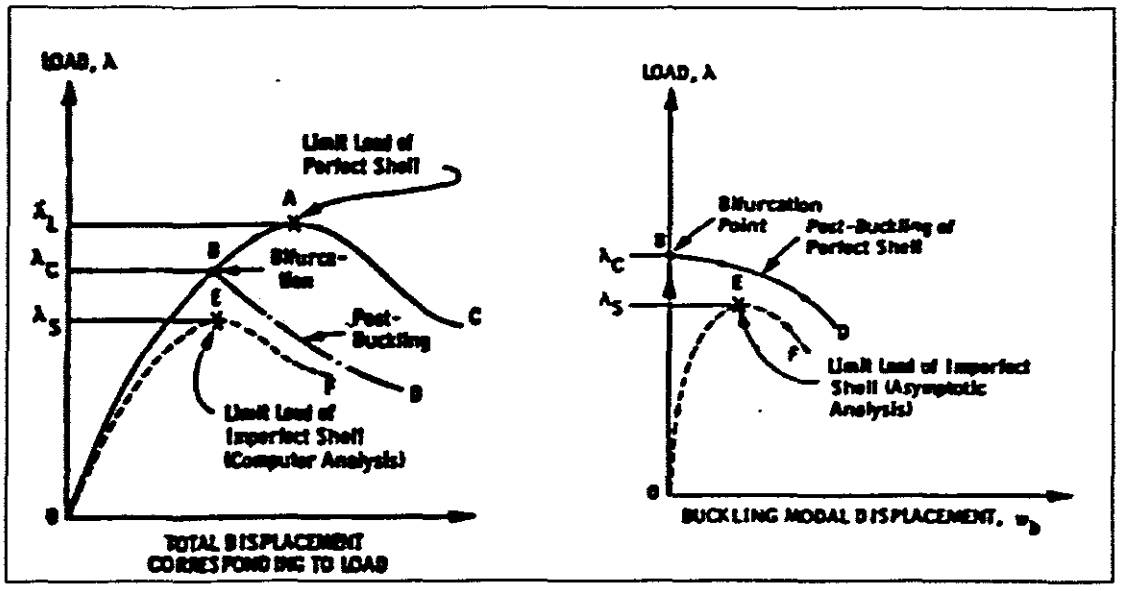

Figure 1.3.2(a) General non-linear analysis

Figure 1.3.2(b) Asymptotic analysis

In laminated composites, failure of one layer does not necessarily imply failure of the entire laminate; the laminate may, in fact, be capable of sustaining higher loads despite a significant change in stiffness. An analogy to this phenomenon is the ability of an in-plane loaded plate to carry loads higher than the buckling load, but at an increase in the amount of deformation per unit of load (a decreased stiffness) as in Figure 1.3.3(a) and 1.3.3(b) below.

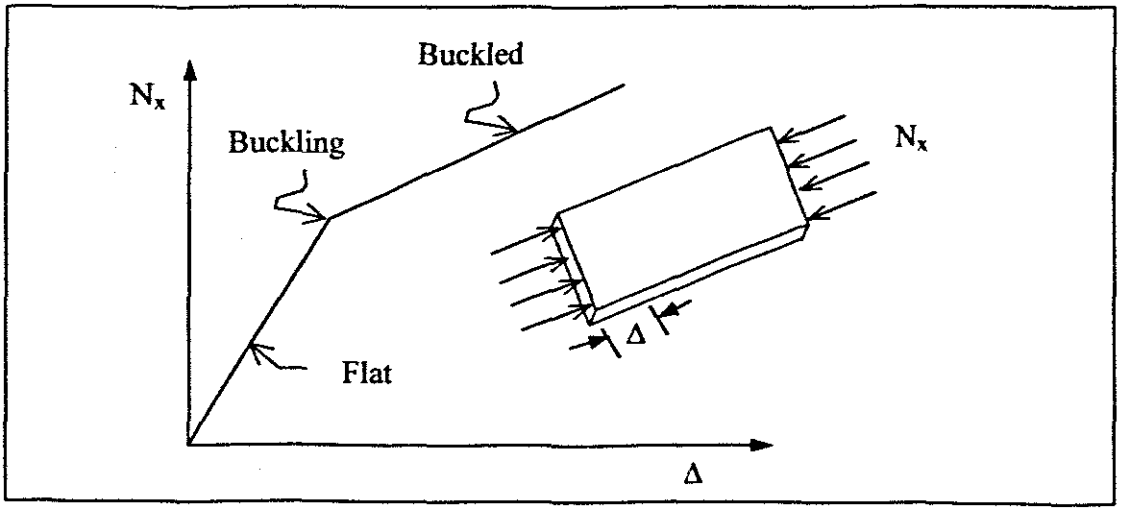

Figure 1.3.3(a) Plate load-deformation behaviour

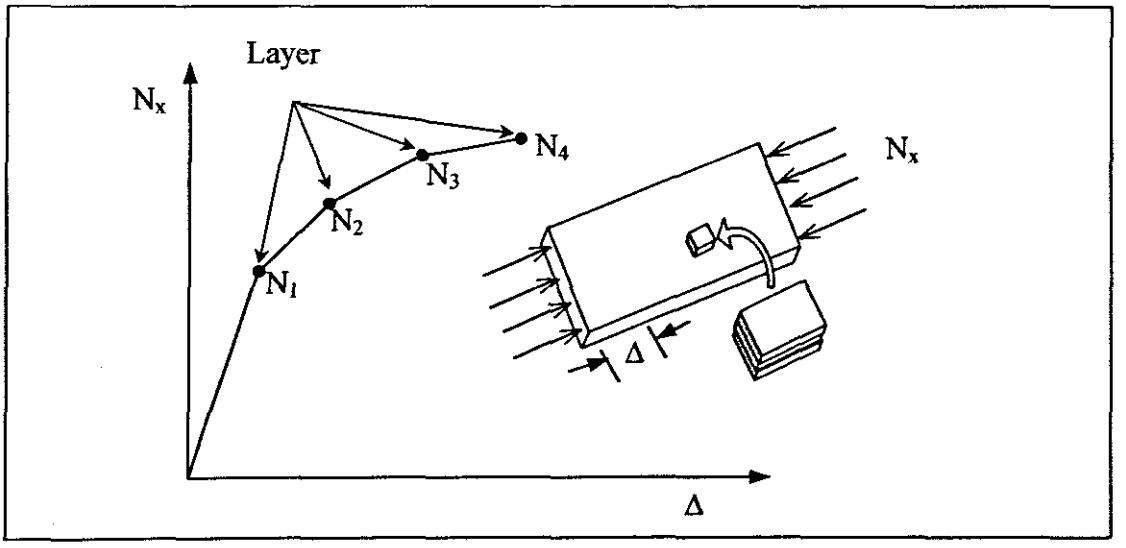

Figure 1.3.3(b) Laminate load-deformation behaviour

All strength theories for composite materials depend on the strength in the principal material directions, which likely do not coincide with principal stress direction. Therefore, the strength of each lamina in a laminate must be assessed in a co-ordinate system that is likely different from those of its neighbouring laminae. This co-ordinate mismatch is but one of the complications that characterises even a macroscopic strength theory. The main factors that are peculiar to laminate strength analysis are:

- laminae strength
- laminae stiffnesses
- laminae coefficient of thermal expansion
- laminae orientations
- laminae thicknesses
- stacking sequence
- curing temperature

The thermomechanical properties, thicknesses, and orientations are important in determining the directional characteristics of strength. The stacking sequence affects the bending and coupling stiffnesses and hence the strengths of the laminate. The curing temperature, or operating versus curing temperature, influences the residual stresses that are developed upon cool-down of the laminate from stress-free elevated temperature curing cycle. In general, if the operating or service temperature is different from the curing temperature, thermal stresses will arise; whether they are called thermal stresses or residual stresses is partly a matter of convenience, but is mainly semantics.

1.4 Choice of Mindlin Plate Element

A plate, though three-dimensional in nature, has the thickness which is much smaller than other dimensions and a three-dimensional analysis would not only be costly but may also lead to equations that are ill-conditioned and difficult to deal with. To make these simplifications, Kirchhoff formulated what is refereed to as the Classical Plate Theory (CPL) with the following assumptions

- straight lines normal to the mid-surface remain straight and normal after deformation,
- the displacement gradients are small,
- the length of a normal remains unchanged, and
- the transverse normal stress is small and it can be neglected.

The analysis of composite structures may take two forms; one is the study of the relationship between the fibre and the matrix at a microscopic level, the micromechanics of the composite, the other is the general behaviour of the entire composite, the macromechanics of the composite.

The classical plate theory does not account for transverse normal and shear deformation but was found to work well with phenomenon such as debonding, delamination and could predict the relationship between the individual layers in a composite. On the other hand Mindlin and Reissner formulated a thick plate theory, normally refereed to as the first-order shear deformation theory (SFDT). This theory removes the normality assumption in Kirchhoff's theory. This means that a straight and normal line does remain straight after deformation, but not necessarily normal. Instead it rotates about an angle according to the application of the load. Consequently excellent results for global response characteristics, such as displacements, natural frequencies and buckling loads are obtained (Wung et al' 1991). But this theory yields poor results for the interlaminar shear stresses. The interlaminar shear stresses obtained from FSDT through the constitutive relations are discontinuous across the laminar interfaces. Thus these results cannot satisfy the lamina interface continuity conditions and the equilibrium conditions, which are the major sources of layer debonding/delamination [32].

Therefore to conduct an analysis such as buckling the Mindlin/Reissner theory must be used. The assumptions made by the first-order shear deformation theory then reduce the three-dimensional nature of the plate into a two-dimensional analysis with references made to the midplane. With FSDT, thermal buckling of composite plates can then be formulated. Though this theory yields poor results for the interlaminar shear stress than the classical plate theory, the main concern of this work is the global response of the composite laminates to the thermal loads applied to them.

Chapter 2

Fundamentals of Elasticity

2.1 Introduction

According to the theory of elasticity, there are nine stress components acting on the front faces of an elemental cube. A stress component σ_{ij} represents the force per unit area in the i direction on the face whose normal is the j direction. Rotational equilibrium requires that $\sigma_{ij} = \sigma_{ji}$ and this leaves six stress components in which $i = j$ are the normal stresses while $i \neq j$ are the shear stresses. The most generalized form of the linear relations between the components of stress and the components of strain, generally known as Hooke's law, can be written in a tensor form as

$$\sigma_{ij} = C_{ijkl}\varepsilon_{kl} \tag{2.1}$$

where σ_{ij} is the stress components and ε_{kl} the strain components. C_{ijkl} represents the material properties. In the formulation of elastic behaviour of plates, we denote the material coordinates of a point in the undeformed reference configuration by

$$\mathbf{x} = (x_1, x_2, x_3)$$

In the deformed configuration the spatial coordinates of the point become

$$\xi = (\xi_1, \xi_2, \xi_3)$$

2.2 Definition of stress

The body-force distribution, which may be represented as a function of position and time, is denoted as $F_i(x_1, x_2, x_3, t)$ and as an intensity function, it is generally evaluated per unit volume of the material acted on. The surface traction, the force distribution that is applied at the boundaries directly from the material outside the domain, are denoted as $T_i(x_1, x_2, x_3, t)$. These are also intensity functions and are given on the basis of per unit area. Considering a vanishingly small rectangular parallelepiped taken at some time t from a continuum and using the superscript to identify the surfaces, the traction vector may be written as

$$T_i^{(v)}(x_1, x_2, x_3, t)$$

where, for example, the Cartesian components of the vector $T^{(1)}$ are $T_1^{(1)}$, $T_2^{(1)}$, $T_3^{(1)}$. The stress components can be represented by employing σ and τ in place of T and moving the superscript down to be the first subscript while deleting the enclosing parenthesis. In general then, we have

$$\sigma_{ij} = \begin{pmatrix} \sigma_{11} & \tau_{12} & \tau_{13} \\ \tau_{21} & \sigma_{22} & \tau_{23} \\ \tau_{31} & \tau_{32} & \sigma_{33} \end{pmatrix} \tag{2.2}$$

where the terms in the main diagonal are called normal stresses, since the force intensity corresponding to these stresses are normal to the surface, while the off-diagonal terms are the shear stresses. Knowing σ_{ij} for a set of axes, that is, for the three orthogonal interfaces at a point, a stress vector $T^{(v)}$ can be determined for an interface at a point having any direction whatever. Thus

$$T_i^{(v)} = \sigma_{ij} v_j$$

where v_j can be considered to give the direction cosines of the unit normal of the interface on which the traction force is desired. σ_{ij} can be shown to form a symmetric array [14], that is

$$\sigma_{ij} = \sigma_{ji}$$

The equation of motion for an element of mass dm at any point P can be found by considering Newton's law:

$$\mathbf{df} = \mathrm{dm}\dot{\mathbf{V}}$$

where **df** is the sum of the total traction force on the element and the total body force on the element and $\dot{\mathbf{V}}$ the acceleration. Integrating the above over some arbitrary spatial domain Ω and a boundary surface Γ, it can be noted as a result of Newton's third law that only traction on the boundary surface do not cancel out so that

$$\oiint_{\Gamma} T_i^{(v)} d\Gamma + \iiint_{\Omega} F_i d\Omega = \iiint_{\Omega} \dot{V} \rho d\Omega \tag{2.3}$$

where ρ is the density of the element. Employing equation $T_i^{(v)} = \sigma_{ij} v_j$ to replace the stress vector $T_i^{(v)}$ by stresses, we obtain

$$\oiint_{\Gamma} \sigma_{ij} v_j d\Gamma + \iiint_{\Omega} F_i d\Omega = \iiint_{\Omega} \dot{V}_i \rho d\Omega \tag{2.4}$$

By employing Gauss divergent theorem for the first integral and collecting terms on integral, we get

$$\iiint_{\Omega} \left[\sigma_{ij,j} + F_i - \dot{V}_i \rho \right] d\Omega = 0 \tag{2.5}$$

Since the domain Ω is arbitrary, it can be concluded that at any point the following must hold

$$\sigma_{ij,j} + F_i = \rho \dot{V}_i \tag{2.6}$$

which is the desired equation of motion.

2.3 Differential equations of motion of a deformed body

In deriving differential equations[1] of motion (differential equations of equilibrium if the body has zero acceleration), the form of the equation depends on the type of orthogonal coordinate axes employed. For small displacements[2], which are the only considerations in this study, no distinction is made between coordinate axes in the deformed state and in the undeformed state. Hence the rectangular[3] coordinate axes (x,y,z) whose directions are parallel to the edge of the deformed volume element. In a box-shaped element discussed previously, six cutting planes are imagined to bound the volume element. In general, the state of stress changes with the location of a point. In particular, the stress components undergo changes from one face of the volume to another face. Body forces (F_x, F_y, F_z) are included in the formulation. Each stress component must be multiplied by the area on which it acts and each body force must be multiplied by the volume of the element since (F_x, F_y, F_z) have dimensions of force per unit volume. The equations of motion for the volume element are obtained by summation of forces and summation of moments. Summation of forces in the x- y- and z-directions, respectively, gives

$$\frac{\partial \sigma_x}{\partial x} + \frac{\partial \tau_{xy}}{\partial y} + \frac{\partial \tau_{xz}}{\partial z} + F_x = 0$$

$$\frac{\partial \sigma_y}{\partial y} + \frac{\partial \tau_{xy}}{\partial x} + \frac{\partial \tau_{yz}}{\partial z} + F_y = 0$$

$$\frac{\partial \sigma_z}{\partial z} + \frac{\partial \tau_{zx}}{\partial x} + \frac{\partial \tau_{yz}}{\partial y} + F_z = 0 \tag{2.7}$$

where $\tau_{xy} = \tau_{yx}$, and $\tau_{xz} = \tau_{zx}$ and F_x, F_y and F_z are the components of body force per unit volume including inertial forces.

2.4 Definition of strain

If we express the undeformed configuration with reference x_i and the deformed configuration with ξ_i, a one-to-one mapping is expected, that is, for some deformation[4];

---

[1] These equations are needed when the theory of elasticity is used to derive load-stress and load-deflection relations for a member.

[2] Additional equilibrium equations of compatibility are needed for the method of theory of elasticity. The derivation employs small displacement approximations and the associated strain-displacement relations, which form the basis of plate formulation.

[3] In other situations it is necessary to use the general form of the differential equations to accommodate other coordinate systems, for example, the cylindrical, the spherical, and so on.

[4] For this deformation $x_1 = u$, $x_2 = v$, $x_3 = w$

$\xi_i = \xi_i(x_1, x_2, x_3)$

A unique inverse to this expression is expected to be of the form

$x_i = x_i(\xi_1, \xi_2, \xi_3)$

By expressing the differentials dx_i and $d\xi_i$ using the above, the measure of deformation of a line segment ds to ds* is found to be

$(ds^*)^2 - (ds)^2 = 2\epsilon_{ij}dx_i dx_j$

$(ds^*)^2 - (ds)^2 = 2\eta_{ij}d\xi_i d\xi_j$

where the Green's strain tensor ϵ_{ij}, expressed as a function of the coordinates in the undeformed state - that is, the so-called Lagrange coordinates, and the Almansi measure of strain [14] η_{ij}, formulated as a function of the coordinates for the deformed state- the so-called Eulerian coordinates, are

$$\epsilon_{ij} = \frac{1}{2}\left(\frac{\partial \xi_k}{\partial x_i}\frac{\partial \xi_k}{\partial x_j} - \delta_{ij}\right) \tag{2.8}$$

$$\eta_{ij} = \frac{1}{2}\left(\delta_{ij} - \frac{\partial x_k}{\partial \xi_i}\frac{\partial x_k}{\partial \xi_j}\right) \tag{2.9}$$

where δ_{ij} is the Kronecker delta.

Introducing the displacement field u_i, defined such that

$u_i = \xi_i - x_i$

the following deformation gradient relation can be written in terms of this equation

$$\frac{\partial x_i}{\partial \xi_j} = \delta_{ij} - \frac{\partial u_i}{\partial \xi_j} \tag{2.10}$$

$$\frac{\partial \xi_i}{\partial x_j} = \frac{\partial u_i}{\partial x_j} + \delta_{ij} \tag{2.11}$$

Substituting these into Equations (2.8) and (2.9) we obtain

$$\epsilon_{ij} = \frac{1}{2}\left(\frac{\partial u_i}{\partial x_j} + \frac{\partial u_j}{\partial x_i} + \frac{\partial u_k}{\partial x_i}\frac{\partial u_k}{\partial x_j}\right) \tag{2.12}$$

$$\eta_{ij} = \frac{1}{2}\left(\frac{\partial u_i}{\partial \xi_j} + \frac{\partial u_j}{\partial \xi_i} - \frac{\partial u_k}{\partial \xi_i}\frac{\partial u_k}{\partial \xi_j}\right) \tag{2.13}$$

where ϵ_{ij} are referred to the initial undeformed geometry and η_{ij} are referred to the deformed or instantaneous geometry of the body.
A restriction to infinitesimal strain, wherein the derivatives of the displacement components are small compared to unity, and neglecting the product of the derivatives of displacement components in Equations (2.12) and (2.13), the following formulation for strain is obtained

$$\epsilon_{ij} = \eta_{ij} = \frac{1}{2}\left(\frac{\partial u_i}{\partial x_j} + \frac{\partial u_j}{\partial x_i}\right)$$

$$= \frac{1}{2}\left(u_{i,j} + u_{j,i}\right) \tag{2.14}$$

In tensor notation, we have

$$\epsilon_{ij} = \begin{pmatrix} \epsilon_{xx} & \epsilon_{xy} & \epsilon_{xz} \\ \epsilon_{yx} & \epsilon_{yy} & \epsilon_{yz} \\ \epsilon_{zx} & \epsilon_{zy} & \epsilon_{zz} \end{pmatrix} \tag{2.15a}$$

or

$$\varepsilon_{ij} = \begin{pmatrix} \varepsilon_x & \frac{1}{2}\gamma_{xy} & \frac{1}{2}\gamma_{xz} \\ \frac{1}{2}\gamma_{yx} & \varepsilon_y & \frac{1}{2}\gamma_{yz} \\ \frac{1}{2}\gamma_{zx} & \frac{1}{2}\gamma_{zy} & \varepsilon_z \end{pmatrix} \tag{2.15b}$$

where the γ_{ij} are the engineering shear strains.

Apart from stretching, a vanishingly small line element, considering the complete mutual relative motion of its endpoints, has the rotation tensor defined by

$$\omega_{ij} = \tfrac{1}{2}\left(u_{i,j} - u_{j,i}\right) \tag{2.16}$$

where ω_{ij} is a skew-symmetric tensor.

Thus the complete representation of a parallelepiped undergoing both deformation and rotation is given as

$$u_{i,j} = \tfrac{1}{2}\left(u_{i,j} + u_{j,i}\right) + \tfrac{1}{2}\left(u_{i,j} - u_{j,i}\right)$$

$$= \epsilon_{ij} + \omega_{ij} \tag{2.17}$$

2.5 Introduction of thermal stresses

The stresses can be written in terms of strains as follows

$$\sigma_x = \lambda e + 2G\epsilon_x$$

$$\sigma_y = \lambda e + 2G\epsilon_y$$

$$\sigma_z = \lambda e + 2G\epsilon_z \qquad (2.18a)$$

where

$\lambda = \frac{\nu E}{(1+\nu)(1-2\nu)}$, $e = \varepsilon_x + \varepsilon_y + \varepsilon_z$, E = Young's modulus, and G = shear modulus.

In index notation this can be written as

$$\sigma_i = \lambda e + 2G\epsilon_i \qquad (2.18b)$$

One method of solution of the problems of elasticity is to eliminate the stress components from Equation (2.18) and the surface forces

$$\bar{F}_x = \sigma_x l + \tau_{xy} m + \tau_{xz} n$$

$$\bar{F}_y = \sigma_y m + \tau_{yz} n + \tau_{xz} l$$

$$\bar{F}_z = \sigma_z n + \tau_{xz} l + \tau_{yz} m \qquad (2.19)$$

where l, m, and n are the direction cosines of the external normal to the surface of the body at the point under consideration. This elimination can be done using Hooke's law and expressing the strain components in terms of displacements by using the strain-displacement relations. In this manner three equations of equilibrium containing only the three unknown functions u, v, w are arrived at, that is

$$(\lambda + G)\frac{\partial e}{\partial x} + G\nabla^2 u + F_x = 0$$

$$(\lambda + G)\frac{\partial e}{\partial y} + G\nabla^2 u + F_y = 0$$

$$(\lambda + G)\frac{\partial e}{\partial z} + G\nabla^2 w + F_z = 0 \qquad (2.20)$$

where

$$\nabla^2 = \frac{\partial^2}{\partial x^2} + \frac{\partial^2}{\partial y^2} + \frac{\partial^2}{\partial z^2}$$

The differential equations of equilibrium in terms of displacement can be extended to cover thermal stress and strain where thermal stresses are defined as

$$\sigma_i = \frac{\alpha_i E T}{1-\nu}$$

where α_i are the coefficient of thermal expansion. The thermal strain are defined as

$$\varepsilon_i = \alpha_i T$$

such that Equation (2.20) becomes

$$(\lambda + G)\frac{\partial e}{\partial x_i} + G\nabla^2 u_i + F_i - \frac{\alpha_i E}{1-2\nu}\frac{\partial T}{\partial x_i} = 0 \qquad (i = 1,2,3) \qquad (2.21)$$

and the displacements u_i produced by the temperature change T are the same as the displacement produced by the body forces

$$F_i = -\frac{\alpha_i E}{1-2\nu}\frac{\partial T}{\partial x_i}$$

and normal tension (or hydrostatic pressure)

$$\sigma_i = \frac{\alpha_i E T}{1-2\nu}$$

are distributed over the surface and proportional at each point to the temperature change at that point. Thus, the total stress produced by nonuniform heating is obtained by superposing hydrostatic pressure on the stresses produced by body forces and surface forces.

Whether strain due to nonuniform heating are suppressed, the same conclusion may be reached and the equilibrium Equation (2.20) must be satisfied [14]

$$\sigma_{ij,j} + \frac{\alpha_i E}{1-2\nu} T_{,x_i}$$

($_{,x}$ is the differentiation with respect to x). Included are the boundary conditions

$$\sigma_{ij} l = \frac{\alpha_i E T}{1-2\nu} l \qquad (i = j = 1,2,3) \qquad \text{and} \qquad (l = l,m,n)$$

Chapter 3

Mindlin Plate Formulation

3.1 Analytical Structure of Mindlin Plate

In the development that follows, u, v and w denote x, y and z components of displacement respectively, and the midplane coincides with the xy-plane. Mindlin plate theory is an assumed strain theory, which offers an alternative to the classical Kirchhoff thin plate theory because in this theory it is possible to allow transverse shear deformation. It is a two dimensional equivalent of Timoshenko beam theory [34]. The motion of a point not on the midsurface is not governed by slopes $w_{,x}$ and $w_{,y}$ as in Kirchhoff theory. Rather, its motion depends on rotations θ_x and θ_y of the lines that were normal to the midsurface of the undeformed plate. This theory is therefore suitable to the analysis of thick, composite, and sandwich plates. The main assumptions are

- displacements are small compared with the plate thickness.
- the stress normal to the midsurface of the plate is negligible.
- normals to the midsurface before deformation remain straight but not necessarily normal to the midsurface after deformation.

It is further assumed that the original cross-section has, after deformation, rotated through an angle θ, where θ is a vector rotation about a given axis. The governing equations are assumed to be the strain-displacement equation, the stress-strain relations, and the equilibrium equation. This results in a five-variable model with u, v, θ_x, θ_y and w, such that the total deformation field is defined as

$$u(x, y, z) = u_0(x, y) - z\theta_x(x, y)$$

$$v(x, y, z) = v_0(x, y) - z\theta_y(x, y)$$

$$w(x, y, z) = w_0(x, y) \tag{3.1}$$

where u_0, v_0 and w_0 are the displacements of the reference surface in the x, y and z direction, respectively, and θ_x, θ_y are the rotations of the transverse normal about the y and x axes in the xz- and yz-planes. The co-ordinate frame is chosen in such a way that the xy-plane coincides with the midplane of the plate. This is shown in Figure 3.1. θ_x and θ_y are small angles of rotation.

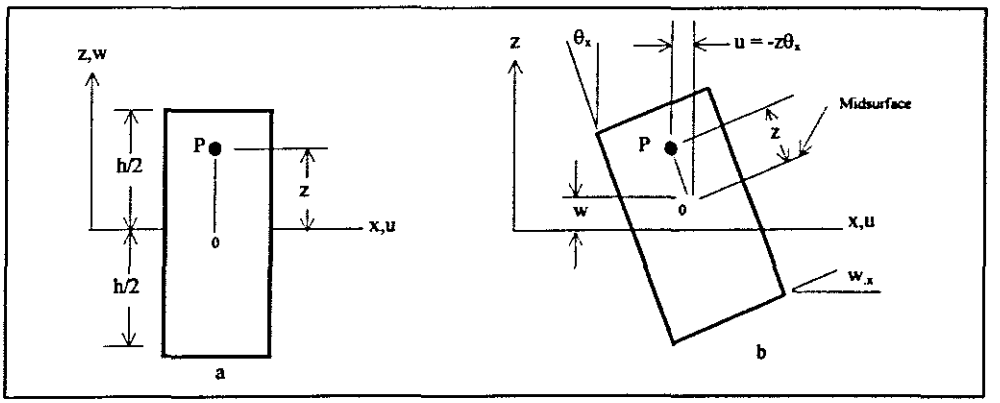

Figure 3.1 Differential element of a plate; (a) before loading, (b) after loading

During the buckling process the incremental displacement components of u, v and w are measured from the configuration immediately prior to buckling and the co-ordinate frame is chosen in such a way that the *xy*-plane coincides with the midplane of the plate.

3.2 Definition of Strains

Firstly we let $\bar{u}$, $\bar{v}$, $\bar{w}$ be the displacement components at any point in the plate, and u, v, w be the corresponding middle-plane quantities, with the subscript "$_0$" being dropped from Eq. (3.1). These quantities are related as follows

$$\bar{u} = u + z\varphi_x \qquad \bar{v} = u + z\varphi_y \qquad \bar{w} = w$$

where $\varphi_x = -w_{,x}$ and $\varphi_y = -w_{,y}$ are rotations relative to the y and x coordinate directions, respectively

The intermediate class of deformation is defined by the limitations that the strains be small compared with unity, the rotations relative to the x and y directions moderately small, and rotations relative to the z direction negligibly small. The following mechanical strains are then defined for the plate:

$$\bar{\varepsilon}_x = \varepsilon_x + z\theta_{x,x} \qquad \bar{\varepsilon}_y = \varepsilon_y + z\theta_{y,y} \qquad \bar{\gamma}_{xy} = \gamma_{xy} + 2z\left(\theta_{x,y} + \theta_{y,x}\right)$$

$$\bar{\gamma}_{yz} = \bar{w}_{,y} - \theta_y \qquad \bar{\gamma}_{xz} = \bar{w}_{,x} - \theta_x$$

while the thermal strains are defined as

$$\varepsilon_{tx} = \alpha_x \Delta T \qquad \varepsilon_{ty} = \alpha_y \Delta T \qquad \varepsilon_{tz} = \alpha_z \Delta T \qquad \gamma_{txy} = 2\alpha_{xy} \Delta T .$$

α_i are the coefficients of thermal expansion and ΔT is the change in temperature. The thermal strains are known to oppose the mechanical strains. In matrix we have;

$$\{\bar{\varepsilon}\} = \left(\varepsilon_x \quad \varepsilon_y \quad \gamma_{xy}\right)^T + z\left(\kappa_x \quad \kappa_y \quad \kappa_{xy}\right)^T - \left(\alpha_x \quad \alpha_y \quad \alpha_{xy}\right)^T \Delta T$$

$$\{\bar{\gamma}\} = \begin{pmatrix} \bar{\gamma}_{xz} & \bar{\gamma}_{yz} \end{pmatrix}^T = \begin{pmatrix} w_{,x} - \theta_x \\ w_{,y} - \theta_y \end{pmatrix} \tag{3.3}$$

where, for the intermediate class of deformation

$$\begin{pmatrix} \varepsilon_x & \varepsilon_y & \gamma_{xy} \end{pmatrix}^T = \begin{pmatrix} u_{,x} & v_{,y} & u_{,y} + v_{,x} \end{pmatrix}^T + \tfrac{1}{2}\begin{pmatrix} \varphi_x^2 & \varphi_y^2 & 2\varphi_x\varphi_y \end{pmatrix}^T$$

$$\begin{pmatrix} \kappa_x & \kappa_y & \kappa_{xy} \end{pmatrix}^T = \begin{pmatrix} \theta_{x,x} & \theta_{y,y} & \theta_{x,y} + \theta_{y,x} \end{pmatrix}^T \tag{3.4}$$

$\bar{\varepsilon}_x$, $\bar{\varepsilon}_y$, $\bar{\gamma}_{xy}$, $\bar{\gamma}_{yz}$ and $\bar{\gamma}_{xz}$ are extensional and shearing strains at any point through the plate thickness and ε_x, ε_y and γ_{xy} denote the corresponding quantities at points on the plate middle plane only. "$_{,x}$" and "$_{,y}$" represent partial differentiation with respect to x and y. The deformation field can also be written in the following form

$$\varepsilon_L = \varepsilon + z\kappa = L_m \mathbf{u} + z L_b \mathbf{u} \qquad \varepsilon_T = L_s \mathbf{u} \tag{3.5}$$

where the indices "m", "b", and "s" stand for membrane, bending and shear respectively. $\varepsilon_L = \{\varepsilon_x, \varepsilon_y, \varepsilon_{xy}\}^T$ and $\varepsilon_T = \{\varepsilon_{yz}, \varepsilon_{xz}\}^T$ contain the in-plane and transversal strain components respectively. $\mathbf{u} = \{u, v, \theta_x, \theta_y, w\}$ is the displacement vector, $\varepsilon = \{u_{,x}, v_{,y}, (u_{,y} + v_{,x})\}^T$ and $\kappa = \{\theta_{x,x}, \theta_{y,y}, (\theta_{x,y} + \theta_{y,x})\}^T$ are the deformation vectors in the reference surface. ($_{,\alpha}$ denotes differentiation with respect to α) The matrices L are given in Section 3.4.

3.3 Stress Resultants in a Plate

A flat plate, like a straight beam, supports transverse loads by bending. The stresses may act on the cross-sections of the plate whose material is homogeneous and linearly elastic. Normal stresses σ_x and σ_y vary linearly with z and are associated with bending moments M_x and M_y. Shear stress τ_{xy} also varies linearly with z and is associated with twisting moment M_{xy}. Normal stress σ_z is considered negligible in comparison with σ_x, σ_y, and τ_{xy}. Transverse shear stresses τ_{yz} and τ_{zx} vary quadratically with z. In general, "plate bending means that external loads have no components parallel to the xy-plane and that $\sigma_x = \sigma_y = \tau_{xy} = 0$. Except for stress τ_{xy}, the foregoing stress patterns are a direct extension of beam theory from one dimension to two. The stress resultants and the moment resultants can be obtained by the integration of stress over the thickness h. They are positive in the same directions as the corresponding stress components and they give the total force per unit length acting at the midplane. In addition to that, there are moments applied at the midplane, which are equivalent to the moments produced by the stresses with respect to the midplane. There are also forces per unit length. All these are defined as

$$\{N\}^T = \begin{pmatrix} N_x, N_y, N_{xy} \end{pmatrix} = \int_{-h/2}^{h/2} \begin{pmatrix} \sigma_x, \sigma_y, \tau_{xy} \end{pmatrix} dz \tag{3.6}$$

$$\{M\}^T = (M_x, M_y, M_{xy}) = \int_{-h/2}^{h/2} (\sigma_x, \sigma_y, \tau_{xy}) z dz \tag{3.7}$$

$$\{V\}^T = (V_x, V_y) = \int_{-h/2}^{h/2} (\tau_{zx}, \tau_{yz}) dz \tag{3.8}$$

The M's are moments per unit length and the V's are forces per unit length. Stresses σ_x, σ_y, and τ_{xy} are largest at the surfaces z = ± h/2, where they have the respective magnitudes $6M_x/h^2$, $6M_y/h^2$, and $6M_{xy}/h^2$ [5]. At arbitrary values of z,

$\sigma_x = 12M_xz/h^3$ $\sigma_y = 12M_yz/h^3$ $\tau_{xy} = 12M_{xy}z/h^3$

Transverse shear stresses are usually small in comparison with σ_x, σ_y, and τ_{xy}. They have the greatest magnitude at z = 0, where $\tau_{yz} = 1.5\ Q_y/h$ and $\tau_{zx} = 1.5Q_x/h$. The membrane stresses σ_x, σ_y, and τ_{xy} are either known *a priory* or calculated by standard static stress analysis.

The thermal stress resultants and the thermal moment resultants are defined as

$$\{N_t\}^T = (N_{tx}, N_{ty}, N_{txy}) = \int_{-h/2}^{h/2} (\sigma_{tx}, \sigma_{ty}, \tau_{txy}) dz \tag{3.9}$$

$$\{M_t\}^T = (M_{tx}, M_{ty}, M_{txy}) = \int_{-h/2}^{h/2} (\sigma_{tx}, \sigma_{ty}, \tau_{txy}) z dz \tag{3.10}$$

where σ_{tx} and σ_{ty}, are thermal stresses in the x and y directions respectively, and τ_{xy} is the thermal stress in the xy plane.

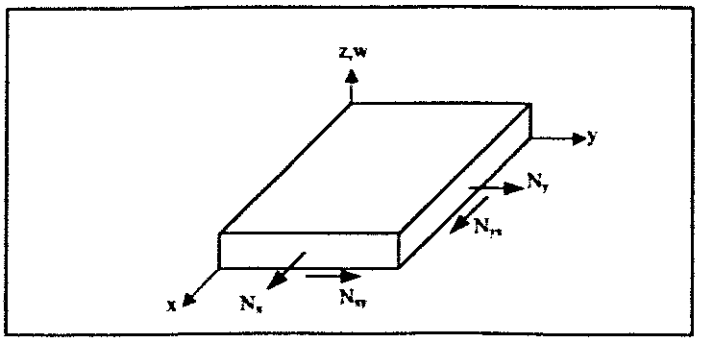

Figure 3.2 Differential element of a flat plate, showing membrane forces

In this theory it can be deduced that w depends only on x and y and that u and v are linear in z. Thus the main assumptions reduce to

$$\mathbf{u} = [u, v, w, \theta_x, \theta_y]^T \tag{3.11}$$

in which u and v are in-plane displacements, w is the lateral displacement normal to the xy-plane. The variables θ_x and θ_y are the normal rotation in the xz and yz planes.

We note that

$$\theta_X = \frac{\partial w}{\partial x} - \phi_X \text{ and } \theta_y = \frac{\partial w}{\partial y} - \phi_y \tag{3.12}$$

where ϕ_x and ϕ_y are the rotations of the normal in the xz and yz-planes respectively and are integrated measures of the transverse shear strain. In thin plate theory it is assumed that ϕ_x and ϕ_y are zero. A typical Mindlin plate is shown in Figure 3.3.

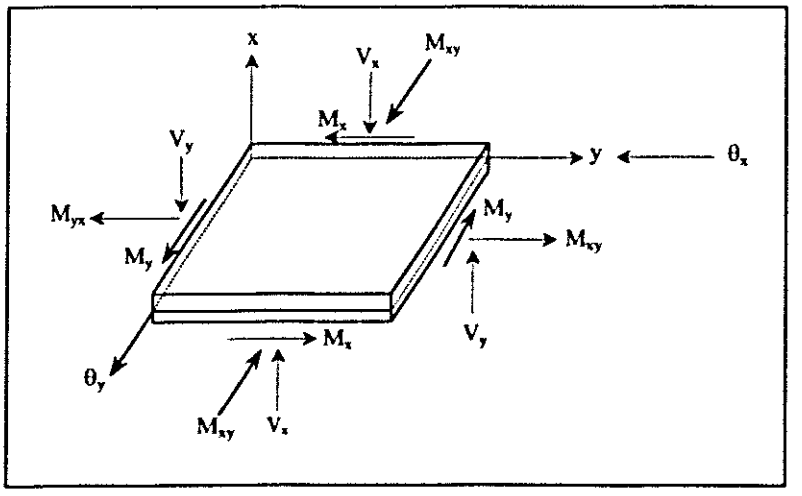

Figure 3.3 Mindlin Plate Rotation

The total stress resultants are

$$\{N\}^T = \begin{bmatrix} N_x \\ N_y \\ N_{xy} \end{bmatrix} - \begin{bmatrix} N_{tx} \\ N_{ty} \\ N_{txy} \end{bmatrix} = \int_{-t/2}^{t/2} \left(\begin{bmatrix} \sigma_x \\ \sigma_y \\ \tau_{xy} \end{bmatrix} - \begin{bmatrix} \sigma_{tx} \\ \sigma_{ty} \\ \tau_{txy} \end{bmatrix} \right) dz \tag{3.13}$$

and the total moment resultants can be written as

$$\{M\}^T = \begin{bmatrix} M_x \\ M_y \\ M_{xy} \end{bmatrix} - \begin{bmatrix} M_{tx} \\ M_{ty} \\ M_{txy} \end{bmatrix} = \int_{-t/2}^{t/2} \left(\begin{bmatrix} \sigma_x \\ \sigma_y \\ \tau_{xy} \end{bmatrix} - \begin{bmatrix} \sigma_{tx} \\ \sigma_{ty} \\ \tau_{txy} \end{bmatrix} \right) z dz \tag{3.14}$$

The shear forces are given by

$$\{V\}^T = \begin{bmatrix} V_x \\ V_y \end{bmatrix} = \int_{-t/2}^{t/2} \begin{pmatrix} \tau_{xz} \\ \tau_{yz} \end{pmatrix} dz \tag{3.15}$$

3.4 Differential Governing Equations of Mindlin Plate

The strains are separated into in-plane and transverse shear groups

$$\kappa = \mathbf{L}\theta \qquad \varepsilon = -z\,\mathbf{L}\,\theta \qquad \gamma = \nabla w - \theta \tag{3.16}$$

In addition to normal bending moments, a twisting moment arises. The introduction of the appropriate constitutive relations enables one to relate all moment components to displacement derivatives. For isotropic elasticity

$$\mathbf{M} = \mathbf{D}\,\mathbf{L}\,\theta \tag{3.17}$$

where, assuming plane stress behaviour in each layer, **D** will be the material properties. The shear force resultants are

$$\mathbf{S} = \alpha\,(\nabla w - \theta) \tag{3.18}$$

Again for isotropic elasticity

$$\alpha = \alpha = \beta G\,h \tag{3.19}$$

The constitutive relations can be generalised to anisotropic or inhomogeneous behaviour such as can be manifested if several layers of material are assembled to form a **composite**. The only apparent difference is the structure of **D** and α matrices, which can always be found by simple integration. The equilibrium relations complete the governing equations for thick and thin plate behaviour. Omitting the in-plane behaviour, we have

$$\mathbf{L}^T\mathbf{M} + \mathbf{S} = \mathbf{0} \tag{3.20}$$

$$\nabla^T\mathbf{S} + \mathbf{q} = \mathbf{0} \tag{3.21}$$

These equations are the basis from which the solutions of both thick and thin plates are formulated. The formulation of a thin plate problem suppresses shear deformation such that

$$\mathbf{S} = \alpha\,(\nabla w - \theta) \tag{3.22}$$

Becomes

$$\nabla w - \theta = \mathbf{0} \tag{3.23}$$

We are now able to write both the mixed and irreducible form of the governing equations. We wish to remain with w as the only variable and this we can do by eliminating **M**, **S** and θ. This elimination is done by applying the operator ∇^T. The result is

$$(\mathbf{L}\,\nabla)^T\,\mathbf{D}\,\mathbf{L}\,\nabla w + \mathbf{q} = \mathbf{0} \tag{3.24}$$

and this is a scalar equation and is irreducible.

In all the above

$$(\mathbf{L}\nabla)^T \equiv \left[\frac{\partial^2}{\partial x^2}, \frac{\partial^2}{\partial y^2}, 2\frac{\partial^2}{\partial x \partial y}\right]$$

For constant **D** this becomes the bihamonic equation of plate flexure.

$$\nabla^4 w = -q\frac{12(1-\nu^2)}{Eh^3} \tag{3.25}$$

For thick plates any (or all) of the independent variables can be approximated independently, leading to a mixed formulation. It is convenient to eliminate **M** and write the system of three equations

$$\mathbf{L}^T \mathbf{D}\, \mathbf{L}\, \theta + \mathbf{S} = \mathbf{0} \tag{3.26}$$

$$\mathbf{S}/\alpha + \theta - \nabla \mathbf{w} = \mathbf{0} \tag{3.27}$$

$$\nabla^T \mathbf{S} = -\mathbf{q} \tag{3.28}$$

This equation system can be reduced further to yield an irreducible form by eliminating shear forces.

$$\mathbf{L}^T \mathbf{D}\, \mathbf{L}\, \theta + \alpha\,(\nabla \mathbf{w} - \theta) = \mathbf{0} \tag{3.29}$$

$$-\nabla^T(\alpha\theta) + \nabla^T(\alpha \nabla \mathbf{w}) = -\mathbf{q} \tag{3.30}$$

The operators and matrices are

$$\kappa = \begin{pmatrix} \theta_{x,x} & \theta_{y,y} & \theta_{x,y} + \theta_{y,x} \end{pmatrix}$$

$$\mathbf{M} = \begin{pmatrix} M_x & M_y & M_{xy} \end{pmatrix}^T$$

$$\varepsilon = \begin{pmatrix} \varepsilon_x & \varepsilon_y & \gamma_{xy} \end{pmatrix}^T$$

$$\nabla w = \begin{pmatrix} \frac{\partial w}{\partial x} & \frac{\partial w}{\partial y} \end{pmatrix}$$

$$\theta = \begin{pmatrix} \theta_x & \theta_y \end{pmatrix}^T$$

$$\mathbf{L} = \begin{pmatrix} \frac{\partial}{\partial x} & 0 & \frac{\partial}{\partial y} \\ 0 & \frac{\partial}{\partial y} & \frac{\partial}{\partial x} \end{pmatrix}^T$$

$$\mathbf{D} = \frac{Et^3}{12(1-\nu^2)}\begin{bmatrix} 1 & \nu & 0 \\ \nu & 1 & 0 \\ 0 & 0 & \frac{1-\nu}{2} \end{bmatrix}$$

The differential operator matrices L_m, L_b and L_s of Section 3.2 are

$$\mathbf{L}_m = \begin{bmatrix} \frac{\partial}{\partial x} & 0 & 0 & 0 & 0 \\ 0 & \frac{\partial}{\partial y} & 0 & 0 & 0 \\ \frac{\partial}{\partial y} & \frac{\partial}{\partial x} & 0 & 0 & 0 \end{bmatrix} \quad \mathbf{L}_b = \begin{bmatrix} 0 & 0 & \frac{\partial}{\partial x} & 0 & 0 \\ 0 & 0 & 0 & \frac{\partial}{\partial y} & 0 \\ 0 & 0 & \frac{\partial}{\partial y} & \frac{\partial}{\partial x} & 0 \end{bmatrix} \quad \mathbf{L}_s = \begin{bmatrix} 0 & 0 & \frac{\partial}{\partial y} & 0 & 1 \\ 0 & 0 & \frac{\partial}{\partial x} & 1 & 0 \end{bmatrix}$$

The governing equations of Mindlin plates can be given as

$$\left(w_{,x} - \theta_x\right)_{,x} + \left(w_{,y} - \theta_y\right)_{,y} + \frac{1}{\beta Gt} q = 0 \tag{3.31}$$

$$w_{,x} - \theta_x + \frac{D}{\beta Gt}\left[\left(\theta_{x,x} + \nu\theta_{y,y}\right)_{,x} \frac{1-\nu}{2}\left(\theta_{x,y} + \theta_{y,x}\right)_{,y}\right] = 0 \tag{3.32}$$

$$w_{,y} - \theta_y + \frac{D}{\beta Gt}\left[\left(\theta_{y,y} + \nu\theta_{x,x}\right)_{,y} \frac{1-\nu}{2}\left(\theta_{x,y} + \theta_{y,x}\right)_{,x}\right] = 0 \tag{3.33}$$

Introducing the following functions

$$\theta_x = \varphi_{,x} + \psi_{,y} \qquad \theta_y = \varphi_{,y} + \psi_{,x} \tag{3.34}$$

the last two equations become

$$\left(w - \varphi + \frac{D}{\beta Gt}\nabla^2\varphi\right)_{,x} - \left(\psi - \frac{1-\nu}{2}\frac{D}{\beta Gt}\nabla^2\psi\right)_{,y} = 0 \tag{3.35}$$

$$\left(w - \varphi + \frac{D}{\beta Gt}\nabla^2\varphi\right)_{,y} - \left(\psi - \frac{1-\nu}{2}\frac{D}{\beta Gt}\nabla^2\psi\right)_{,x} = 0 \tag{3.36}$$

According to the theory of complex analysis, we have

$$w = \varphi - \frac{D}{\beta Gt}\nabla^2\varphi \qquad \psi - \frac{1-\nu}{2}\frac{D}{\beta Gt}\nabla^2\psi = 0 \tag{3.37}$$

and

$$\nabla^4\varphi = q \tag{3.38}$$

φ is referred to as the displacement function, and ψ is called shear deformation function. A single governing equation of w can be derived as

$$\nabla^4 w = \frac{1}{D}\left(1 - \frac{D}{\beta G t}\nabla^2\right)q \tag{3.39}$$

Using the stress-strain relations,

$$\begin{pmatrix}\gamma_{xz,z}\\ \gamma_{yz,z}\\ \varepsilon_z\end{pmatrix} = 0 \qquad \begin{pmatrix}\gamma_{xz}\\ \gamma_{yz}\end{pmatrix} = \frac{1}{G'}\begin{pmatrix}\tau_{xz}\\ \tau_{yz}\end{pmatrix} \tag{3.40}$$

where $G' = \kappa^2 G = \dfrac{\pi^2}{12G}$

and denoting the plate thickness by h and time by t, Mindlin [22] includes the effects of rotary inertia[1] with the result that the displacements are expressed as

$$\frac{D}{2}\left[(1-\nu)\nabla^2\theta_x + (1+\nu)\frac{\partial \Phi}{\partial x}\right] - \kappa^2 Gh\left(\theta_x + \frac{\partial w}{\partial x}\right) = \frac{\rho h^3}{12}\frac{\partial^2 \theta_x}{\partial t^2}$$

$$\frac{D}{2}\left[(1-\nu)\nabla^2\theta_y + (1+\nu)\frac{\partial \Phi}{\partial y}\right] - \kappa^2 Gh\left(\theta_y + \frac{\partial w}{\partial y}\right) = \frac{\rho h^3}{12}\frac{\partial^2 \theta_y}{\partial t^2}$$

$$\kappa^2 Gh\left(\nabla^2 w + \Phi\right) + q = \rho h \frac{\partial^2 w}{\partial t^2} \tag{3.41}$$

where $\Phi = \dfrac{\partial \theta_x}{\partial x} + \dfrac{\partial \theta_y}{\partial y}$ and ∇^2 is the Laplace's two dimensional operator. κ is a constant selected to modify the relation between the average transverse shear and strain. ρ is the density of the plate.

The constitutive relationships are given in the form

$$\sigma = \mathbf{D}\varepsilon \tag{3.42}$$

where

$$\sigma = \begin{bmatrix} M_x & M_y & M_{xy} & V_y & V_y \end{bmatrix}^T$$

M_x and M_y are the direct bending moments and M_{xy} is the twisting moment. The quantities V_x and V_y are the shear forces in the xz and yz planes. For isotropic elastic material

[1] See Mindlin for a full treatment

$$\mathbf{D}=\begin{bmatrix} D & \nu D & 0 & 0 & 0 \\ \nu D & D & 0 & 0 & 0 \\ 0 & 0 & \frac{(1-\nu)}{2}D & 0 & 0 \\ 0 & 0 & 0 & S & 0 \\ 0 & 0 & 0 & 0 & S \end{bmatrix}$$

in which for a plate of thickness h

$$D=\frac{Eh^3}{12(1-\nu^2)} \quad \text{and} \quad S=\frac{Gh}{1.2}$$

where G is the shear modulus and the factor 1.2 is a shear correction term.

Finally the governing equation for a Mindlin plate, including Equations (3.37), is

$$\left(\nabla^2-\frac{\rho}{G'}\frac{\partial^2}{\partial t^2}\right)\left(D\nabla^2-\frac{\rho h^3}{12}\frac{\partial^2}{\partial t^2}\right)w=\rho h\frac{\partial^2 w}{\partial t^2} \tag{3.43}$$

which is a two dimensional analogue of Timoshenko's beam equation. If the rotatory inertia terms are omitted and the transverse shear deformation is neglected, equation (3.43) reduces to

$$D\nabla^4 w+\rho h\frac{\partial^2 w}{\partial t^2}=p \tag{3.44}$$

which is referred to as the Lagrange's equation. Mindlin's theory involves the modelling (neglect) of the in-plane strain gradient.

Chapter 4

Constitutive Equations of Laminated Composites Plates

4.1 Introduction

An anisotropic body in the most general case has 21 independent elastic constants. An isotropic body, on the other hand, has only two independent elastic constants. In such a body, when a tensile stress is applied in the z direction, a tensile strain ε_z results in that direction. In addition to this, because of the Poisson ratio effect, two equal compressive strains ($\varepsilon_x = \varepsilon_y$) result in the x and y directions. In a generally anisotropic body, the two transverse strains are not equal. In fact, in such a body, tensile loading can result in tensile as well as shear strains. A composite containing uniaxially aligned fibers will have a plane of symmetry perpendicular to the fiber direction (that is, material on one side of the plane will be the mirror image of the material on the other side). Such a material will have 13 independent elastic constants. Additional symmetry elements, depending on the fiber arrangements, can be present.

4.2 Elastic Constants of a Composite Material

As discussed in Chapter 2, from the theory of elasticity, there are nine stress components acting on the front faces of an elemental cube. A stress component σ_{ij} represents the force per unit area in the i direction on the face whose normal is the j direction. Rotational equilibrium requires that $\sigma_{ij} = \sigma_{ji}$ and this leaves six stress components in which $i = j$ are the normal stresses while $i \neq j$ are the shear stresses. The most generalized form of Hooke's law can be written in a tensor form as

$$\sigma_{ij} = C_{ijkl}\varepsilon_{kl} \tag{4.1}$$

which, when expanded, will have 81 elastic constants. C_{ijkl} are the elastic constants or stiffnesses. In the discussion that follows, C_{ijkl} will be represented by C_{mn}, σ_{ij} by σ_m and ε_{kl} by ε_n as per the following procedure

ij or kl	11	22	33	23	31	12
m or n	1	2	3	4	5	6

where 4, 5, and 6 now represent the state of shear, this then gives us

$$\sigma_m = C_{mn}\varepsilon_n .$$

It can be shown that $\sigma_{mn} = \sigma_{nm}$. Conversely,

$$\varepsilon_n = S_{mn}\sigma_m$$

where S_{mn}, the compliance matrix, is the inverse of the stiffness matrix C_{mn}. In the expanded form, we get a symmetric matrix, which gives 21 independent elastic constants in the most general case. For most materials, this number of independent elastic constants is further reduced because of the various symmetry elements present. For isotropic materials where elastic properties are independent of direction, only two constants are independent, that is C_{11} and C_{12} (or S_{11} and S_{12}). In practice, use is frequently made of the elastic constants such as Young's modulus E, Poisson ratio ν, shear modulus G, and bulk modulus K. However, only two of these are independent because E, G, ν, and K are interrelated by

$E = 2G(1 + \nu)$ and $K = E/3(1-2\nu)$.

The relationship between these engineering constants and compliances are

$$E = \frac{1}{S_{11}} \qquad \nu = -\frac{S_{12}}{S_{11}} \qquad G = \frac{1}{2}(S_{11} - S_{12})$$

and the compliances are related to the stiffnesses by

$$S_{11} = \frac{C_{11} + C_{12}}{(C_{11} - C_{12})(C_{11} + 2C_{12})} \qquad S_{12} = -\frac{C_{12}}{(C_{11} - C_{12})(C_{11} + 2C_{12})}$$

4.3 Macromechanics of Composites

A lamina, the unit building block of a composite, can be considered to represent a state of generalized plane stress. This implies that the through thickness stress components are zero. Thus, $\sigma_3 = \sigma_4 = \sigma_5 = 0$, that is, using the rectangular Cartesian coordinates, $\sigma_z = \tau_{yz} = \tau_{zx} = 0$, and this reduces the expanded form of the elastic constant matrix even further in that the terms involving the z-axis are eliminated. The equations thus produced describe the stress-strain relationship for an isotropic lamina, for example, an aluminum sheet. A fiber-reinforced lamina, however, is not an isotropic material. It is an orthotropic material; that is, it has three mutually perpendicular axes of symmetry. A fiber-reinforced lamina generally contains unidirectionally oriented fibers, and is quite thin (about 0.1mm). These thin laminae are stacked in a specific order of fiber orientation, cured, and bonded into a laminated composite. The behaviour of a laminated composite depends on the characteristics and the directionality of the individual laminae. Three-dimensional orthotropy requires nine independent elastic constants, while bidimensional orthotropy requires only four. For an isotropic material (two or three-dimensional) two independent elastic constants are needed. When the terms with indices 16 and 26 are taken as zero, we get a special case of orthotropy when the principal material axes of symmetry (fiber direction and the direction transverse to it coincide with the principal loading direction). However, if the material symmetry axes and the geometry axes do not coincide, which is a more general case of orthotropy, then a fully populated elastic constant matrix is obtained. In a generally orthotropic lamina wherein there are

nonzero 16 and 26 terms, a unidirectional normal stress σ_x has both normal as well as shear strains as responses and vice versa: that is, there is a coupling between the normal and shear effects. In the case of a specially orthotropic lamina where the 16 and 26 terms are zero, there are normal stresses producing normal strains and shear stresses producing shear strains and vice versa. In this case there is no coupling between the normal and shear components. Figure 4.3.1 of the following page shows a lamina with unidirectional fibers embedded in a homogeneous matrix.

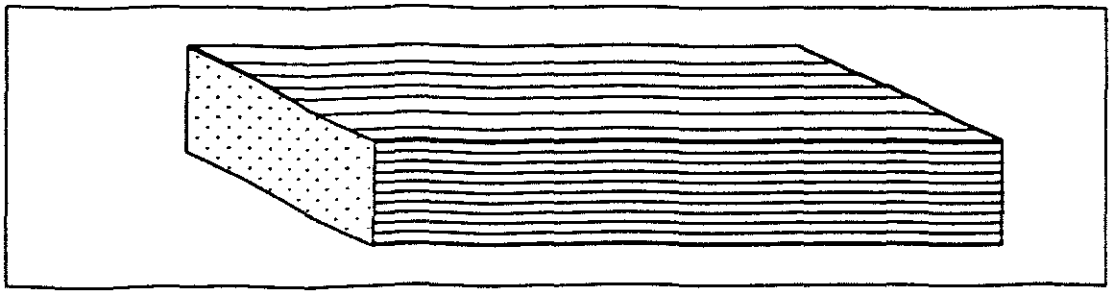

Figure 4.3.1 Homogeneously orthotropic plate

When the natural (or material) axes coincide with the geometric axes, the relationship between the engineering constants (E_1, E_2, G_6, ν_1, and ν_2) and the reduced stiffness' are found to be

$$Q_{11} = \frac{E_1}{1-\nu_1\nu_2} \qquad Q_{22} = \frac{E_2}{1-\nu_1\nu_2} \qquad Q_{12} = \frac{\nu_1 E_2}{1-\nu_1\nu_2} = \frac{\nu_2 E_1}{1-\nu_1\nu_2} \qquad Q_{66} = G_6$$

whiles the relationship between the engineering constants and the compliance are

$$S_{11} = 1/E_1 \quad S_{22} = 1/E_2 \quad S_{12} = -\nu_1/E_1 = \nu_2/E_2 \quad S_{66} = 1/G_6$$

The conventional material constants can be referred to the geometric axes x-y.

4.4 Laminated Composite Plates

Composite structures are fabricated by stacking up thin sheets of unidirectional composites called plies in an appropriate orientation sequence dictated by elastic theory. Bonding together two or more laminae makes in particular, laminated fibrous composites. The individual unidirectional laminae or plies are oriented in such a manner that the resulting structural component has the desired mechanical and/or physical characteristics in different directions. This is shown in Figure 4.4.1. Thus, one exploits the inherent anisotropy of fibrous composites to design a composite material having the appropriate properties. The displacements, like in plate analysis, are presented as u, v, and w in the x, y, and z directions, respectively. The rotations are also presented as θ_x and θ_y. For $i \neq j$, ε_{ij} represents engineering shear strain components equal to twice the tensorial shear components. The assumptions that are made in analyzing the composite plates are very similar to those made for ordinary plate analysis. These are:

- The laminate thickness is small compared to its lateral dimensions. This means that the stresses acting on the interlaminar planes in the interior of the laminate, that is, away from the free edges, are negligibly small.
- There exists a perfect bond between any two laminae. This implies that the laminae cannot slide over each other and the displacements across the bond are continuous.
- There exists a perfect bond between the matrix and the fibrous material.
- There are no empty spaces in the whole laminated composite.

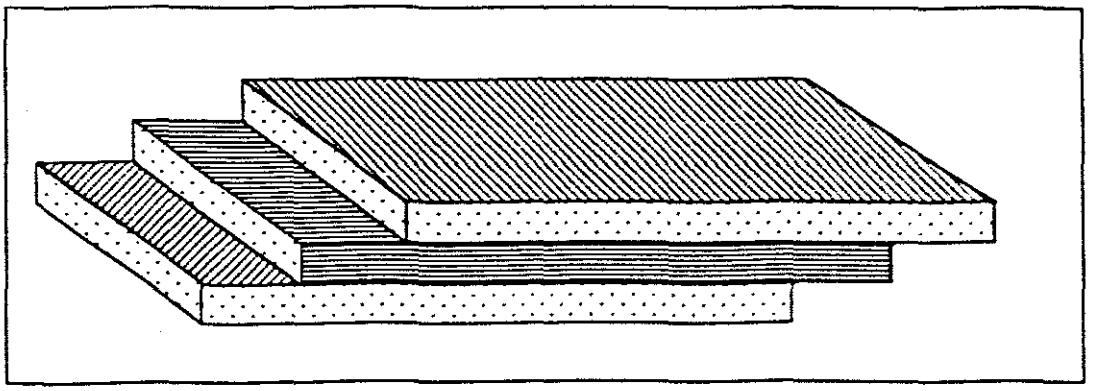

Figure 4.4.1 A laminated composite plate

With these assumptions the laminate behaviour can be reduced to a two-dimensional analysis of the laminate midplane. The coordinate frame is also chosen in such a way that the xy-plane coincides with the midplane of the plate. Based on the above postulates, a composite made of n stacked layers or plies, with thickness h and applying the analysis to the k-th layer, we have a constitutive relationship which will be formulated as the discussion continues.

In the analysis that follows, it may be necessary to generalize the case where the operating temperature of the laminate differs from the temperature at which it was laminated and cured. Effectively, this means that there are stresses produced owing to the restriction of thermally induced expansion or contraction of a body. These stresses, unlike in a uniformly heated free-plate which experience normal strains but no thermal stress, occur when a plate experiences a nonuniform temperature field, or if the displacements are prevented from occurring freely or if the material displays anisotropic properties. According to the Duhamel-Neumann law [8], the stress-strain relations of the m-th layer is given by

$$[\sigma]_m = [Q]_m(\varepsilon - \alpha\Delta T)_m \tag{4.2}$$

where α_{11}, α_{22}, and α_{33} are thermal expansion coefficients in the principal directions. ΔT is the temperature rise. The full version of equation (4.2) is given in Appendix C. In Equation (4.2)

$$Q_{11} = C_{11} - \frac{C_{14}C_{14}}{C_{44}} \qquad Q_{12} = C_{12} - \frac{C_{24}C_{14}}{C_{44}} \qquad Q_{22} = C_{22} - \frac{C_{24}C_{24}}{C_{44}}$$

$$Q_{33} = C_{33} \quad Q_{55} = C_{55} \quad Q_{66} = C_{66}$$

The correspondence between these terms and the usual engineering constants that might be given for a simple orthotropic layer in a laminate is

$$Q_{11} = \frac{E_1}{1-\nu_{12}\nu_{21}} \qquad Q_{12} = \frac{\nu_{12}E_2}{1-\nu_{12}\nu_{21}} = \frac{\nu_{21}E_1}{1-\nu_{12}\nu_{21}} \qquad Q_{22} = \frac{E_2}{1-\nu_{12}\nu_{21}}$$

$$Q_{33} = G_{12} \qquad Q_{55} = G_{13} \qquad Q_{66} = G_{23}$$

In the derivation of the above equation, the stresses and strains are defined in the principal directions (1, 2, and 3) for that orthotropic lamina. However, in angle-ply laminated plates the principal directions of orthotropy of each individual lamina do not coincide with the geometric coordinate frame. The detailed microstructural nature (the micromechanical analysis of a thin unidirectional lamina that are used as input to the macromechanical analysis) is ignored (Figure 4.4.2)

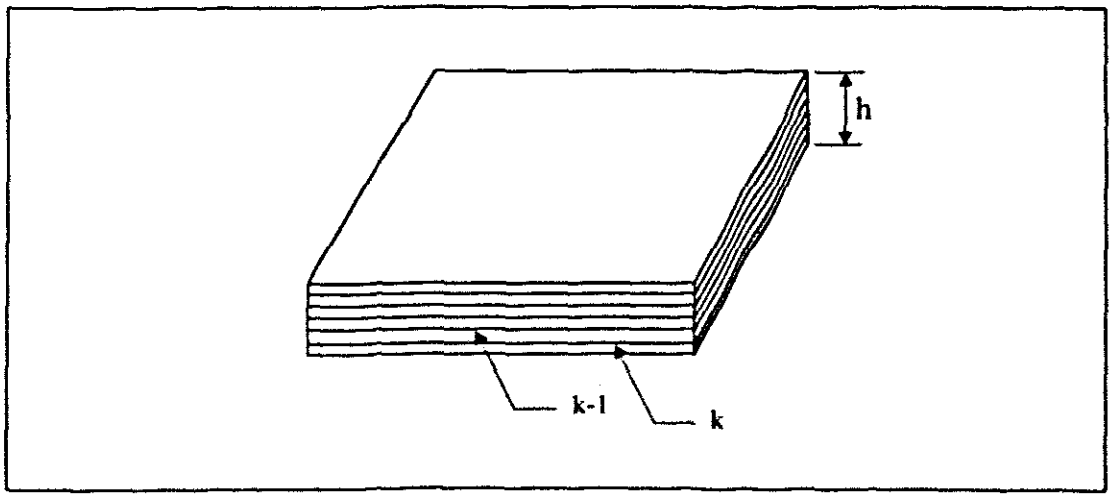

Figure 4.4.2 A laminated composite plate

It is necessary then to use the transformed reduced stiffness

$$[\sigma]^{x-y} = [\bar{Q}_{ij}]\{\varepsilon_i\} - [\bar{Q}_{\alpha ij}]\{\alpha_i\}\Delta T \tag{4.3}$$

where the thirteen constants $\bar{Q}_{ij}$ are related to the nine Q_{ij} through the usual transformation law. This $\bar{Q}_{ij}$ matrix (written in full in Equation B.1.6) is called the transformed reduced stiffness matrix because it is obtained by transforming Q_{ij} (specially orthotropic) to $\bar{Q}_{ij}$ (generally orthotropic) according to

$$P_{ij} = r_{ik}r_{jl}P_{kl} \tag{4.4}$$

where P_{ij} is a second-rank tensor, and r_{ik} and r_{jl} are the direction cosines. Figure 4.4.3 shows the situation for a unidirectional composite lamina where two sets of axes do not coincide.

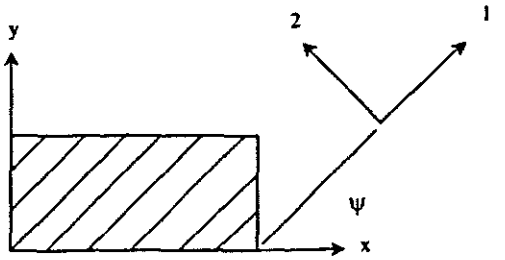

Figure 4.4.3 An off-axis unidirectional lamina

Angle ψ is positive when the x-y axes are rotated counterclockwise with respect to the 1-2 axes.

The strains are as defined in Chapter 3 and Appendix B gives the transformation of the stress-strain matrix. Both the stresses and strains are second-rank tensors. Although $\overline{Q}_{ij}$ is a completely filled matrix, only four of its components are independent: $\overline{Q}_{16}$ and $\overline{Q}_{26}$ are linear combinations of the other four.

The stress resultants and the moment resultants are obtained by integration of stress over the thickness h with Equation (4.3) and summing over the number of layers N, from a particular layer to the k-th layer. Also present are the shear forces. These are defined as

$$\left(N_x \quad N_y \quad N_{xy}\right)=\sum_{k=1}^{n}\left(\sigma_x \quad \sigma_y \quad \tau_{xy}\right)\int_{h_{k-1}}^{h_k} dz \tag{4.5}$$

$$\left(M_x \quad M_y \quad M_{xy}\right)=\sum_{k=1}^{n}\left(\sigma_x \quad \sigma_y \quad \tau_{xy}\right)\int_{h_{k-1}}^{h_k} z\,dz \tag{4.6}$$

$$\left(V_x \quad V_y\right)=\sum_{k=1}^{n}\left(\tau_{xz} \quad \tau_{yz}\right)\int_{h_{k-1}}^{h_k} dz \tag{4.7}$$

These stress resultants, having the dimensions of force per unit length, are positive in the same directions as the corresponding stress components. These resultants give the total force per unit length acting at the midplane. Using equation (4.3), the stress resultants are given by

$$\begin{bmatrix}\{N\}\\ \{M\}\\ \{V\}\end{bmatrix}=\begin{bmatrix}[A] & [B] & 0\\ [B] & [D] & 0\\ 0 & 0 & [\overline{A}]\end{bmatrix}\begin{bmatrix}\{\bar{\varepsilon}\}\\ \{\bar{\kappa}\}\\ \{\bar{\gamma}\}\end{bmatrix}-\begin{bmatrix}\{N_t\}\\ \{M_t\}\\ 0\end{bmatrix} \tag{4.8}$$

where

$$\left(A_{ij} \quad B_{ij} \quad D_{ij}\right)=\sum_{k=1}^{N}\left[\overline{Q}_{ij}\right]_k\left(1 \quad z \quad z^2\right)\int_{h_{k-1}}^{h_k} dz \qquad (i,j = 1, 2, 6)$$

$$\overline{A}_{ij} = b\sum_{k=1}^{N}\left[\overline{Q}_{ij}\right]_k \int_{h_{k-1}}^{h_k} dz \qquad (i,j = 4, 5) \tag{4.9}$$

b is the shear correction factor [36].
The extensional stiffness A_{ij}, flexural-extensional coupling stiffness B_{ij}, and flexural stiffness D_{ij} of the plate are defined in Appendix B. The state of stress developed in the plate very much depends on the lay-up and boundary conditions, and it is this stress state that is responsible for plate buckling rather than the applied one. Equation (4.8) is the constitutive model of the laminated composite plate and is the basis from which buckling analysis can be carried out.

4.5 Special Cases of Laminated Stiffnesses

There are cases of laminated composites for which the stiffnesses take on certain simplified values as opposed to the general form of Equation 4.9. Many of the cases result from the common practice of constructing laminates from laminae that have the same material properties and thickness, but have different orientations of their principal material directions relative to one another and relative to the laminate axes as discusses above. These may be listed as follows

4.5.1 Single-layered Configurations

These include

- **Single isotropic layer**

  The resultant forces are dependent only on the in-surface strains of the laminate middle surface, and the resultant moments are dependent only on the curvatures of the middle surface. There is no coupling between bending and extension of a single isotropic layer

- **Single specially orthotropic layer**

  As with a single isotropic layer, the resultant forces depend only on the in-surface strains, and the resultant moments depend only on the curvature. However, this type of laminated contains the lamina stiffness Q_{ij}.

- **Single generally orthotropic layer**

  This laminate contains the stiffness $\overline{Q}_{ij}$ with no coupling between bending and extension. In contrast to both an isotropic layer and a specially orthotropic layer, the extensional forces depend on shearing strain as well as on extensional strain. Also, the resultant shearing force, N_{xy}, depends on the extensional strains ε_x and ε_y,

as well as on the shearing strain γ_{xy}. Similarly, the moment resultants all depend on both the curvatures κ_x and κ_y, and on the twist κ_{xy}.

- **Single anisotropic layer**

  The only difference in appearance between a single generally orthotropic layer and an anisotropic layer is that the latter has lamina stiffnesses, Q_{ij}, whereas the generally orthotropic layer has stiffnesses $\overline{Q}_{ij}$.

4.5.2 Symmetric Laminates

For laminates that are symmetric in both geometry and material properties about the middle surface, the general stiffness equations, Equation (4.9), simplify considerably. In particular, because of the symmetry of the $\left(\overline{Q}_{ij}\right)_k$ and the thickness t_k, all the coupling stiffness, that is, the B_{ij}, can be shown to be zero. The elimination of coupling between bending and extension has two ramifications. First, such laminates are usually much easier to analyze than laminates with coupling. Second, symmetric laminates do not have a tendency to twist from the inevitable thermally induced contractions that occur during cooling following the curing process. Consequently, symmetric laminates are commonly used unless special circumstances require an unsymmetric laminate. For example, part of the function of a laminate may be to serve as a heat shield, but the heat comes from only one side; thus, an unsymmetric laminate is likely to be used.

- **Symmetric laminates with multiple isotropic layers**

  If multiple isotropic layers of various thicknesses are arranged symmetrically about a middle surface from both a geometric and a material property standpoint, the resulting laminate does not exhibit coupling between bending and extension.

- **Symmetric laminates with multiple specially orthotropic layer**

  Because of the analytical complications involving the stiffnesses A_{16}, A_{26}, D_{16}, and D_{26}, a laminate is desired that does not have these stiffnesses. Laminates can be made with orthotropic layers that have principal material directions aligned with the laminate axes. If the thicknesses, locations, and material properties of the laminae are symmetric about the middle surface of the laminate, there is no coupling between bending and extension. Because $\left(\overline{Q}_{16}\right)_k$ and $\left(\overline{Q}_{26}\right)_k$ are zero, the stiffnesses A_{16}, A_{26}, D_{16}, and D_{26}, vanish. Also, the stiffness B_{ij} are zero because of symmetry. This type of laminate could therefore be called a specially orthotropic laminate in analogy to a specially orthotropic lamina. A very common special case of symmetric laminates with multiple specially orthotropic layers occur when the laminae are all of the same thickness and material properties, but have their major principal material directions alternating at 0^0 and 90^0 to the laminate axes, for example, $0^0/90^0/0^0$. Such laminates are called *regular symmetric cross-ply laminates.*

- **Symmetric laminates with multiple generally orthotropic layers**

  A laminate of multiple generally orthotropic layers that are symmetrically disposed about the middle surface exhibits no coupling between bending and extension; that is; the B_{ij} are zero. All the A_{ij} and D_{ij} are required because of coupling between normal forces and shearing strain, shearing force and normal strains, normal moments and twist, and twisting moment and normal curvatures. Such coupling is evidenced by the A_{16}, A_{26}, D_{16}, and D_{26} stiffnesses. A special subclass of this class of symmetric laminates is the *regular symmetric angle-ply laminate*. Such laminates have orthotropic laminae of equal thicknesses. The adjecent laminae have opposite signs of the angle of orientation of the principal material properties with respect to the laminate axes, for example, $+\theta/-\theta/+\theta$. Thus, for symmetry, there must be an odd number of layers.

- **Symmetric laminates with multiple anisotropic laters**

  The general case of a laminate with multiple anisotropic layers symmetrically disposed about the middle surface does not have any stiffness simplifications other than the elimination of the B_{ij} by vitue of symmetry. The A_{16}, A_{26}, D_{16}, and D_{26}, stiffnesses all exist and do not necessarily go to zero as the number of layers is increased. Many of the stiffness simplifications possible for other laminates cannot be achieved for this class.

4.5.3 Antisymmetric Laminates

Symmetry of a laminate about the middle surface is often desirable to avoid coupling between bending and extension. However, many physical applications of laminated composites require nonsymmetric laminates to achieve design requirements. For example, coupling is a necessary feature to make jet turbine fan blades with pretwist. As a further example, if the shear stiffness of a laminate of made laminae with unidirectional fibers must be increased, one way to achieve this requirement is to position layers at some angle to the laminate axes. To stay within weight and cost requirements, an even number of such layers may be necessary at orientations that alternate from layer to layer, e.g., $+\psi/-\psi/+\psi/-\psi$. Therefore, symmetry about the middle surface is destroyed and the behavioural characteristics of the laminate can be substantially changed from the symmetry case. Although the example laminate is not symmetric, it is antisymmetric about the middle surface, and certain stiffness simplifications are possible. Two important classes of antisymmetric laminates are

- **Antisymmetric cross-ply laminates**

  An antisymmetric cross-ply laminate consists of an even number of orthotropic laminae laid on each other with principal material directions alternating at 0^0 and 90^0 to the laminate axes. Such laminates do not have A_{16}, A_{26}, D_{16}, and D_{26}, but do have coupling between bending and extension. A *regular antisymmetric cross-ply laminate* is defined to have laminae all of equal thickness and is common because of simplicity of fabrication. As the number of layers increases, the coupling stiffness B_{ij} can be shown to approach zero.

- **Antisymmetric angle-ply laminates**

  An antisymmetric angle-ply laminate has laminae orientated at $+\psi$ degrees to the laminate coordinate axes on one side of the middle surface and corresponding equal thickness laminae oriented at $-\psi$ degrees on the other side. A *regular antisymmetric angle-ply laminate* has laminae all of the same thickness for ease of fabrication. This class of laminates can be further restricted to have a single value of ψ as opposed to several orientations. The coupling stiffnesses B_{16} and B_{26} can be shown to go to zero as the number of layers in the laminate increases for a fixed laminate thickness.

4.5.4 Nonsymmetric Laminates

No special reduction of the stiffnesses is possible when t_k is arbitrary. That is, coupling between bending and extension can be obtained by unsymmetric arrangement about the middle surface of isotropic layers with different material properties and possibly (but not necessarily) different thicknesses. Thus, coupling between bending and extension is not a manifestation material orthotropy but rather of laminate heterogeneity; that is, a combination of both geometric and material properties.

Chapter 5

Buckling Equations of Laminated Composite Plates

5.1 Non-linear Equilibrium Equations

From elementary mechanics we know that a static conservative system is in equilibrium if its potential energy is stationary and the equilibrium is stable if the potential energy is a relative minimum. This criterion will be applied to formulate both the prebuckling equilibrium equation and the buckling equation of the laminated composite plate and is carried out in Appendix C. For a conservative structural system, the total potential energy of a loaded structure is defined as the sum of the strain energy of the structure itself and the potential energy of the applied load.

$$\Pi = \Pi_{Strain} + \Pi_{Load} \tag{5.1}$$

For $\Pi_{Load} = 0$, the strain energy (which is the product of the internal strains caused by the internal stresses in the composite material, we have

$$\Pi = \tfrac{1}{2}\iiint\left[\bar{\sigma}_x\bar{\varepsilon}_x + \bar{\sigma}_y\bar{\varepsilon}_y + \bar{\sigma}_z\bar{\varepsilon}_z + \bar{\tau}_{xy}\bar{\gamma}_{xy} + \bar{\tau}_{xz}\bar{\gamma}_{xz} + \bar{\tau}_{yz}\bar{\gamma}_{yz}\right]dxdydz \tag{5.2}$$

Omission of $\bar{\gamma}_{xz}$ and $\bar{\gamma}_{yz}$ according to the basic approximation of the Mindlin theory and substituting equation (4.3) from Chapter 4 into Equation (5.2) and using the stress resultant and moment resultant definitions of Chapter 3, the potential energy equation of a laminated composite plate is found to be

$$\begin{aligned}\Pi = \tfrac{1}{2}\iint\Big(&\{\varepsilon\}^T[A]\{\varepsilon\} + \{\varepsilon\}^T[B]\{\kappa\} + \{\kappa\}^T[B]\{\varepsilon\} + \{\kappa\}^T[D]\{\kappa\} + \{\bar{\gamma}\}^T[\bar{A}]\{\bar{\gamma}\}\Big)dxdy \\ &-\tfrac{1}{2}\iint\Big(\{\varepsilon\}^T[N_t] + \{\kappa\}^T[M_t]\Big)dxdy\end{aligned} \tag{5.3}$$

The first variations of the total potential energy may be written as

$$\begin{aligned}\delta^{(1)}\Pi = &\iint\Big(\{\varepsilon\}^T[A]\{\delta\varepsilon\} + \{\varepsilon\}^T[B]\{\delta\kappa\} + \{\kappa\}^T[B]\{\delta\varepsilon\} + \{\kappa\}^T[D]\{\delta\kappa\} + \{\bar{\gamma}\}^T[\bar{A}]\{\bar{\delta\gamma}\}\Big)dxdy \\ &- \iint\Big([N_t]\{\delta\varepsilon\} + [M_t]\{\delta\kappa\}\Big)dxdy\end{aligned} \tag{5.4}$$

where $\delta^{(1)}\Pi$ is the sum of the first-order terms in the expression for the change in potential energy. To carry out the necessary operations in order to arrive at a more convenient form of the non-linear equilibrium equations, Equation (5.4) is rewritten as

$$\delta^{(1)}\Pi = \iint\left(\left[\overline{N}\right]^T\{\delta\varepsilon\} + \left[\overline{M}\right]^T\{\delta\kappa\} + \left[\overline{V}\right]^T\{\delta\bar{\gamma}\} - \left[N_t\right]^T\{\delta\varepsilon\} - \left[M_t\right]\{\delta\kappa\}\right)dxdy \tag{5.5}$$

where

$$\left(\left[\overline{N}\right]\ \left[\overline{M}\right]\ \left[\overline{V}\right]\right)^T = \begin{pmatrix} \overline{N}_x & \overline{N}_y & \overline{N}_{xy} \\ \overline{M}_x & \overline{M}_y & \overline{M}_{xy} \\ \overline{V}_{xz} & \overline{V}_{yz} & 0 \end{pmatrix} \tag{5.6}$$

$$\left(\{\delta\varepsilon\}\ \{\delta\kappa\}\ \{\delta\bar{\gamma}\}\right)^T = \begin{pmatrix} \delta\varepsilon_x & \delta\varepsilon_y & \delta\gamma_{xy} \\ \delta\kappa_x & \delta\kappa_y & \delta\kappa_{xy} \\ \delta\bar{\gamma}_{xz} & \delta\bar{\gamma}_{yz} & 0 \end{pmatrix} \tag{5.7}$$

so that after integration by parts we get the following,

$$\begin{aligned}
\delta^{(1)}\Pi = &-\iint\left\{\left(\overline{N}_{x,x} - N_{tx,x}\right) + \left(\overline{N}_{xy,x} - N_{txy,x}\right)\right\}\delta u dxdy \\
&-\iint\left\{\left(\overline{N}_{y,y} - N_{ty,y}\right) + \left(\overline{N}_{xy,y} - N_{txy,y}\right)\right\}\delta v dxdy \\
&-\iint\left\{\left(\overline{M}_{x,x} - M_{tx,x}\right) + \left(\overline{M}_{xy,y} - M_{txy,y}\right) - \overline{V}_x\right\}\delta\theta_x dxdy \\
&-\iint\left\{\left(\overline{M}_{y,y} - M_{ty,y}\right) + \left(\overline{M}_{xy,x} - M_{txy,x}\right) - \overline{V}_y\right\}\delta\theta_y dxdy \\
&-\iint\left\{\overline{V}_{y,y} + \overline{V}_{x,x} + \left(\overline{N}_x - N_{tx}\right)w_{,xx} + 2\left(\overline{N}_{xy} - N_{txy}\right)w_{,xy} + \left(\overline{N}_y - N_{ty}\right)w_{,yy}\right. \\
&+\left(N_{x,x} - N_{tx,x}\right)w_{,x} + \left(N_{xy,y} - N_{txy,y}\right)w_{,x} \\
&\left.+\left(\overline{N}_{xy,x} - N_{tx,x}\right)w_{,y} + \left(\overline{N}_{y,y} - N_{ty,y}\right)w_{,y}\right\}\delta w dxdy \\
&+ \text{Boundary terms}
\end{aligned} \tag{5.8}$$

The boundary terms are listed in the Appendix C. From the principle of total potential energy we equate the first variation to zero and get a strong form of the non-linear equilibrium equation.

$$\left(\overline{N}_x - N_{tx}\right)_{,x} + \left(\overline{N}_{xy} - N_{txy}\right)_{,y} = 0$$

$$\left(\overline{N}_y - N_{ty}\right)_{,y} + \left(\overline{N}_{xy} - N_{txy}\right)_{,x} = 0$$

$$\overline{V}_{y,y} + \overline{V}_{x,x} + \left(\overline{N}_x - N_{tx}\right)w_{,xx} + 2\left(\overline{N}_{xy} - N_{txy}\right)w_{,xy} + \left(\overline{N}_y - N_{ty}\right)w_{,yy} +$$

$$\left(\overline{N}_x - N_{tx}\right)_{,x} w_{,x} + \left(\overline{N}_{xy} - N_{txy}\right)_{,y} w_{,x} + \left(\overline{N}_{xy} - N_{txy}\right)_{,x} w_{,y} + \left(\overline{N}_y - N_{ty}\right)_{,y} w_{,y} = 0$$

$$\left(\overline{M}_x - M_{tx}\right)_{,x} + \left(\overline{M}_{xy} - M_{txy}\right)_{,y} - \overline{V}_x = 0$$

$$\left(\overline{M}_y - M_{ty}\right)_{,y} + \left(\overline{M}_{xy} - M_{txy}\right)_{,x} - \overline{V}_x = 0 \qquad (5.9)$$

Using the definition in N, M, and V the full form of equation (5.9) is

$$\begin{aligned} &A_{11}u_{,xx} + A_{12}v_{,xy} + A_{16}\left(2u_{,xy} + v_{,xx}\right) + A_{26}v_{,yy} + A_{66}\left(u_{,yy} + v_{,xy}\right) \\ &+ B_{11}\theta_{x,xx} + B_{12}\theta_{y,xy} + B_{16}\left(2\theta_{x,xy} + \theta_{y,xx}\right) + B_{26}\theta_{y,yy} + B_{66}\left(\theta_{x,yy} + \theta_{y,xy}\right) = N_{tx,x} + N_{txy,y} \end{aligned}$$

$$\begin{aligned} &A_{12}u_{,xy} + A_{16}u_{,xx} + A_{22}v_{,yy} + A_{26}\left(u_{,yy} + 2v_{,xy}\right) + A_{66}\left(u_{,xy} + v_{,xx}\right) \\ &+ B_{12}\theta_{x,xy} + B_{22}\theta_{y,yy} + B_{16}\theta_{x,xx} + B_{26}\left(\theta_{x,yy} + 2\theta_{y,xy}\right) + B_{66}\left(\theta_{x,xy} + \theta_{y,xx}\right) = N_{txy,x} + N_{ty,y} \end{aligned}$$

$$A_{44}\left(w_{,yy} + \theta_{y,y}\right) + A_{45}\left(2w_{,xy} + \theta_{x,y} + \theta_{y,x}\right) + A_{55}\left(w_{,xx} + \theta_{x,x}\right) = \overline{N}_x w_{,xx} + 2\overline{N}_{xy} w_{,xy} + \overline{N}_y w_{,yy}$$

$$\begin{aligned} &B_{11}u_{,xx} + B_{12}v_{,xy} + B_{16}\left(2u_{,xy} + v_{,xx}\right) + B_{26}v_{,yy} + B_{66}\left(u_{,yy} + v_{,xy}\right) \\ &+ D_{11}\theta_{x,xx} + D_{12}\theta_{y,xy} + D_{16}\left(2\theta_{x,xy} + \theta_{y,xx}\right) + D_{26}\theta_{y,yy} + D_{66}\left(\theta_{x,yy} + \theta_{y,xy}\right) \\ &- A_{45}\left(w_{,y} + \theta_y\right) - A_{55}\left(w_{,x} + \theta_x\right) = M_{tx,x} + M_{txy,y} \end{aligned}$$

$$\begin{aligned} &B_{12}u_{,xy} + B_{16}u_{,xx} + B_{22}v_{,yy} + B_{26}\left(u_{,yy} + 2v_{,xy}\right) + B_{66}\left(u_{,xy} + v_{,xx}\right) \\ &+ D_{12}\theta_{x,xy} + D_{22}\theta_{y,yy} + D_{16}\theta_{x,xx} + D_{26}\left(\theta_{x,yy} + 2\theta_{y,xy}\right) + D_{66}\left(\theta_{x,xy} + \theta_{y,xx}\right) \\ &- A_{44}\left(w_{,y} + \theta_y\right) - A_{45}\left(w_{,x} + \theta_x\right) = M_{txy,x} + M_{ty,y} \end{aligned} \qquad (5.10)$$

It is noted that w, θ_x and θ_y are zero for prebuckling analysis and the plate still maintains its initial flat configuration.

5.2 Linear Stability Equations

To investigate the possible existence of adjacent equilibrium configurations, we give small increments to the displacement variables and examine the two adjacent configurations represented by the displacements before and after the increment, as follows

$$u = u_0 + u_1 \qquad v = v_0 + v_1 \qquad w = w_0 + w_1 \qquad \theta_x = \theta_{x0} + \theta_{x1} \qquad \theta_y = \theta_{y0} + \theta_{y1} \qquad (5.11)$$

where $(u_0, v_0, w_0, \theta_{x0}, \theta_{y0})$ is the configuration on the primary equilibrium path and $(u_1, v_1, w_1, \theta_{x1}, \theta_{y1})$ is the virtual increment. This is a perturbation method to analyse the loss of stability. Introduction into Equation (5.3) is seen to give terms that are linear, quadratic, and cubic in the u_0, v_0, w_0 and u_1, v_1, w_1 displacement components. In the new equations, the terms in u_0, v_0, w_0 alone add to zero because (u_0, v_0, w_0) is an equilibrium configuration, and terms that are quadratic and cubic in u_1, v_1, w_1 may be omitted because of the smallness of the incremental displacement. Thus the resulting equation is homogeneous and linear in u_1, v_1, w_1, with variable coefficients in u_0, v_0, w_0. The coefficients u_0, v_0, w_0, however, are governed by the original non-linear equations. For this reason it is desirable to limit the range of applicability of the linearized equation by requiring that u_0, v_0, w_0 be confined to configurations that are governed by the linear equilibrium equations. The second variation of the total potential energy is the sum of all terms in the expression for the potential energy increment that are quadratic in u_1, v_1 and w_1. This results in a simplified and linearized form of the buckling equation. The second-order terms together are called the second variation of Π and are denoted by $\delta^{(2)}\Pi$, where, for instance,

$$\left(\delta\varepsilon_x\right)^2 = u_{1,x}^2 + u_{0,x}\varphi_{x1}^2 \text{, and so on.} \tag{5.12}$$

This is applied to the strain terms of the second variation and we rewrite the resulting equation is a simpler form

$$\delta^{(2)}\Pi = \iint\left([N_1]^T\{\varepsilon_1\} + [M_1]^T\{\kappa_1\} + [V_1]^T\{\gamma_1\} + [N_0]^T\begin{Bmatrix} \frac{1}{2}\varphi_{x1}^2 \\ \frac{1}{2}\varphi_{y1}^2 \\ \varphi_{x1}\varphi_{y1} \end{Bmatrix}\right)dxdy \tag{5.13}$$

where $[N_1]^T$, $\{\varepsilon_1\}$, $[M_1]^T$, $\{\kappa_1\}$, $[V_1]^T$, $\{\gamma_1$, and $[N_0]^T$ are listed in Appendix C. Integration by parts as in Section 5.1, we obtain

$$\begin{aligned}\delta\left(\delta^{(2)}\Pi\right) = &-\iint\left\{N_{x1,x} + N_{xy1,y}\right\}\delta u_1 dxdy - \iint\left\{N_{y1,y} + N_{xy1,x}\right\}\delta v_1 dxdy \\ &- \iint\left\{M_{x1,x} + M_{xy1,y} - V_{x1}\right\}\delta\theta_{x1}dxdy - \iint\left\{M_{y1,y} + M_{xy1,x} - V_{y1}\right\}\delta\theta_{y1}dxdy \\ &- \iint\left\{V_{y1,y} + V_{x1,x} + N_{x0}w_{1,xx} + 2N_{xy0}w_{1,xy} + N_{y0}w_{1,yy}\right. \\ &\quad \left. + \left(N_{x0,x} + N_{xy0,y}\right)w_{1,x} + \left(N_{y0,x} + N_{xy0,y}\right)w_{1,y}\right\}\delta w_1 dxdy \\ &\quad + \text{Boundary terms}\end{aligned} \tag{5.14}$$

where the thermal loads $N_{\alpha x}$, $N_{\alpha y}$ and $N_{\alpha xy}$ will be converted into equivalent mechanical loads by the terms N_{x0}, N_{y0} and N_{xy0}. The boundary terms result from integration by parts of the second variation of the total potential energy and are listed in the Appendix C. When the variation of equation (5.14) is set equal to zero, that is

$$\delta\left(\delta^{(2)}\Pi\right)=0 \tag{5.15}$$

five equations, which govern the buckling of laminated composite plates, are derived.

$$N_{x1,1}+N_{xy1,y}=0$$

$$N_{y1,y}+N_{xy1,x}=0$$

$$M_{x1,x}+M_{xy1,y}-Q_{x1}=0$$

$$M_{y1,y}+M_{xy1,x}-Q_{y1}=0$$

$$\begin{aligned}&V_{y1,y}+V_{x1,x}+N_{x0}w_{1,xx}+2N_{xy0}w_{1,xy}+N_{y0}w_{1,yy}+\\&\left(N_{x0,x}+N_{xy0,y}\right)w_{1,x}+\left(N_{y0,y}+N_{xy0,x}\right)w_{1,y}=0\end{aligned} \tag{5.16}$$

where the subscript denotes a variation of the principal symbol from its value in the prebuckled equilibrium state. Thus, the terms N_{x1}, M_{x1}, ... are variations of forces and moments, respectively, from a membrane prebuckled equilibrium state. The terms δw_1 and, by implication, δu_1 and δv_1 are variations in displacement from the same flat prebuckled state. If the prebuckled state is a membrane, then $\delta w = w$. The applied in-plane loads $\bar{N}_x, \bar{N}_y$, and $\bar{N}_{xy}$ enter the mathematical formulation of the eigenvalue problem as coefficients of the curvatures rather than as "loads" on the right-hand side of the equation. The essence of the eigenvalue problem is to determine the smallest applied loads, $\bar{N}_x$, and so on, that cause buckling. An important consequence of this type of problem is that the magnitude of the deformations after buckling cannot be determined without resorting to large deflection considerations; that is, the deformations are indeterminate when only the above equations are available.

The boundary conditions for buckling problems are applied only to the buckling deformations since the prebuckling deformations are assumed to be a membrane state. On of the distinguishing features of an eigenvalue problem is that all the boundary conditions are homogeneous, that is, zero. These boundary conditions, as listed in Appendix C, could be different for each edge of a plate, so the number of combinations of possible boundary conditions is enormous.

These equations give the exact solutions of the critical buckling temperature and they are quite difficult to solve. The Finite Element Method, which gives the approximate solution (depending on the type of element used), is used to solve the problem. Equation (5.14) forms the basis for the finite element formulation that is the topic of the next chapter.

Chapter 6

Finite Element Modelling of Laminated Composite Plates

6.1 Introduction

Standard finite elements based on Mindlin's assumptions have one important advantage over elements based on classical Kirchhoff's thin plate theory. Mindlin plate elements require only C^0 continuity of the lateral displacement w and the independent normal rotations θ_x and θ_y. However, elements based on classical thin plate Kirchhoff theory require C^1 continuity. In other words, $w_{,x}$ and $w_{,y}$ as well should ideally be continuous across element interface although this condition is relaxed in non-conforming plate elements. Thus, it would appear that Mindlin plate elements are simpler to formulate and they have the added advantage of being able to model shear-weak as well as shear-stiff plates. If transverse shear effects are present in the plate they are automatically modelled with Mindlin elements. Some of the conditions that are satisfied by the Mindlin plate element are:

6.1.1 Compatibility

This means that the displacements within the elements across the element boundary must be continuous. Compatibility is one of the ways of verifying the convergence of the numerical solution to the exact solution. Physically, compatibility ensures that *no gaps* occur between elements when assemblage is loaded. When only translational degrees of freedom are defined at the element nodes, only continuity in the displacement u, v, or w, which are applicable, must be preserved. However, when rotational degrees of freedom are also defined that are obtained by differentiation of the transverse displacement (such as in the formulation of the plate bending element), it is also necessary to satisfy element continuity in the corresponding first displacement derivatives. This is the consequence of the kinematic assumption on the displacement over the depth of the plate bending element; that is, the continuity in the displacement w and the derivatives $\partial w/\partial x$ and/or $\partial w/\partial y$ along the respective element edges ensures continuity of displacement over the thickness of adjoining elements. Compatibility is automatically ensured between truss and beam elements because they join only at the nodal points, and compatibility is relatively easy to maintain in two-dimensional plane strain, plane stress, and axisymmetric analysis and in three-dimensional analysis, when only u, v, and w degrees of freedom are used as nodal point variables. However, the requirements of compatibility are difficult to satisfy in plate bending analysis, and particularly in thin shell analysis if the rotations are derived from the transverse displacements. For this reason, much emphasis has been directed toward the development of plate and shell elements, in which the displacements and rotations are variables.

6.1.2 Completeness

This means that the displacement functions of the element must be able to represent the *rigid body displacements* and the *constant strain states*.

Rigid body displacements are those displacement modes that the element must be able to undergo as a rigid body without stresses being developed in it. The number of element rigid body modes is equal to the number of element degrees of freedom minus the number of element straining modes (or natural modes).

Constant strain state: We imagine that more and more elements are used in the assemblage to represent the structure. Then in the limit as each element approaches a very small size, the strain in each element approaches a constant value, and any complex variation of strain within the structure can be approximated.

6.1.3 Completeness condition on an element assemblage

As the finite element mesh is refined (i.e., the size of the element gets smaller), each element should approach a constant strain condition, so the second condition on convergence of an assemblage of incompatible finite elements, where the element may be of any size, is that the elements together can represent constant strain conditions. This is not a condition on a single element but on an assemblage of elements. That is, although an individual element is able to represent all constant strain states, when the element is used in an assemblage, the incompatibilities between elements may prohibit constant strain states from being represented.

6.1.4 Patch test

This is to investigate whether an assemblage of nonconforming elements is complete. In this test a specific element is considered and a patch of elements is subjected to the minimum displacement boundary conditions to eliminate all rigid body modes and to the boundary nodal point forces that by an analysis should result in constant stress conditions. If for any patch of elements the element stresses actually represent the constant stress conditions and all nodal point displacements are correctly predicted, we say that the element passes the patch test. Since a patch may also consist of only a single element, this test ensures that the element itself is complete and that the completeness condition is also satisfied by any element assemblage. The number of constant stress states in a patch depends of course on the actual number of constant stress states that pertain to the mathematical model.

6.1.5 Incompatible modes

The completeness condition must always be satisfied, and this condition is not affected by the size of the element. On the other hand the compatibility can be relaxed somewhat at the expense of not obtaining a monotonically convergent solution, provided that when relaxing this requirement, the essential ingredients of the completeness condition are not lost. Sometimes satisfactory finite element analysis results are obtained although some continuity requirements between displacement-based elements in the mesh employed are violated. The violation happens when

- The nodal point layout is such that interelement continuity is not preserved
- Elements are used that contain interelement incompatibility.

6.2 Mindlin Plate Element

In this section use will be made of the symbol H to denote the strain-displacement matrix for both the Mindlin plate model and the formulation of the buckling equation for laminated composite plate. The context in which this symbol is used will be clarified

Interpolation of displacements and normal rotation in a bilinear element: Nodal degrees of freedom consist of lateral deflection w_i and rotations θ_{xi} and θ_{yi} of midsurface normals. The corresponding deflections and rotations within an element are obtained by independent shape functions interpolations:

$$w = \Sigma N_i w_i \qquad \theta_x = \Sigma N_i \theta_{xi} \qquad \theta_y = \Sigma N_i \theta_{yi} \tag{6.2.1}$$

If we introduce an unknown column in an element e, the above can be written in matrix form as

$$\mathbf{u}^e = \sum_{i=1}^{n} \mathbf{N}_i^e \mathbf{a}_i^e \tag{6.2.2}$$

in which the function $\mathbf{N}_i^e$ are used to interpolate both the nodal lateral displacement w and the normal rotation θ_x, θ_y of an n-noded element. The shape function $\mathbf{N}_i^e$ are expressed in terms of the natural (local) element co-ordinate system (ξ,η). $\mathbf{u}^e$ is the element displacement vector and $\mathbf{a}_i^e$ is the vector of variables for node i in the element e.

Interpolation of strains, B-matrix: The changes of curvature may be written as

$$\boldsymbol{\varepsilon}_b = \sum_{i=1}^{n} \mathbf{H}_{bi}^e \mathbf{a}_i^e \tag{6.2.3}$$

where $\mathbf{H}_{bi}^e$ is the curvature-displacement matrix associated with e, and the shear strains can be put as

$$\boldsymbol{\varepsilon}_s = \sum_{i=1}^{n} \mathbf{H}_{si}^e \mathbf{a}_i^e \tag{6.2.4}$$

where $\mathbf{H}_{si}^e$ is the shear-displacement matrix.

Stress-strain matrix D: Using the constitutive equations, we have

$$\mathbf{M}^e = -\mathbf{D}\boldsymbol{\varepsilon}_b^e = -\mathbf{D}\sum_{i=1}^{n} \mathbf{H}_{bi}^e \mathbf{a}_i^e = -\sum_{i=1}^{n} \mathbf{D}\mathbf{H}_{bi}^e \mathbf{a}_i^e = -\sum_{i=1}^{n} \mathbf{D}_{bi}^e \mathbf{a}_i^e \tag{6.2.5}$$

and

$$\mathbf{S}^e = \alpha Gh \sum_{i=1}^{n} \mathbf{H}_{si}^e \mathbf{a}_i^e = \sum_{i=1}^{n} \mathbf{D}_{si}^e \mathbf{a}_i^e \tag{6.2.6}$$

where $\mathbf{D}_{bi}^e = \mathbf{D}\mathbf{H}_{bi}^e$ is the moment-curvature matrix, and $\mathbf{D}_{si}^e = \alpha Gh \mathbf{H}_{si}^e$ is the shear force-shear strain matrix. Then stress-strain matrix $\mathbf{D}$ of the element is defined as

$$\sigma = \begin{Bmatrix} \mathbf{M}^e \\ \mathbf{S}^e \end{Bmatrix} = \sum \begin{bmatrix} \mathbf{D}_{bi}^e \\ \mathbf{D}_{si}^e \end{bmatrix} \mathbf{a}_i^e = \sum_{i=1}^{n} \mathbf{D}_i^e \mathbf{a}_i^e \tag{6.2.7}$$

Element stiffness matrix $\mathbf{K}^e$: Having the above relations of the element, we can derive stiffness matrix of the element from virtual work principle, neglecting point loads or couples, the contribution to the total potential energy from element e may be expressed as

$$\Pi^e = \sum_{i=1}^{n} \sum_{j=1}^{n} \frac{1}{2} \iint \left[\mathbf{a}_i^e\right]^T \left\{ \left[\mathbf{H}_{bi}^e\right]^T \mathbf{D} \mathbf{H}_{bj}^e + \alpha Gh \left[\mathbf{H}_{si}^e\right]^T \mathbf{H}_{sj}^e \right\} \mathbf{a}_j^e dxdy - \sum_{i=1}^{n} \iint \left[\mathbf{a}_i^e\right]^T \left[\mathbf{N}_i^e\right]^T \begin{bmatrix} q & 0 & 0 \end{bmatrix}^T dxdy$$

$$= \sum_{i=1}^{n} \sum_{j=1}^{n} \left[\mathbf{a}_i^e\right]^T \left\{ \mathbf{K}_{bij}^e + \mathbf{K}_{sij}^e \right\} \mathbf{a}_j^e - \sum_{i=1}^{n} \left[\mathbf{a}_i^e\right] \mathbf{f}_i^e \tag{6.2.8}$$

where $\mathbf{K}_{bij}^e$ and $\mathbf{K}_{sij}^e$ are the contributions to the submatrix of the element stiffness linking nodes i and j and respectively associated with the bending and shear strain energies. $\mathbf{f}^e$ is the element force vector. They are defined as

$$\mathbf{K}_{bij}^e = \frac{1}{2} \iint \left[\mathbf{H}_{bi}^e\right]^T \mathbf{D} \mathbf{H}_{bj}^e dxdy \tag{6.2.9a}$$

$$\mathbf{K}_{sij}^e = \frac{1}{2} \alpha Gt \iint \left[\mathbf{H}_{si}^e\right]^T \mathbf{H}_{sj}^e dxdy \tag{6.2.9b}$$

$$\mathbf{f}_i^e = \iint \left[\mathbf{N}_i^e\right]^T \begin{bmatrix} q & 0 & 0 \end{bmatrix}^T dxdy \tag{6.2.9c}$$

The transverse shear stiffness: This is computed by matching the shear response for the case of the plate bending about one axis, using a parabolic variation of transverse shear stress in each layer. The approach is outlined in Appendix A. For now we define the transverse shear stiffness of the section of a shear flexible element as

$$\bar{K}_{xy}^{ts} = \beta_p K_{xy}^{ts} \tag{6.2.10}$$

where

$\bar{K}_{xy}^{ts}$ are the components of the section shear stiffness (x, y = 1,2 refer to the default surface direction on the plate)

β_p is a dimensionless factor that is used to prevent the shear stiffness from becoming too large in thin plates and is defined as

$$\beta_p = 1/\left(1 + 0.25x10^{-4}\,\frac{A}{h^2}\right) \qquad (6.2.11)$$

where A is the area of the element and h is the thickness of the plate; and K_{xy}^{ts} is the actual shear stiffness of the section. In the present analysis, where we have a homogeneous plate made of a linear, orthotropic elastic material, and the strong material direction aligns with the element's local 1-direction, the transverse shear stiffness is given as

$$K_{11}^{ts} = \tfrac{5}{6}G_{13}h, \qquad K_{22}^{ts} = \tfrac{5}{6}G_{23}h, \qquad K_{12}^{ts} = 0.0.$$

G_{13} and G_{23} are the material's shear moduli in the out-of-plane direction. The number 5/6 is the shear correction coefficient that results from matching the transverse shear energy to that for a three-dimensional structure in pure bending. The present analysis uses the same value.

Bilinear isoparametric element: A bilinear element has an advantage that the node values are only needed to construct the element. Because of its simplicity, it is widely used in the finite element formulation. The isoparametric (local) co-ordinates (ξ, η) in a plane are shown in Fig.6.2.1. For a typical 4-noded element, the axes ξ and η pass through midpoints of opposite sides. Axes ξ and η need not be orthogonal, neither do they need to be parallel to the global x and y co-ordinate axis. The sides of the element are at $\xi = \pm 1$ and $\eta = \pm 1$. The global co-ordinate x and y within the element are defined by

$$x = \sum_{i=1}^{4} N_i x_i \quad \text{and} \quad y = \sum_{i=1}^{4} N_i y_i \qquad (6.2.12)$$

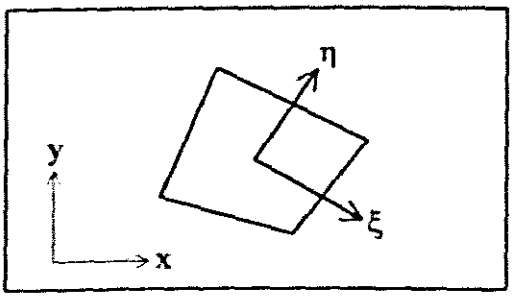

Figure 6.2.1 Isoparametric Bilinear Element

The shape function of a bilinear isoparametric element N_i and their derivatives are expanded in Appendix D. The Jacobean matrix of the bilinear isoparametric element is also given in the same Appendix.

Isoparametric representation of Mindlin plate: The contribution to the stiffness matrices and load vector of the Mindlin plate may be written as

$$\mathbf{K}_{bij}^{e} = \tfrac{1}{2}\int_{-1}^{+1}\int_{-1}^{+1}\left[\mathbf{H}_{bi}^{e}\right]^{T}\mathbf{D}\mathbf{H}_{bi}^{e}\,\det(J)\,d\xi d\eta$$

$$\mathbf{K}_{sij}^{e} = \tfrac{1}{2}\alpha G h \int_{-1}^{+1}\int_{-1}^{+1} \left[\mathbf{H}_{si}^{e}\right]^{T} \mathbf{H}_{sj}^{e} \det(J) d\xi d\eta$$

$$\mathbf{f}_{i}^{e} = \int_{-1}^{+1}\int_{-1}^{+1} \left[\mathbf{N}_{i}^{e}\right]^{T} \begin{bmatrix} q & 0 & 0 \end{bmatrix} \det(J) d\xi d\eta \qquad (6.2.13)$$

For an isoparametric element, the integration must be calculated in the local co-ordinate system. The element stiffness matrix is $\mathbf{K}_{ij}^{e} = \mathbf{K}_{bij}^{e} + \mathbf{K}_{sij}^{e}$.

6.3 Finite Element Formulation of Buckling

The problem is solved by dividing the region Ω of the plate into n-noded quadrilateral finite elements, each with five degrees-of-freedom per node. Using the same shape function associated with node i(i = 1, 2,... n), for interpolating the variation in each element, we can write

$$\mathbf{u}_{1}^{e} = \sum_{i=1}^{n} \mathbf{N}_{i}^{e} \mathbf{d}_{1}^{i(e)} \qquad (6.3.1)$$

where $\mathbf{N}_{i}^{e}$ are the interpolation functions and are used to interpolate the nodal in-plane displacements u_1 and v_1, and the lateral displacement w_1 as well as the normal rotation θ_{x1}, θ_{y1}. The shape function $\mathbf{N}_{i}^{e}$ are expressed in terms of the natural (local) element co-ordinate system (ξ, η). $\mathbf{u}_{1}^{e}$ is the element displacement vector and $\mathbf{d}_{1}^{i(e)}$ is the vector of variables for node i in the element e. We note that $\mathbf{d}_{1}^{i(e)}$ now contains the in-plane displacements u and v, i.e $\mathbf{d}_{1}^{i(e)} = \{u_1, v_1, w_1, \theta_{x1}, \theta_{y1}\}$.

Interpolation of strains, H-matrix: The normal strains are given by

$$\varepsilon_{1t}^{e} = \sum_{i=1}^{n} \mathbf{H}_{ti}^{e} \mathbf{d}_{1}^{i(e)} \qquad (6.3.2)$$

The change of curvature may be written as

$$\varepsilon_{1b}^{e} = \sum_{i=1}^{n} \mathbf{H}_{bi}^{e} \mathbf{d}_{1}^{i(e)} \qquad (6.3.3)$$

where $\mathbf{H}_{bi}^{e}$ is the curvature-displacement matrix associated with element e.
The shear strains can be written as

$$\varepsilon_{1s}^{e} = \sum_{i=1}^{n} \mathbf{H}_{si}^{e} \mathbf{d}_{1}^{i(e)} \qquad (6.3.4)$$

where $\mathbf{H}_{si}^{e}$ is the shear-displacement matrix. $\mathbf{H}$ is called the strain-displacement matrix.

Stress matrix σ: There are no temperature terms in the second variation of the total potential energy. The bending stress and the shear stress of a laminated composite are defined as

$$\sigma^e = \sum_{i=1}^{n} \left(\mathbf{A}\mathbf{H}_{ti}^e + \mathbf{B}\mathbf{H}_{bi}^e \right) \mathbf{d}_1^{i(e)} \tag{6.3.5}$$

and

$$\tau^e = \sum_{i=1}^{n} \bar{\mathbf{A}}\mathbf{H}_{si}^e \mathbf{d}_1^{i(e)} \tag{6.3.6}$$

where $\mathbf{A}$, $\mathbf{B}$ and $\bar{\mathbf{A}}$ are material property matrices of the laminated composite.

Stress-strain matrix: Using the constitutive equations, we have

$$\{N_1\}^e = \left[[A][H_{ti}^e] + [B][H_{bi}^e] \right] \{d_1^i\}^e$$

$$\{M_1\}^e = \left[[B][H_{ti}^e] + [D][H_{bi}^e] \right] \{d_1^i\}^e$$

$$\{Q_1\}^e = \left[[\bar{A}][H_{si}^e] \right] \{d_1^i\}^e \tag{6.3.7}$$

6.4 Buckling Equations of a Laminated Composite Plate

Substitution of Equation (6.3.7) into the second variation of the total potential energy (Equation 5.13) gives;

$$\begin{aligned}
\delta\left(\delta^{(2)}\Pi\right)^e = -\sum_{i=1}^{n} \iint \{ & \left([A][H_{ti,x}^e] + [B][H_{bi,x}^e] + [A][H_{ti,y}^e] + [B][H_{bi,y}^e] \right) \{d_1^i\}^e \delta u_1 \\
& + \left([A][H_{ti,y}^e] + [B][H_{bi,y}^e] + [A][H_{ti,x}^e] + [B][H_{bi,x}^e] \right) \{d_1^i\}^e \delta v_1 \\
& + \left([B][H_{ti,x}^e] + [D][H_{bi,x}^e] + [B][H_{ti,y}^e] + [D][H_{bi,y}^e] - [\bar{A}][H_{si}^e] \right) \{d_1^i\}^e \delta\theta_{x1} \\
& + \left([B][H_{ti,y}^e] + [D][H_{bi,y}^e] + [B][H_{ti,x}^e] + [D][H_{bi,x}^e] - [\bar{A}][H_{si}^e] \right) \{d_1^i\}^e \delta\theta_{y1} \\
& + \left([B][H_{ti,xx}^e] + [D][H_{bi,xx}^e] + 2\left([B][H_{ti,xy}^e] + [D][H_{bi,xy}^e] \right) \right. \\
& \left. + [B][H_{ti,yy}^e] + [D][H_{bi,yy}^e] \right) \{d_1^i\}^e \delta w_1 \\
& + \left(N_{x0}[N_{i,xx}^e] + 2N_{xy0}[N_{i,xy}^e] + N_{y0}[N_{i,yy}^e] \right. \\
& \left. + \left(N_{x0,x} + N_{xy0,y} \right)[N_{i,x}^e] + \left(N_{y0,x} + N_{xy0,x} \right)[N_{i,y}^e] \right) \{d_1^i\}^e \delta w_1 \} dxdy
\end{aligned}$$

$$= \left([K_1]^e \delta u_1 + [K_2]^e \delta v_1 + [K_3]^e \delta\theta_{x1} + [K_4]^e \delta\theta_{y1} + [K_5]^e \delta w_1 + [K_6]^e \delta w_1 \right) \{d_1^i\}^e \tag{6.4.2}$$

where $[K_i]^e$ ($i = 1,\ldots5$) are defined in Appendix D

For arbitrary δu_1, δv_1, δw_1, $\delta\theta_{x1}$, $\delta\theta_{y1}$, and making $\delta\left(\delta^{(2)}\Pi\right) = 0$, we have

$$\left([\mathbf{K}]^e + [\mathbf{K}_\sigma]^e\right)\{\mathbf{d}_1^i\}^e = \mathbf{0} \tag{6.4.3}$$

where

$$[\mathbf{K}]^e = [\mathbf{K}_1]^e + [\mathbf{K}_2]^e + [\mathbf{K}_3]^e + [\mathbf{K}_4]^e + [\mathbf{K}_5]^e$$

Substituting into the total potential energy leads to the formulation of the structural stiffness matrix $[\mathbf{K}]$ and the geometric stiffness matrix $[\mathbf{K}_\sigma]$ for the entire domain, such that

$$\left([\mathbf{K}] + [\mathbf{K}_\sigma]\right)\{\mathbf{u}\} = \{\mathbf{0}\} \tag{6.4.4}$$

where $\{\mathbf{u}\}$ is still the vector of nodal displacement as discussed above.

A level of stress $[\mathbf{K}_\sigma]$ is sought such that a solution $\{\mathbf{u}\}$ other than $\{\mathbf{u}\} = \mathbf{0}$ is possible. The use of this stiffness matrix implies that prebuckling rotations are either ignored or are zero, and is referred to as the classical buckling analysis. A reference level of loading is first applied to the structure and a standard linear static analysis is carried out to obtain membrane stresses in the elements. We refer to this loading as $\{\mathbf{u}\}_{ref}$ and the stress stiffness matrix generated as $[\mathbf{K}_\sigma]_{ref}$. Using λ as a scalar multiplier for the next load level, that is

$$[\mathbf{K}_\sigma] = \lambda[\mathbf{K}_\sigma]_{ref}$$

leads to the load vector being

$$\{\mathbf{R}\} = \lambda\{\mathbf{R}\}_{ref}$$

This implies that multiplying all loads by λ also multiplies the intensity of the stress field by λ but does not change the distribution of stresses. Since the external loads do not change during an infinitesimal buckling displacement, an eigenvalue problem, whose lowest eigenvalue λ_{cr} is associated with the buckling, is defined. Thus

$$\left([\mathbf{K}] + \lambda_{cr}[\mathbf{K}_\sigma]_{ref}\right)\{\mathbf{u}\} = \{\mathbf{0}\} \tag{6.4.5}$$

and the critical or buckling load is

$$\{\mathbf{R}\}_{cr} = \lambda_{ref}\{\mathbf{R}\}_{ref} \tag{6.4.6}$$

The eigenvector $\{\mathbf{u}\}$ associated with λ_{cr} defines the buckling mode. The combination of numerical/mechanical aspects is essential for the accurate prediction of the non-linear structural behaviour of composites (where instead of secant stiffness matrix, we use tangent stiffness matrix) in the prebuckling, buckling and postbuckling regime.

Chapter 7

Computer Simulation and Numerical Results

7.1 Introduction

The study is performed using a 4 x 4, 9-noded doubly curved thin shell element, with reduced integration and five degrees of freedom per node (S9R5). However, to account for the transverse shear deformation, the transverse shear stiffness (as discussed in the previous chapter and in Appendix A) of 5/6 is introduced in the ABAQUS input file.

7.1.1 Isotropic Square Plate

In order to establish a benchmark or the integrity of the present analysis, the critical buckling temperatures of a simply supported square isotropic plate subjected to a uniform temperature increase are compared with those of Chandrashekhara [9] in Table 7.1. The dimensions are

a = b = 10mm and thickness t = 0.1mm

with the following boundary conditions

- Simply supported edges

  $x = 0,a$ $\qquad u_0 = w_0 = \theta_y = 0$

  $y = 0,b$ $\qquad v_0 = w_0 = \theta_x = 0$

- Clamped edges

  $x = 0,a$ $\qquad u_0 = v_0 = w_0 = \theta_x = \theta_y = 0$

  $y = 0,b$ $\qquad u_0 = v_0 = w_0 = \theta_x = \theta_y = 0$

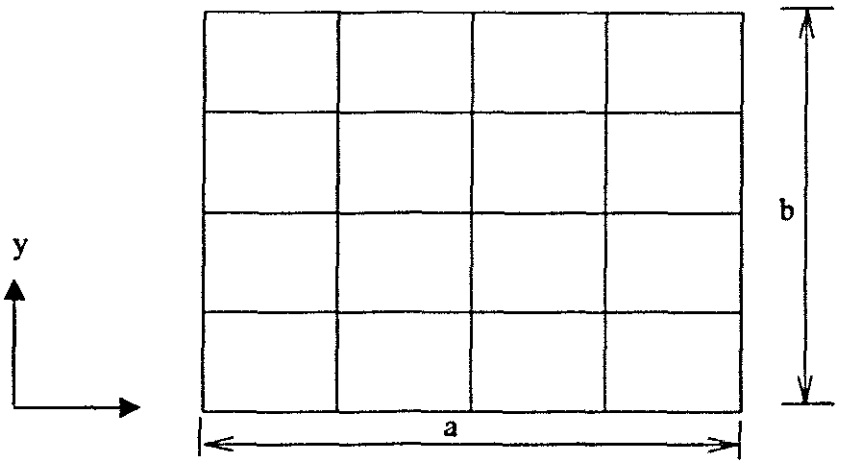

Figure 7.1.1 Square plate buckling study

The following nondimensional buckling temperatures were obtained in the ABAQUS computer simulations.

E = 1.0 GPa, ν = 0.3, a/t = 100, a = b = 10, α = 1.0 x 10^{-6}/°C

a/b	$\alpha T_{cr} \times 10^{-3}$	
	Present	Chandrashekhara [9]
0.25	0.6730	0.6727
0.50	0.7916	0.7913
0.75	0.9892	0.989
1.00	1.2659	1.2657
1.25	1.6214	1.6234
1.50	2.0558	2.0561
1.75	2.5691	2.5696
2.00	3.1607	3.1617
2.25	3.8311	3.8324
2.50	4.5798	4.5817
2.75	5.4068	5.4096
3.00	6.3118	6.3144

Table 7.1 Comparison of nondimensional critical buckling temperature for a simply supported isotropic thin plate

The results of the present analysis and reference [9] are in excellent agreement. Figure 7.2 on page 54 shows a deformed rectangular plate under uniform temperature distribution.

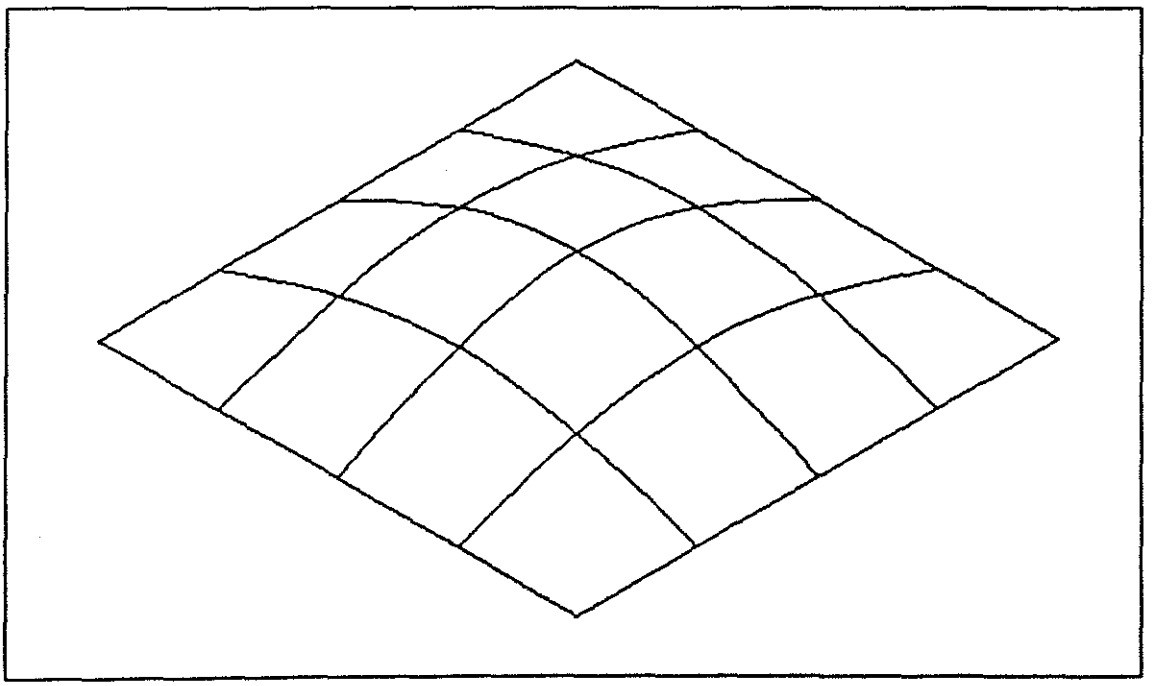

Table 7.1.2 Buckling mode of a typical rectangular isotropic plate

The next step is to change the properties of the isotropic plate to the one of a laminated composite according to the discussions from Chapters 1 to 6, and this is done throughout the remainder of this chapter.

7.2 Laminated Square Plate

The first block in the ABAQUS input data defines the mesh, that is, the nodes and their co-ordinates, and the elements (in this case the S9R5 element as defined in ABAQUS). The nodes and the elements are generated automatically by the *NGEN and *ELGEN (see the copy of an Input File in APPENDIX E). They are also grouped into sets using *NSET and ELSET respectively. The properties associated with the shell elements used in this COMPOSITE analysis are:

- the thickness of the plate
- the number of integration points
- the material, in this case the lamina and
- the orientation of each layer

These are repeated as often as is necessary to vary the number of layers being used. The LAMINA type elastic option is used to define the linear elastic moduli, and these are given in the input file and Table 7.2.

The thermal expansion coefficients of the composite are defined with *EXPANSION option and are also tabled in Table 7.2. A rectangular system of orientation is used to specify a local axis system and this concept is explained further in the ABAQUS User' Manual [1]. The *STEP option begin the analysis and is followed by *BUCKLE which controls the eigenvalue buckling estimation. In this estimation three eigenvalues are extracted, although in some instances the number of eigenvalues is increased to increase the number of iterations. Finally the boundary conditions are applied as described in Chapter 7.1.

In the analysis of a laminated, orthotropic, composite plate, each layer has the same material properties. The effects of the various parameters are studied and the graphs are used to show the trends as these parameters are changed. Two sets of graphs are shown for each type of analysis, one for simply supported edges and another for clamped edges. Unless otherwise stated, each lamina has the following material properties;

ν_{12}	α_{11}	α_{12}	K_{11}	K_{22}	E_{11}	E_{22}	G_{12}	G_{13}	G_{23}
0.28	0.02	22.5	2.987	2.587	181.0	10.30	7.17	7.17	6.21

Table 7.2 Material properties of a composite

where the 1-direction is along the fibres, the 2-direction is transverse to the fibres in the surface of the lamina, and the 3-direction is normal to the lamina, Figure 7.2 (a). E_{11}, E_{22}, G_{12}, G_{13} and G_{23} are in 10^9 Pascals and α_{11} and α_{12} are in 10^{-6} per degrees Celsius. Figure 7.2 (b) shows the dimensions and co-ordinates of a typically stacked laminate.

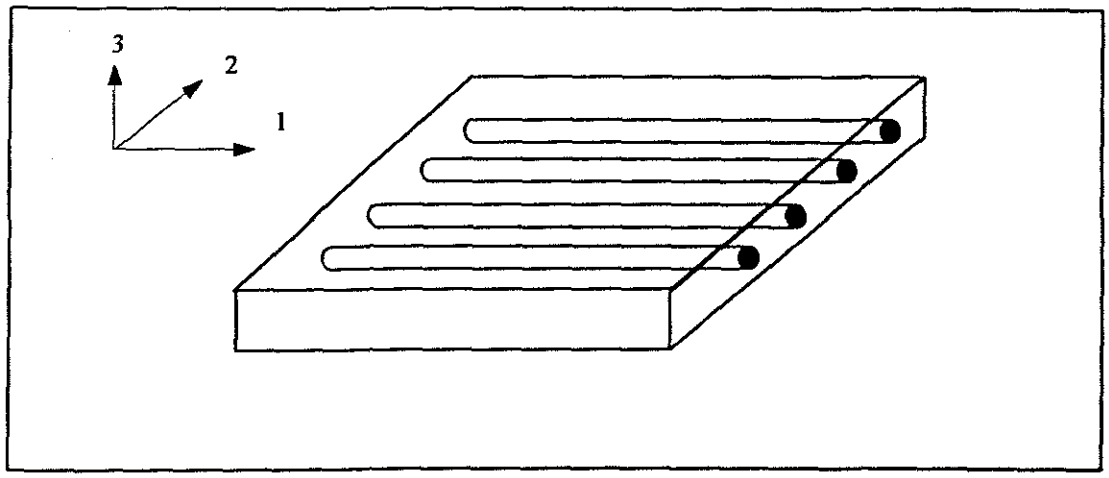

Figure 7.2(a) A typical lamina

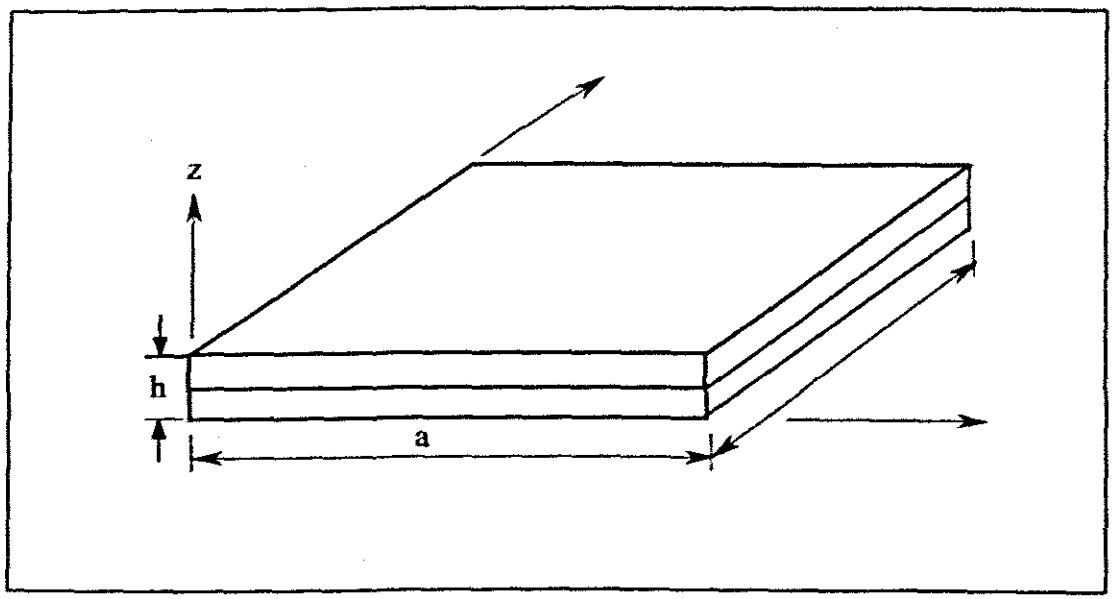

Figure 7.2(b) Geometry of a typical two-layered laminated square plate

7.2.1 Effect of ply orientation

Figure 7.2.1.1 shows the critical buckling temperature T_{cr} versus lamination angle ψ for a simply supported and clamped plate. The variation in lamination angle ψ may result in large changes of T_{cr} as shown by the figure. Also the critical buckling temperature for a given thickness of laminated plates increases as the number of layers, N, increases. The maximum value of T_{cr} occurs at $\psi = 45^0$ for clamped N = 4 and N = 8 plates. However, the reverse phenomenon is observed in two-layer laminates. This is because bending-stretching coupling stiffness reach their maximum values at stacking layers N=2 and decrease rapidly as N increases.

Clamped

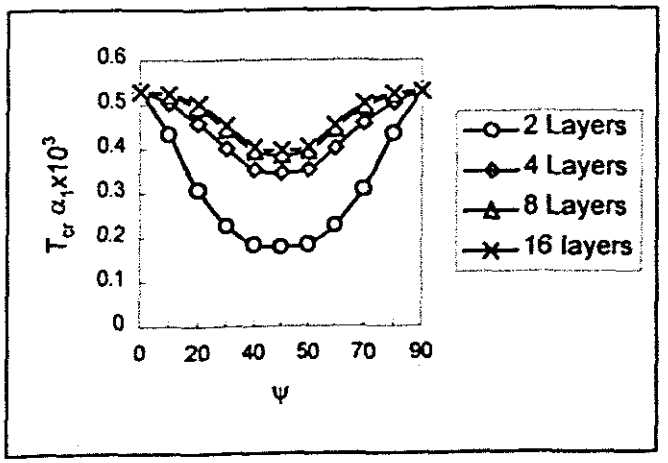

ψ	2 Layers	4 layers	8 Layers	16 Layers
0	0.5290	0.5290	0.5290	0.5290
10	0.4354	0.5037	0.5200	0.5241
20	0.3082	0.4580	0.4932	0.5019
30	0.2265	0.4015	0.4432	0.4525
40	0.1843	0.3534	0.3941	0.4041
45	0.1786	0.3457	0.3859	0.3958
50	0.1843	0.3534	0.3941	0.4041
60	0.2265	0.4015	0.4432	0.4535
70	0.3082	0.4580	0.4932	0.5019
80	0.4354	0.5037	0.5200	0.5241
90	0.5290	0.5290	0.5290	0.5290

Simply Supported

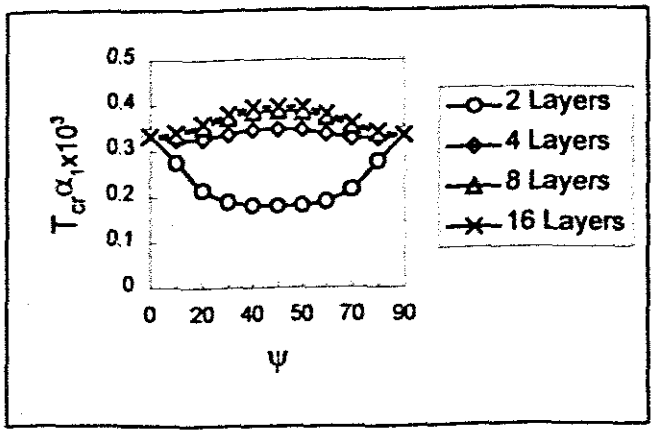

ψ	2 Layers	4 Layers	8 Layers	16 Layers
0	0.3332	0.3332	0.3332	0.3332
10	0.2754	0.3252	0.3373	0.3404
20	0.2149	0.3259	0.3525	0.3591
30	0.1886	0.3362	0.3716	0.3804
40	0.1796	0.3446	0.3843	0.3941
45	0.1787	0.3458	0.3860	0.3960
50	0.1796	0.3446	0.3843	0.3941
60	0.1886	0.3362	0.3716	0.3804
70	0.2149	0.3259	0.3525	0.3591
80	0.2754	0.3252	0.3373	0.3404
90	0.3332	0.3332	0.3332	0.3332

Figure 7.2.1.1 Effect of ply orientation on the critical buckling temperature of laminates ($a/t = 20$, $a/b = 1$)

Figure 7.2.1.2 gives a summary of the buckling modes predictions for N = 2. We note that the eigenvalue of the first buckling mode or (eigenmode) is smaller than the eigenvalue of the second buckling mode, and so on. These buckling modes are the same for N = 4, N = 8 and N = 16.

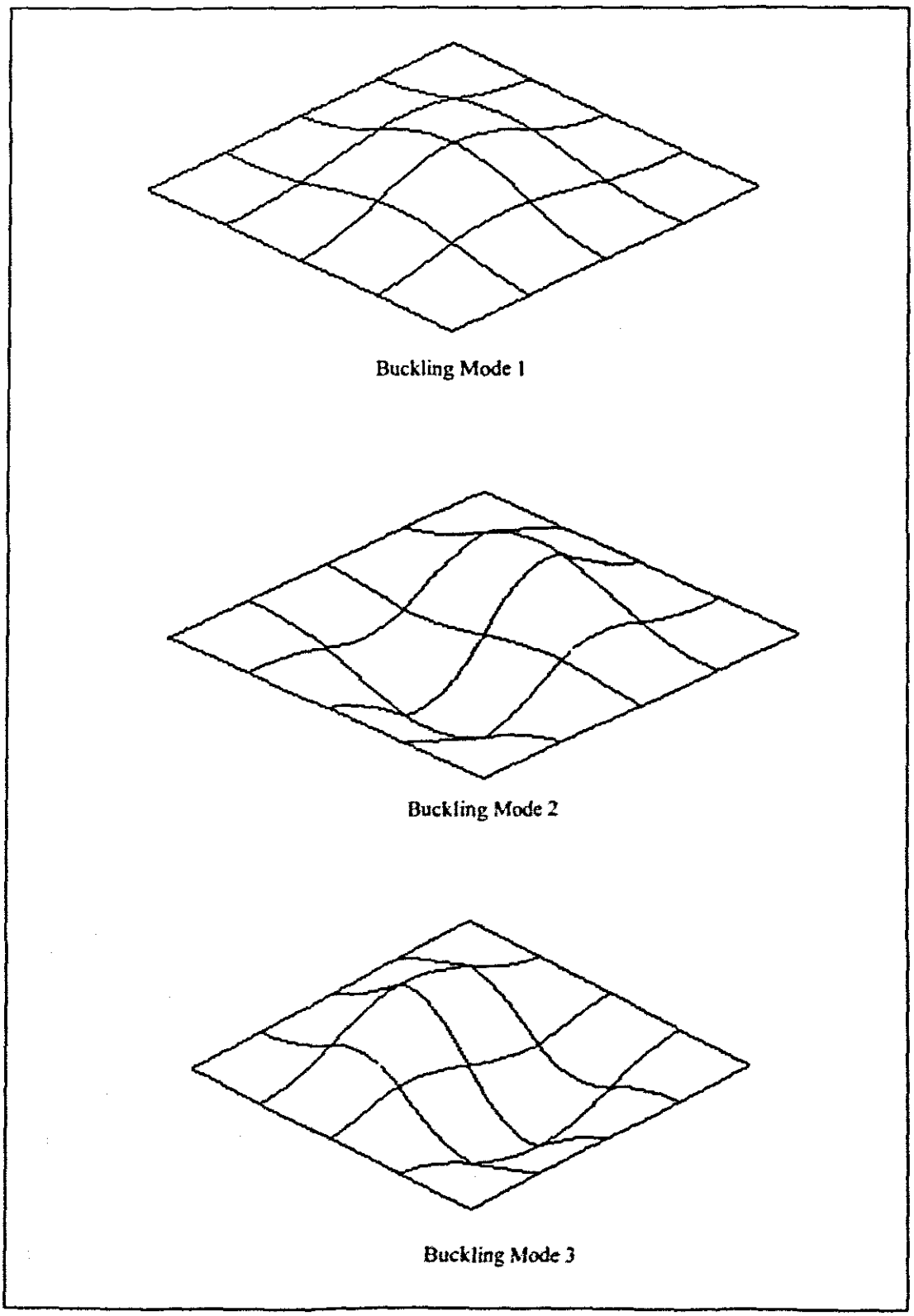

Figure 7.2.1.2 Buckling modes of a laminated square plate

7.2.2 Effect of plate thickness ratio

Figures 7.2.2 depicts the effects of plate thickness ratio a/t on the critical buckling temperature for a square laminated plates having lamination angle $\psi = 45^0$. It is shown that the thermal buckling loads decrease with an increase in laminate thickness. This is in agreement with Ref. [33]. It is evident that the rigidity and hence the critical temperature decreases rapidly as the plate thickness ratio increases. This is because the stiffness of the laminate is greatly reduces when it becomes relatively thin. The effect of the number of stacking layers N on T_{cr} is insignificant when a/t is large.

Clamped

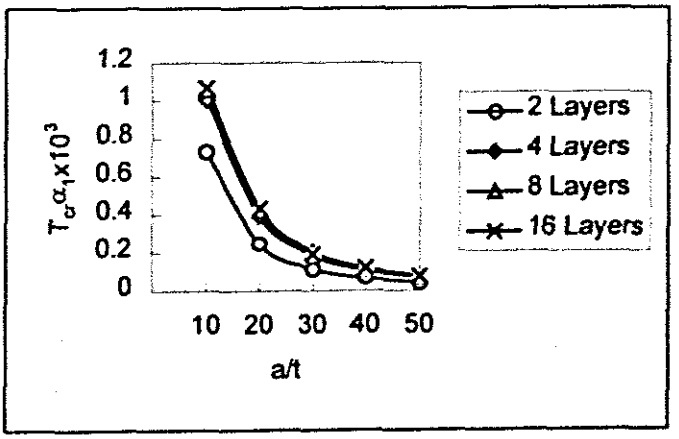

a / t	2 Layers	4 Layers	8 Layers	16 Layers
10	0.7317	1.002	1.0541	1.0663
20	0.2428	0.3888	0.4234	0.4320
30	0.1121	0.1841	0.2018	0.1891
40	0.0636	0.1053	0.1156	0.1182
50	0.0409	0.0678	0.0745	0.0761

Simply Supported

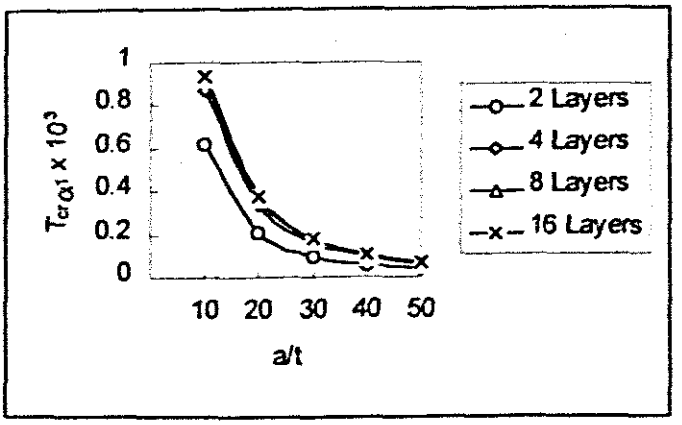

a / t	2 Layers	4 Layers	8 Layers	16 Layers
10	0.6161	0.8698	0.9208	0.9330
20	0.2079	0.3358	0.3665	0.3741
30	0.0961	0.1583	0.1736	0.1775
40	0.0546	0.0904	0.0993	0.1015
50	0.0351	0.0582	0.0633	0.0623

Figure 7.2.2 Effect of plate thickness on the critical buckling temperature of laminates (a/b = 1, $\psi = 45^0$)

7.2.3 Effect of aspect ratio a / b

The effect of aspect ratio a/b on the critical temperature is illustrated in Figure 7.2.3.1. It can be seen that T_{cr} goes up as the plate aspect ratio increases. Since geometry has a significant influence on in-plane loaded structures, it is expected that the buckling load of a laminate will be greatly influenced by the change in the plate geometry. However, for a thermally loaded laminate, the graph shows that at a/b ≥ 1.2 the critical buckling temperature increases proportionally with the increase in the aspect ratio. There is no change of the buckling mode shape with the variation of aspect ratio, since the curves go up smoothly without any cusp, more especially for a/b > 1.8.

Clamped

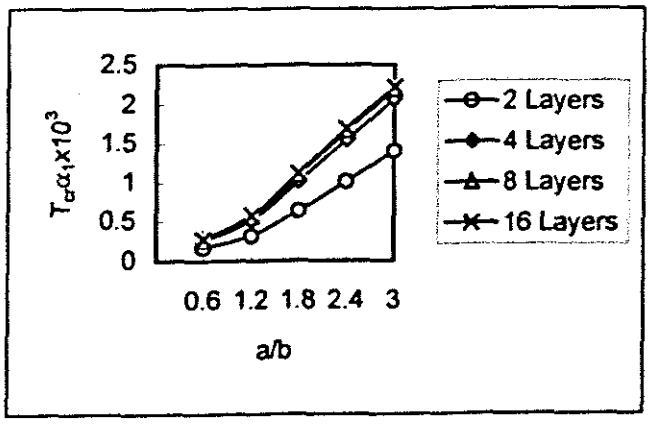

a/b	2 Layers	4 Layers	8 Layers	16 Layers
0.6	0.1676	0.2518	0.2718	0.2767
1.2	0.3187	0.5162	0.5626	0.5740
1.8	0.6327	1.0088	1.0928	1.1132
2.4	1.0082	1.5472	1.6603	1.6875
3	1.3979	2.0573	2.1867	2.2172

Simply Supported

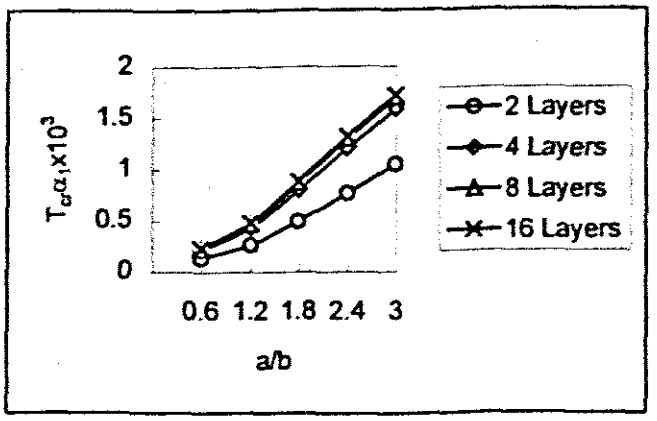

a/b	2 Layers	4 Layers	8 Layers	16 Layers
0.6	0.1376	0.2110	0.2287	0.2331
1.2	0.2657	0.4334	0.4733	0.4832
1.8	0.4951	0.8002	0.8696	0.8866
2.4	0.7676	1.2028	1.2967	1.3194
3	1.0478	1.5846	1.6935	1.7194

Figure 7.2.3.1 Effect of aspect ratio on the critical buckling temperature of laminates ($a / t = 20$, $\psi = 45^0$)

The buckling mode shapes for different aspect ratios are shown in Figure 7.2.3.2 below.

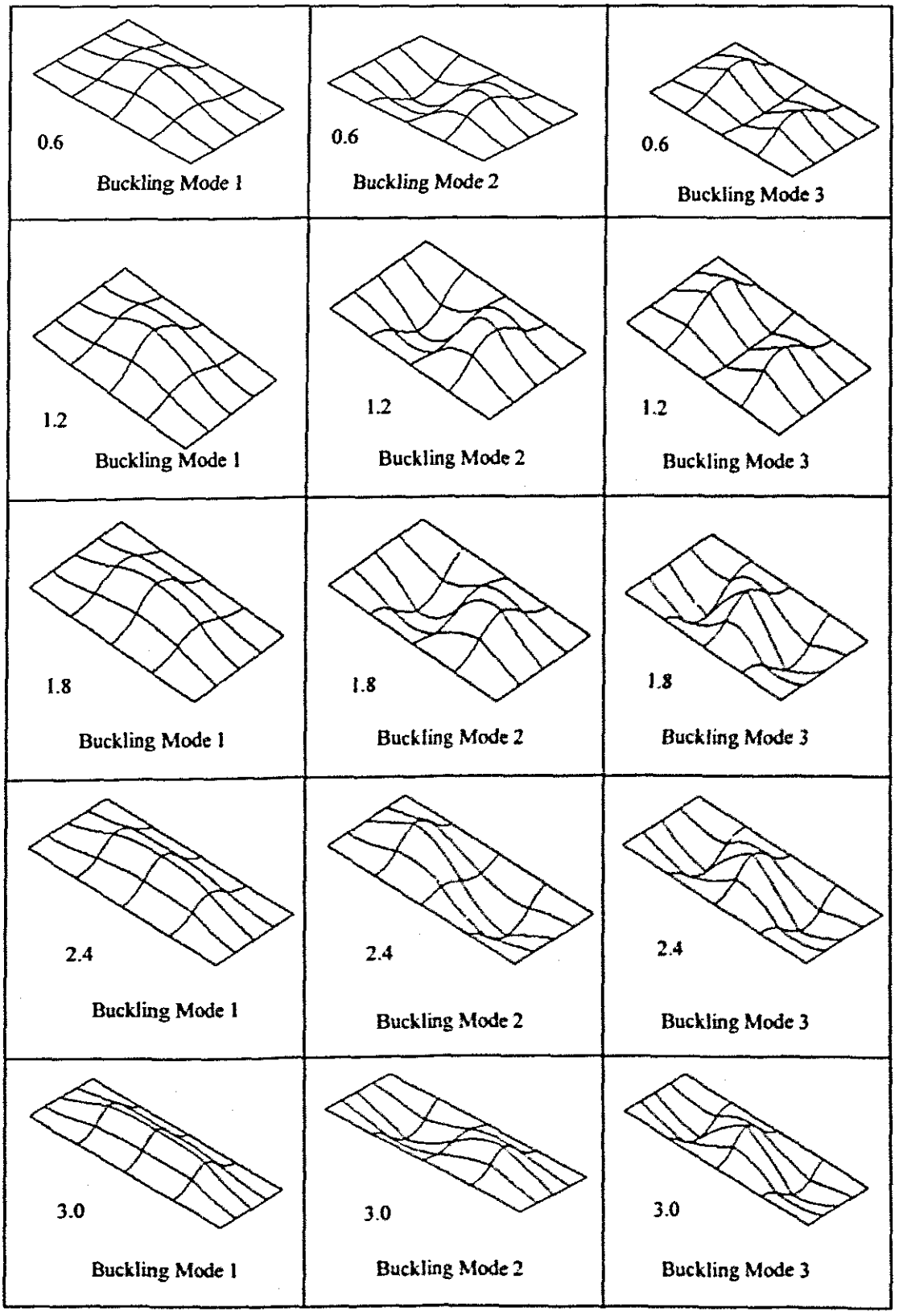

Figure 7.2.3.2 Buckling mode shapes for each of the aspect ratios

7.2.4 The effect of the modulus ratio E_1 / E_2

Figure 7.2.4 shows the influence of the modulus ratio E_1/ E_2 on critical buckling temperature. It is observed that in a simply supported plate of N = 4, N= 8 and N = 16, T_{cr} increases with increase of modulus ratio and plotted curves are rather flat when $E_1 / E_2 \geq 10$. The increase in the number of layers means the increase in the material substance and hence the rigidity of a laminate. The interaction of the various stiffnesses means greater ability of the laminate to withstand buckling loads. For simply supported edges, Figure 7.2.4 shows that the boundaries have less influence on the modulus ratio of a laminate. The graph of N = 2 for the simply supported and clamped plates shows that the plate is more susceptible to buckling as a result of the change in E_1 / E_2.

Clamped

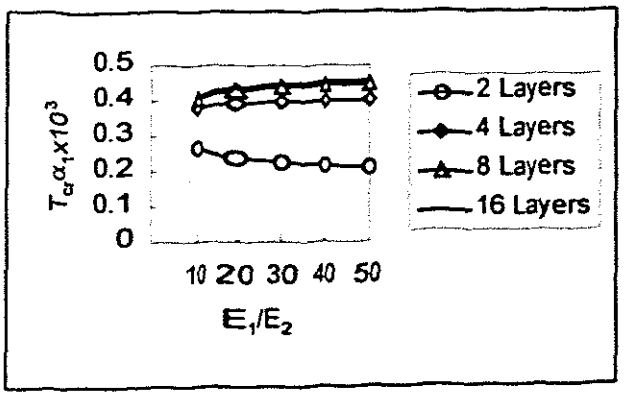

E1/E2	2 Layers	4 Layers	8 Layers	16 Layers
10	0.2656	0.3788	0.4057	0.4123
20	0.2380	0.3907	0.4270	0.4359
30	0.2245	0.3960	0.4366	0.4467
40	0.2163	0.399	0.4422	0.4529
50	0.2107	0.4009	0.4459	0.4570

Simply Supported

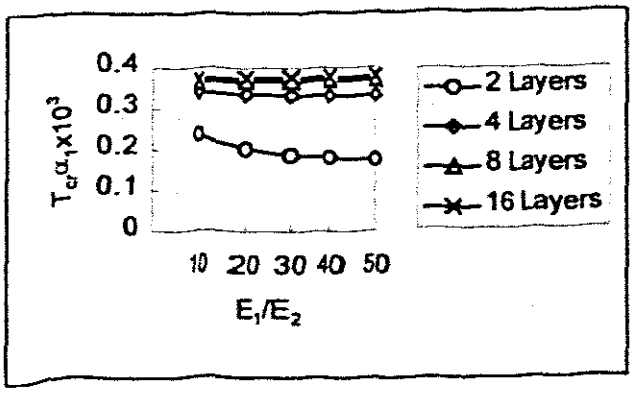

E_1/E_2	2 Layers	4 Layers	8 Layers	16 Layers
10	0.2371	0.3395	0.3640	0.3701
20	0.2022	0.3349	0.3668	0.3747
30	0.1870	0.3326	0.3676	0.3762
40	0.1784	0.3312	0.3679	0.3770
50	0.1728	0.3303	0.3681	0.3775

Figure 7.24 Effect of the modulus ratio on the critical buckling temperature of laminates ($a / b = 1, a / t = 20, \psi = 45^0$)

7.2.5 The effect of thermal expansion coefficient ratio α_2/α_1

The effect of thermal expansion coefficient ratio α_2 / α_1 on the critical temperature is shown in Figure 7.2.5. The higher the ratio of thermal expansion coefficients, the higher the value of T_{cr}. This means that the thermal coefficient of expansion has a linear relationship with the buckling temperature of a laminate. It is pointed out that in the present analysis α_1 was varied while α_2 was left constant. An increase in the coefficient of expansion means that more temperature has to be applied to cause buckling on a laminated composite. The interaction of the different coefficients of the different materials in a laminate has a tendency to increase the temperature needed to cause buckling. We note that in Ref. [11] the opposite trend is observed for T_{cr} versus as α_1 is varied. The expansion coefficients of a laminated composite have a direct influence on the buckling temperature as expected from the strain equations of Chapter 3.

Clamped

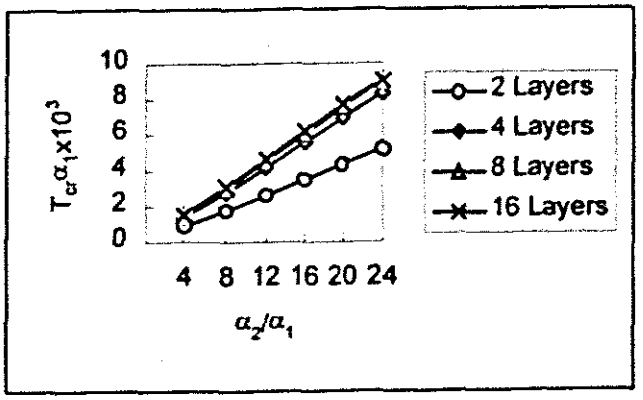

α_2/α_1	2 Layers	4 Layers	8 Layers	16 Layers
4	0.8633	1.3825	1.5057	1.5362
8	1.7266	2.7651	3.0115	3.0723
12	2.59	4.1476	4.5172	4.6085
16	3.4533	5.5301	6.023	6.1446
20	4.3166	6.9127	7.5287	7.6808
24	5.1799	8.2952	9.0344	9.0217

Simply Supported

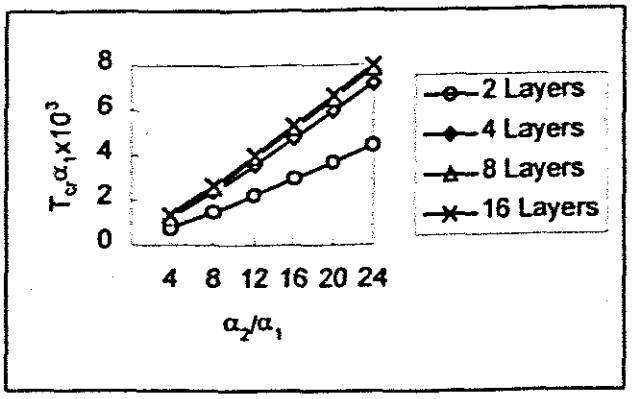

α_2/α_1	2 Layers	4 Layers	8 Layers	16 Layers
4	0.7394	1.194	1.3032	1.3302
8	1.4789	2.3879	2.6063	2.6604
12	2.2183	3.5819	3.9095	3.9907
16	2.9577	4.7758	5.2127	5.3209
20	3.6971	5.9698	6.5159	6.6511
24	4.4366	7.1637	7.819	7.9813

Figure 7.2.5 Effect of thermal expansion ratio on the critical buckling temperature of laminates ($a / b = 1$, $a / t = 20$, $\psi = 45^0$)

7.2.6 The effect of boundary conditions

Figure 7.2.6 shows the effect of boundary condition on the variation of critical temperature. The boundary condition has a strong impact on the critical temperature T_{cr}, as shown in the figure. Also, the variation of T_{cr} for different aspect ratios is presented in Figure 7.2.6 for both simply supported and clamped plates with N = 4 in order to compare the effect of the boundary condition. It can be seen that the critical temperatures of clamped cases are higher than those of the simply supported cases. This is because of the enhanced stiffness of the laminate by the clamping of the laminate. The simply supported edges make the plate susceptible to buckling, as the edges are not restricted from expanding. The effect of the aspect ratio was discussed in Section 7.6.3.

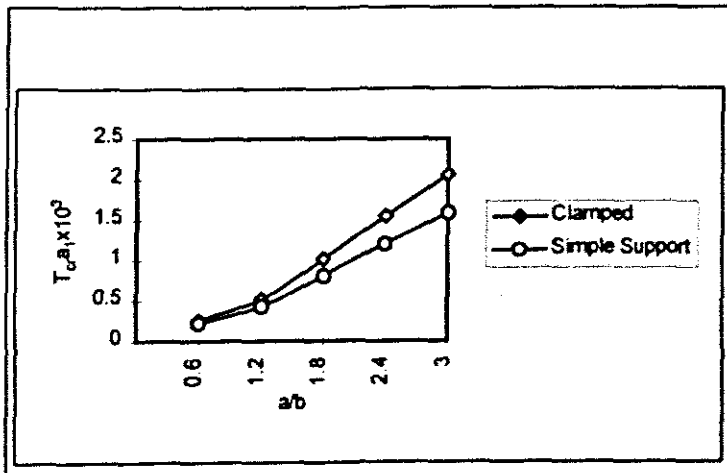

a/b	Clamped	Simply Supported
0.6	0.2518	0.2110
1.2	0.5162	0.4334
1.8	1.0088	0.8002
2.4	1.5472	1.2028
3	2.0573	1.5848

Figure 7.2.6 Influence of boundary condition and aspect ratio on the critical buckling temperature of laminates (a/t =20, N = 4, $\psi = 45^0$)

It has been seen that of all the variables that were used to study the behaviour of a laminated plate, the number of layers affects the buckling temperature the most. For two layers, the bending-stretching coupling is at the maximum and as the number of layers increases, the laminate approaches orthotropy and the critical buckling temperature decreases.

7.3. Plate with a square hole

The same analyses are performed as in the previous section but with a rectangular hole as shown in Figure 7.3. The outside dimensions are 10mm by 10mm and the square hole is 5mm by 5mm. The values in this section are *not* to be compared with the results in the previous section. This is because of the difference in the number of elements, and the fact that the present plate was constructed with a different type of element; the 8-noded shell element with 5 degrees of freedom and reduced integration (S8R5). The aim here is to study the general behaviour of a laminate with a rectangular hole.

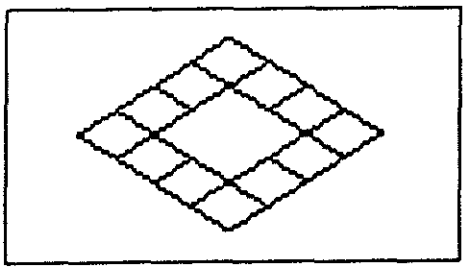

Figure 7.3 Plate with a square hole

7.3.1 Effect of ply orientation

Similar trends are observed as in Section 7.2 where the critical buckling temperature increases with the increase in the number of layers N, with the clamped edges having a higher value.

Clamped

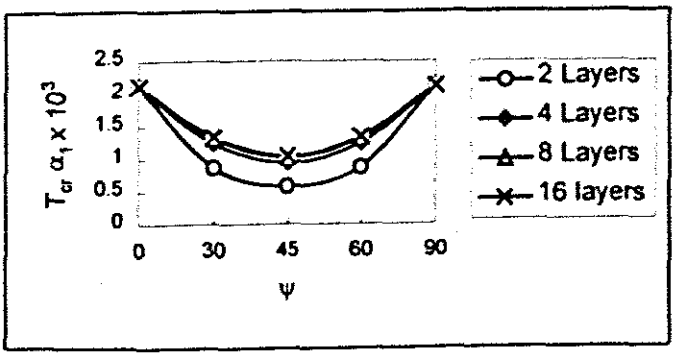

ψ	2 Layers	4 Layers	8 Layers	16 Layers
0	2.1112	2.1112	2.1111	2.1112
30	0.8699	1.2437	1.3213	1.3398
45	0.5802	0.9454	1.0239	1.0428
60	0.8699	1.2437	1.3213	1.3398
90	2.1112	2.1112	2.1112	2.1111

Simply supported

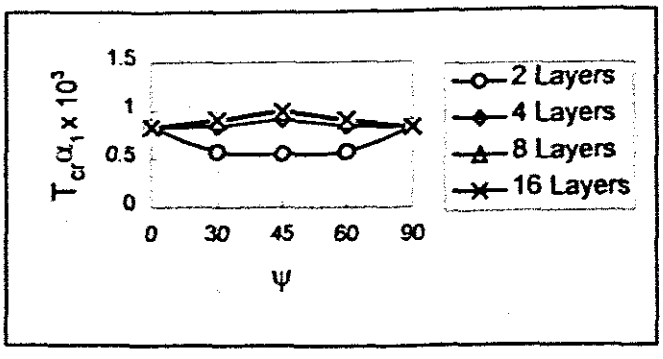

ψ	2 Layers	4 Layers	8 Layers	16 Layers
0	0.8275	0.8275	0.8275	0.8275
30	0.5754	0.8386	0.8919	0.9046
45	0.5536	0.9032	0.9774	0.9953
60	0.5754	0.8386	0.8919	0.9046
90	0.8275	0.8275	0.8275	0.8275

Figure 7.3.1.1 Effect of ply orientation on the critical buckling temperature of laminates (a/t = 20, a/b = 1)

Figure 7.3.1.2 shows the first three buckling modes of a 2-layered laminate with a stacking sequence of $0^0/0^0$. Of significance in this diagram is the deformation of the inner edges where there is stress concentration at the corners.

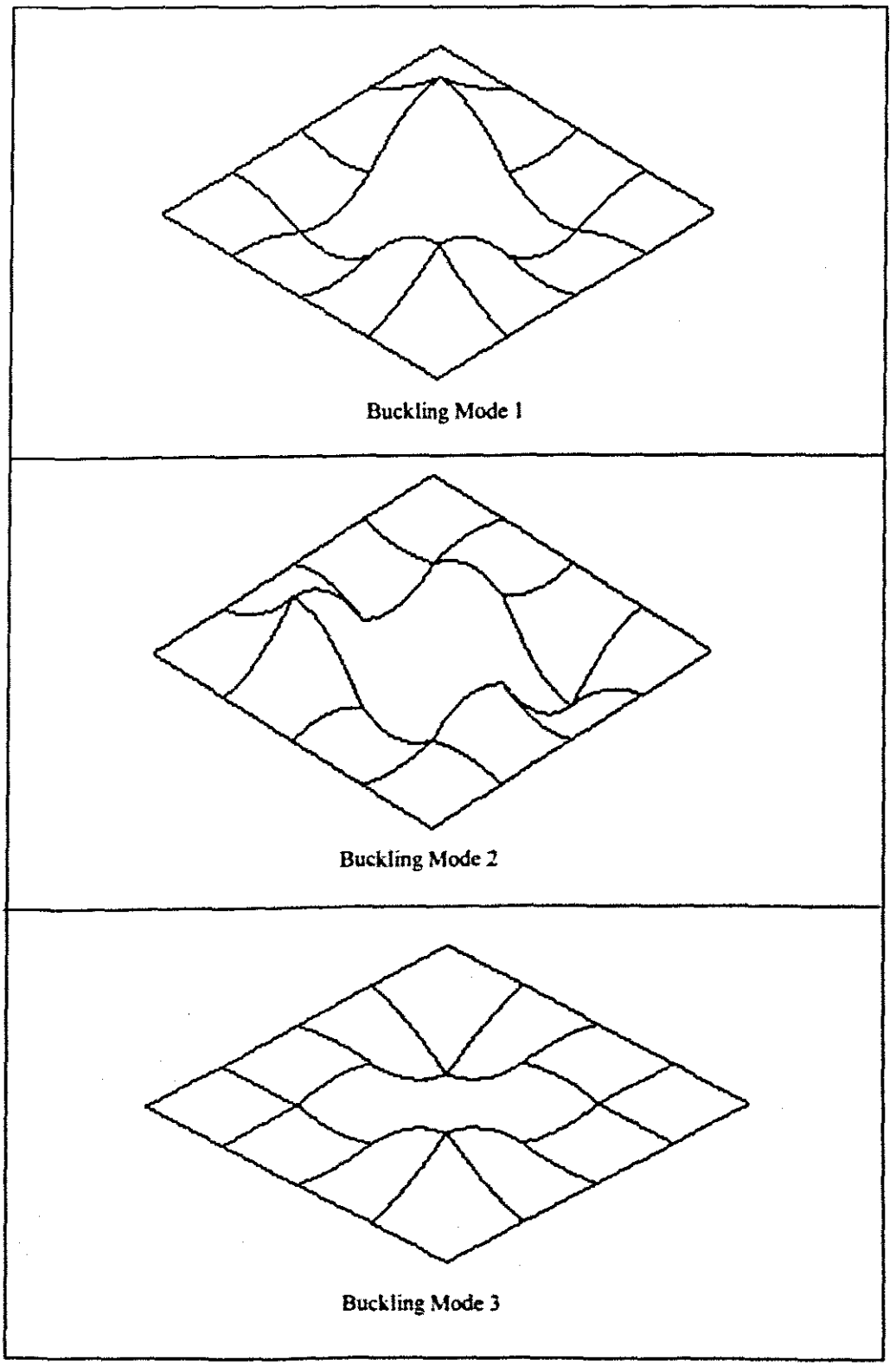

Figure 7.3.1.2 Buckling mode predictions for a laminated plate with a square hole

7.3.2 *Effects of plate thickness ratio*

For a simply supported plate, the critical buckling temperature is lower for N = 2 and it increases as the number of layer increases. The trend for N=2 is slightly different from N = 4, 8 and 16. There is not much difference as the number of layers is increased from 2. This shows that for a given lamination thickness, the increase in the number of plies has little effect on the critical buckling loads in a laminate with a rectangular cut-out. For a clamped plate, the graphs show a similar pattern for any given number of plies. This is because the edges in a clamped laminate are always kept together and the interaction of the various material properties is prevented from acting independently.

Clamped

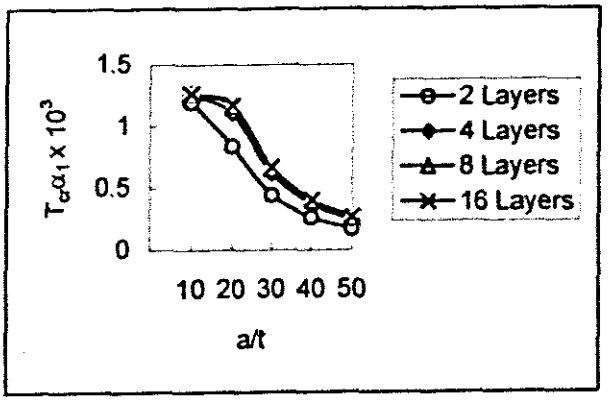

a/t	2 Layers	4 Layers	8 Layers	16 Layers
10	1.1948	1.2567	1.2627	1.2639
20	0.8350	1.1007	1.1563	1.1695
30	0.4405	0.6143	0.6540	0.6638
40	0.2602	0.3687	0.3942	0.4005
50	0.1696	0.2418	0.2589	0.2632

Simply Supported

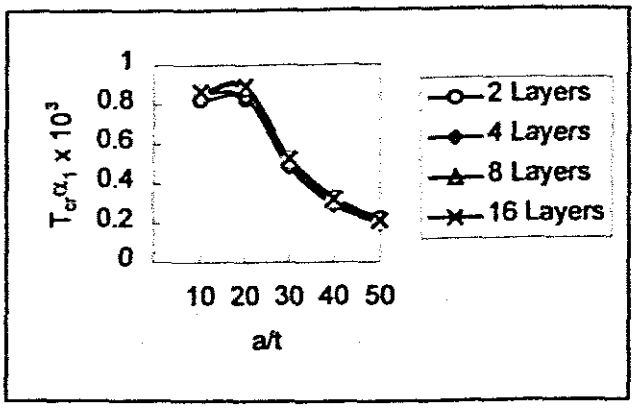

a/t	2 Layers	4 Layers	8 Layers	16 Layers
10	0.8197	0.8581	0.8638	0.865
20	0.8275	0.8343	0.8800	0.891
30	0.523	0.4819	0.5167	0.5253
40	0.3266	0.2911	0.3135	0.3190
50	0.2174	0.1913	0.2063	0.2100

Figure 7.3.2 Effects of plate thickness ratio on the critical buckling temperature of laminates ($a/b = 1$, $\psi = 45^0$)

7.3.3 The effect of the modulus ratio E_1 / E_2

When N = 2, the effects are quite significant and T_{cr} decreases as the modulus ratio increases. For more layers, the effect is not so significant and the graphs tend to flatten out as the modulus ratio is increased. This situation was observed in a normal laminate of Section 7.2.4 and a similar explanation can be given as in Section 7.2.4

Clamped

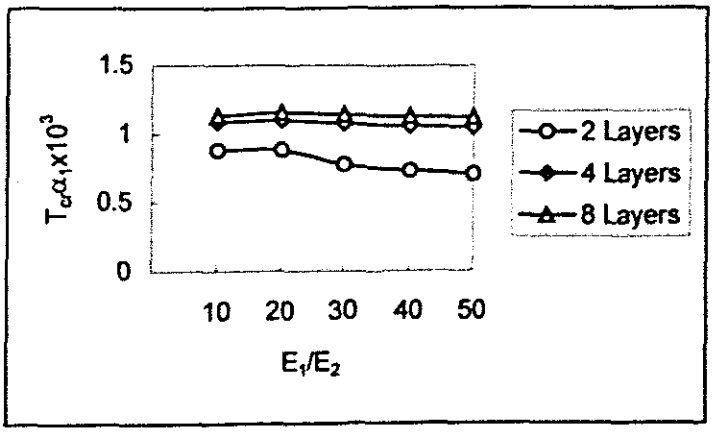

E_1/E_2	2 Layers	4 Layers	8 Layers
10	0.8810	1.0862	1.1303
20	0.8823	1.0975	1.1538
30	0.7758	1.0755	1.1386
40	0.7378	1.0612	1.1291
50	0.7103	1.0517	1.123

Simply Supported

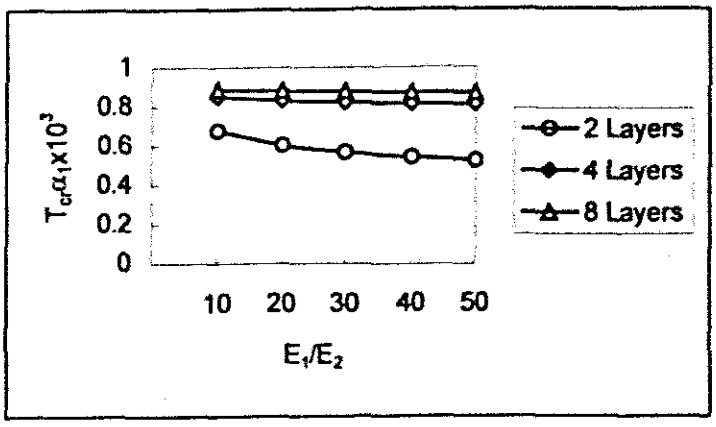

E1/E2	2 Layers	4 Layers	8 Layers
10	0.6765	0.8491	0.8852
20	0.6023	0.8311	0.8788
30	0.5650	0.8219	0.8753
40	0.542	0.8162	0.8730
50	0.5261	0.8125	0.8716

Figure 7.3.3 Effect of the modulus ratio on the critical buckling temperature of laminates ($a / t = 20, \psi = 45^0$)

The increase in the number of layers does not change the overall behaviour of the laminates with a rectangular hole, both with simply supported and clamped edges.

7.3.4 The effect of thermal expansion coefficient ratio α_2/α_1

Figure 7.3.4 depicts a situation where the critical buckling temperature increases with the increase in the expansion coefficient ratio. A similar situation was seen for a plate in Section 7.2.5. This means that the influence of the expansion coefficient is independent of the shape of the laminated, but rather this thermal coefficient influences the critical buckling temperature of the laminate linearly.

Clamped

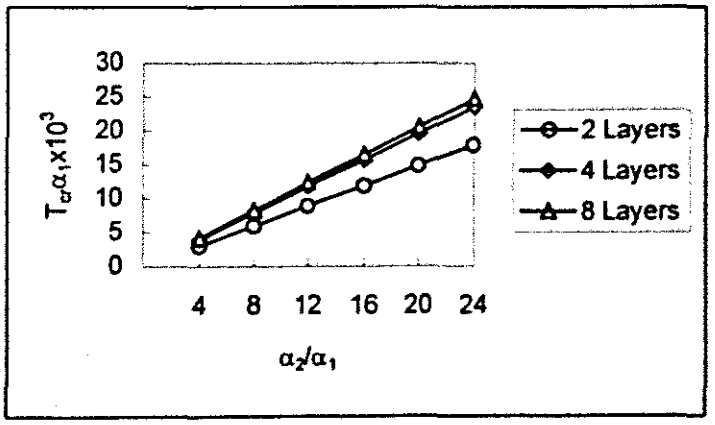

α_2/α_1	2 Layers	4 Layers	8 Layers
4	2.9689	3.9137	4.1112
8	5.9379	7.8274	8.2224
12	8.9068	11.741	12.334
16	11.876	15.655	16.445
20	14.845	19.568	20.556
24	17.845	23.482	24.667

Simply Supported

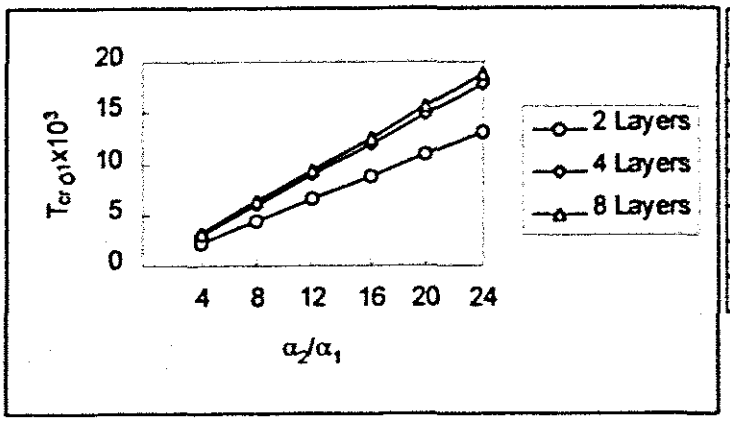

α_2/α_1	2 Layers	4 Layers	8 Layers
4	2.1878	2.9666	3.1291
8	4.3756	5.9333	6.2582
12	6.5634	8.8999	9.3872
16	8.7512	11.867	12.516
20	10.939	14.833	15.645
24	13.127	17.8	18.774

Figure 7.3.4 The effect of thermal expansion coefficient ratio on the critical buckling temperature of laminates ($a/b = 1$, $a/t = 20$, $\psi = 45^0$)

As this section was meant to study the overall behaviour of a laminated plate with a rectangular cut-out, it can be concluded that the laminate thickness plays a significant role in the buckling behaviour of structures as observed in Figure 7.3.2. The other variables, that is, the lamination angle, the modulus ratio and the coefficient of thermal expansion, do not alter the general behaviour of laminates under thermal loading.

7.4 Plate with a circular hole

Figure 7.4 shows a plate with a 4mm-diameter hole. It is meshed with the S9R5 element as the other plate in section 7.2. t is the plate thickness and the boundary conditions are applied on the outer edges while the hole has free supports. The plate dimensions are such that a = b = 20mm and the hole has a diameter of 4mm. Similar analyses are performed as in the previous sections, and once again the results in this section are *independent* of the two previous sections. This analysis is intended to observe the general behaviour of a laminated plate with a central cut-out.

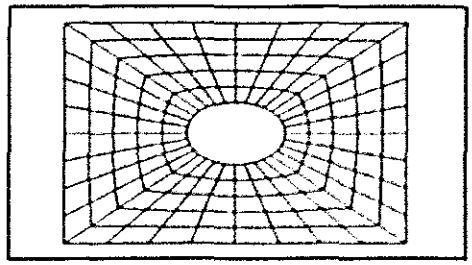

Figure 7.4 Plate with a circular hole

7.4.1 Effects of ply orientation

Figure 7.4.1.1 shows that for a simply supported plate, the minimum value occurs at $\psi = 45^0$, and for a clamped plate the maximum occurs at the same orientation angle. The buckling temperature is seen to increases as the number of layers increases. The same behaviour was observed in the two previous sections.

Clamped

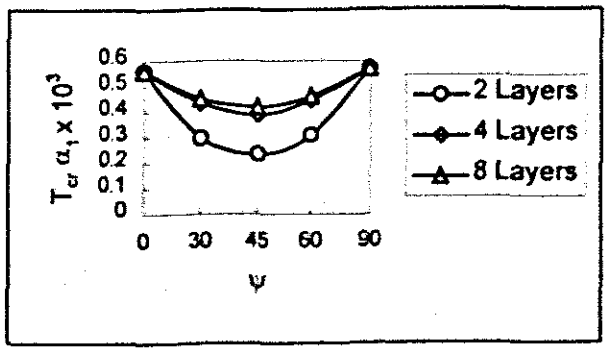

ψ	2 Layers	4 Layers	8 Layers
0	0.5582	0.5582	0.5582
30	0.2998	0.4343	0.4519
45	0.2339	0.3887	0.4172
60	0.3076	0.4457	0.4611
90	0.5694	0.5694	0.5694

Simply Supported

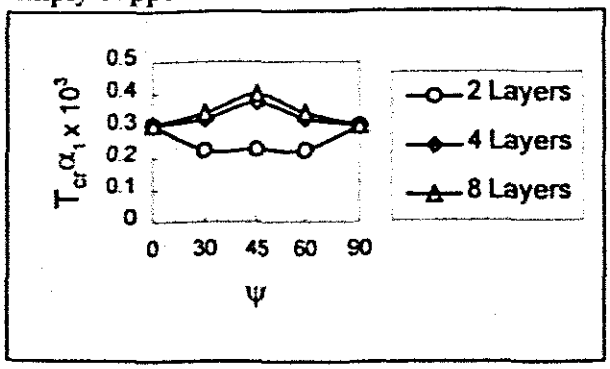

ψ	2 Layers	4 Layers	8 Layers
0	0.3029	0.3029	0.3029
30	0.2233	0.3221	0.3393
45	0.2267	0.3731	0.3987
60	0.2233	0.3221	0.3393
90	0.3029	0.3029	0.3029

Figure 7.4.1.1 Effect of ply orientation on the critical buckling temperature of laminates (e.g. $30^0/-30^0\ldots$)(a/t = 20, a/b = 1)

Figure 7.4.1.2 shows the different buckling mode shapes for an initially flat 2-layered simply supported square plate with a central cut-out. The different lamination angles are also shown and the shapes were tilted to show the side profiles.

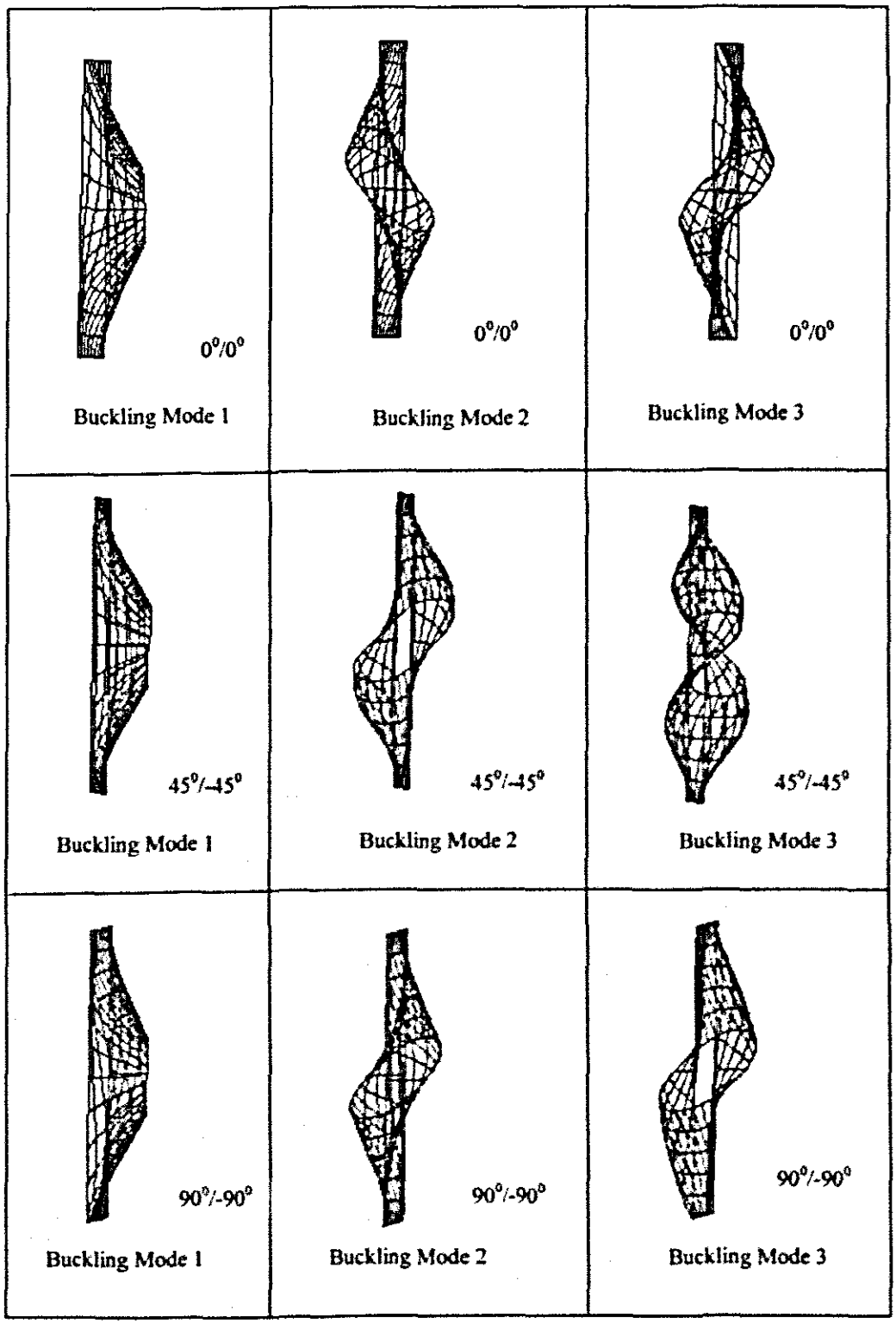

Figure 7.4.1.2 Buckling mode predictions for a laminated plate with a circular hole

Figure 7.3.1.2 shows the different buckling modes for a laminated plate with a square hole and clamped boundary conditions. The effects of the boundary conditions are evident from the deformed meshes.

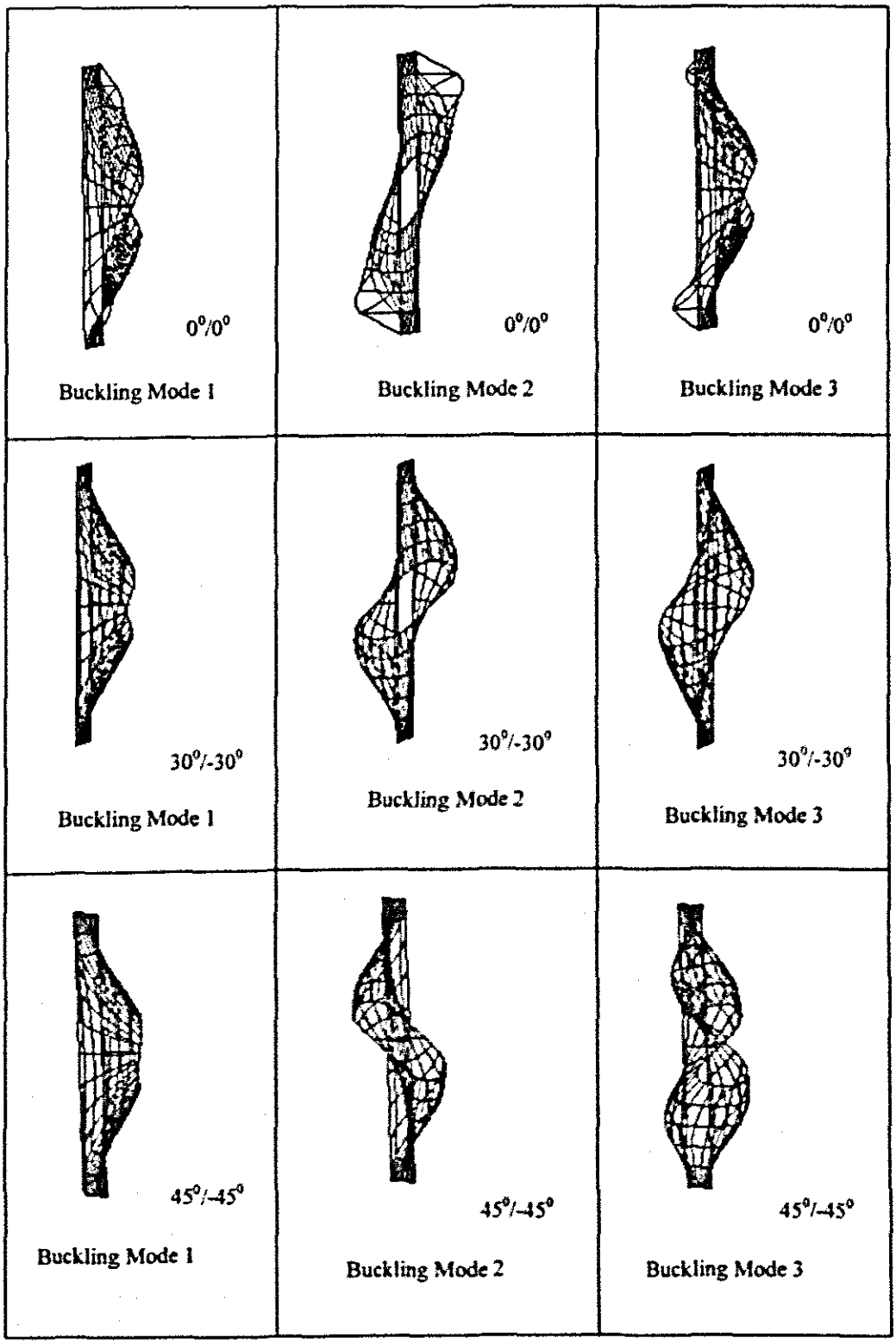

Figure 7.3.1.2 Buckling mode predictions for a laminated plate with a circular hole

7.4.2 Effects of plate thickness ratio

Figure 7.4.2 shows the effects of plate thickness ratio on the critical buckling temperature of laminates for both the simply supported and clamped edges. In both instances, the maximum buckling load occurs at about a/t = 20 and then the graph decreases rapidly until a/t = 30, from where it decreases gradually. From the tables next to the graphs, it is seen that the difference between the simply supported and the clamped boundary conditions for a given number of layers is small.

Clamped

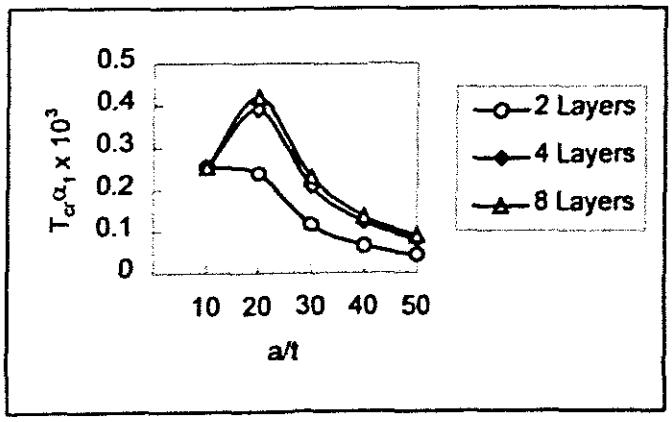

a / t	2 Layers	4 Layers	8 Layers
10	0.2509	0.2510	0.2514
20	0.2339	0.3887	0.4172
30	0.1130	0.2052	0.2269
40	0.0648	0.1204	0.1339
50	0.0417	0.0783	0.0872

Simply Supported

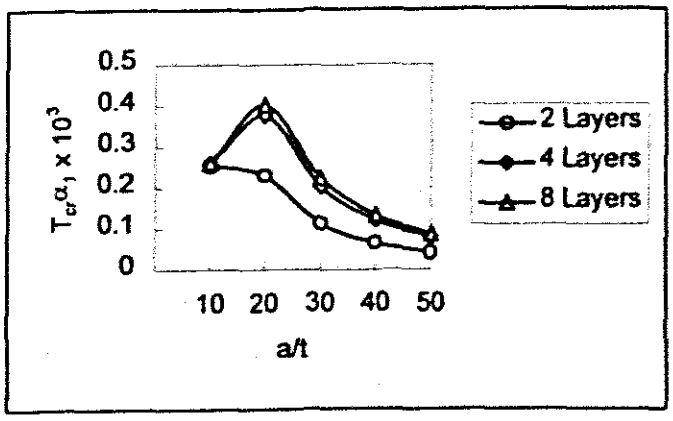

a / t	2 Layers	4 Layers	8 Layers
10	0.2514	0.2565	0.2571
20	0.2267	0.3731	0.3987
30	0.1097	0.1995	0.2207
40	0.0629	0.1169	0.1301
50	0.0405	0.0760	0.0847

Figure 7.4.2 Effects of plate thickness ratio on the critical buckling temperature of laminates ($a/b = 1, \psi = 45^0$)

At $10 > a/t < 20$ the laminate is relatively thick and can support a certain amount of buckling load. When the thickness of the plate is reduced, so does the ability of the plate to withstand load, and thus the critical buckling temperature decreases. This is explained by the fact that when the thickness of the plate is reduced, the coupling effect of the individual laminae is reduced and laminate stiffness is increased, rapidly between a/t = 20 and a/t = 30, and steadily thereafter.

7.4.3 Effect of aspect ratio

From Figure 7.4.3.1 the critical buckling temperature is a maximum at a/b = 1.2 and it decreases rabidly at a/b > 1.2. For a/b ≥ 1.8 the behaviour is the same for N = 2, N = 4 and N = 8 in both the simply supported and the clamped edges. Also the values are nearly similar. The critical buckling temperature decreases very rapidly after a/b =1.8 and this is because of the significant influence of the geometry on the ability of the structure to withstand buckling loads. This point will be explained further in Section 7.6 when the effect of geometry on the critical buckling temperature of a laminate is investigated. For now we concentrate on the *overall* performance of the laminate with a hole as compared to the overall performance of a 'normal" laminate.

Clamped

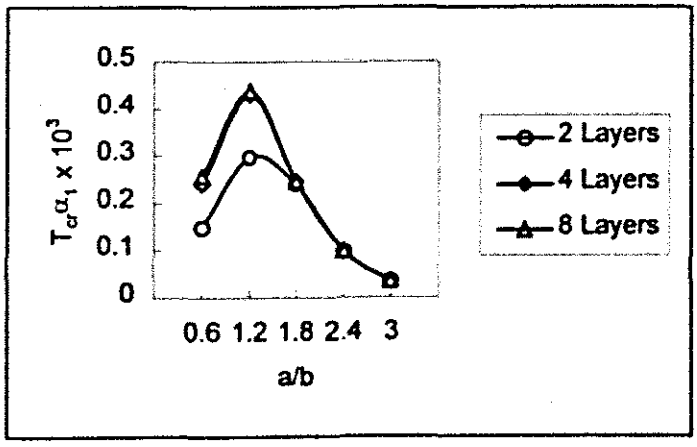

a/b	2 Layers	4 Layers	8 Layers
0.6	0.1478	0.2402	0.2572
1.2	0.2973	0.429	0.4355
1.8	0.2394	0.2454	0.2462
2.4	0.0991	0.1008	0.1011
3	0.0367	0.0370	0.0371

Simply Supported

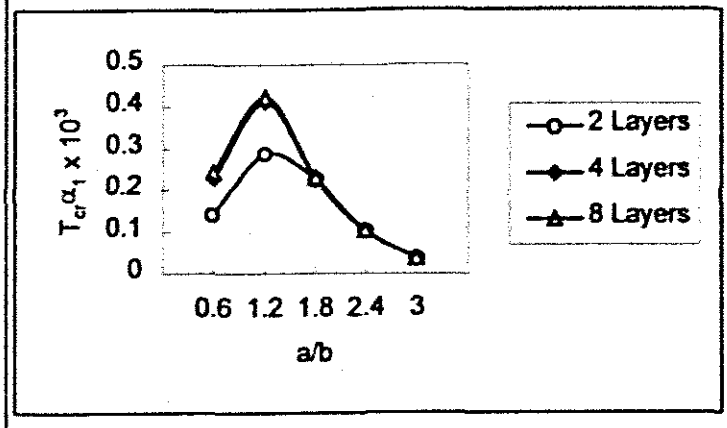

a/b	2 Layers	4 Layers	8 Layers
0.6	0.1409	0.2281	0.2435
1.2	0.2850	0.4099	0.4219
1.8	0.2252	0.2289	0.2294
2.4	0.1020	0.1026	0.1026
3	0.0375	0.0377	0.0377

Figure 7.4.3.1 Effect of aspect ratio on the critical buckling temperature of laminates ($a/t = 20$, $\psi = 45^0$)

At present we conclude that a central cut-out alters the general behaviour of a plate significantly from that of a "normal" plate

Figure 7.4.3.2 and Figure 7.4.3.3 show the different buckling modes for the different aspect ratios of 2-layered laminated composite plate with a circular hole at the centre. We observe that the edges of a simply supported plate are less affected, although a different behaviour would be expected from the clamped edges, where the deformation is fully restricted.

Simply supported

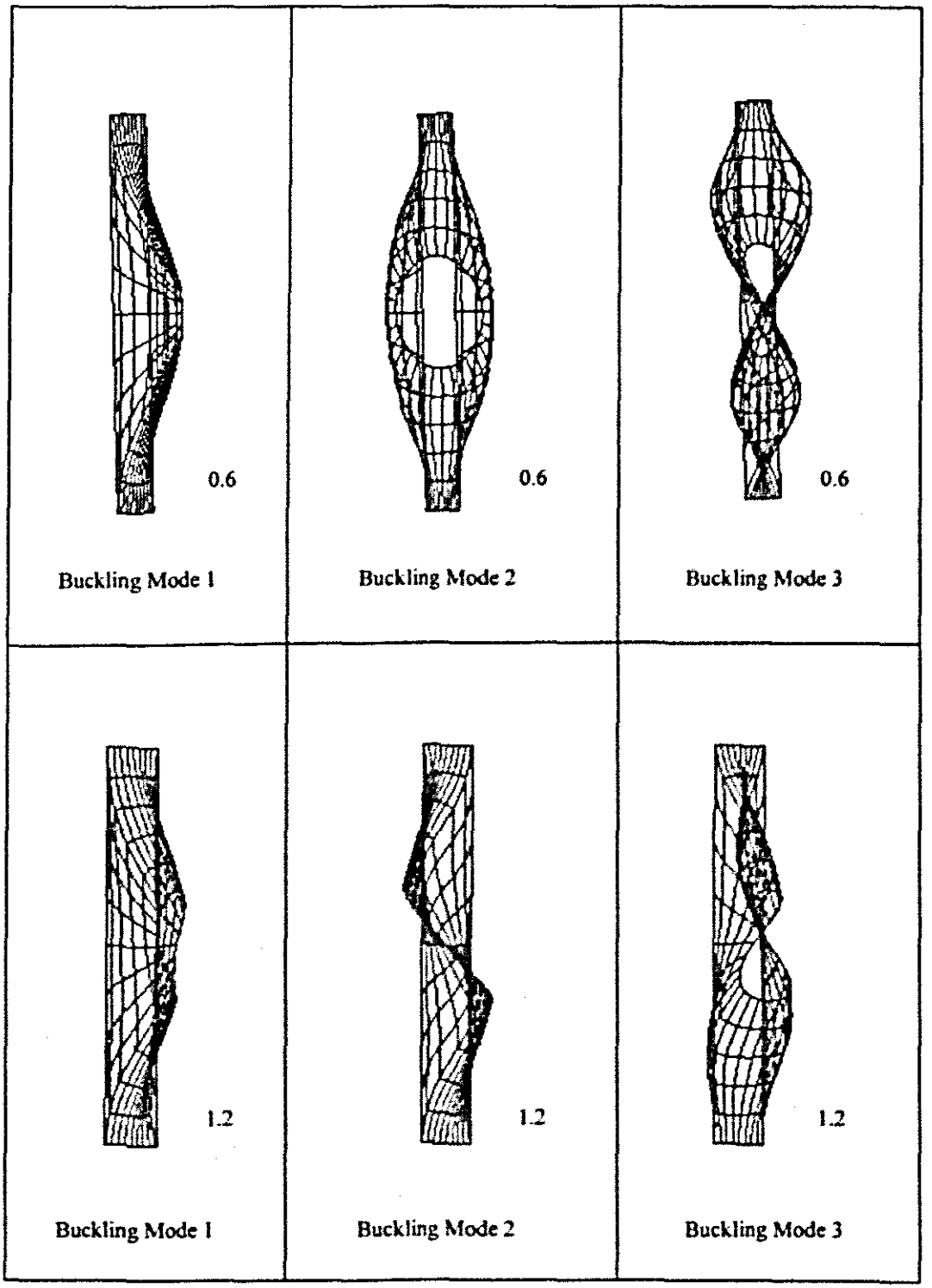

Figure 7.4.3.2 Buckling mode shapes for each of the aspect ratios

Simply supported (continued)

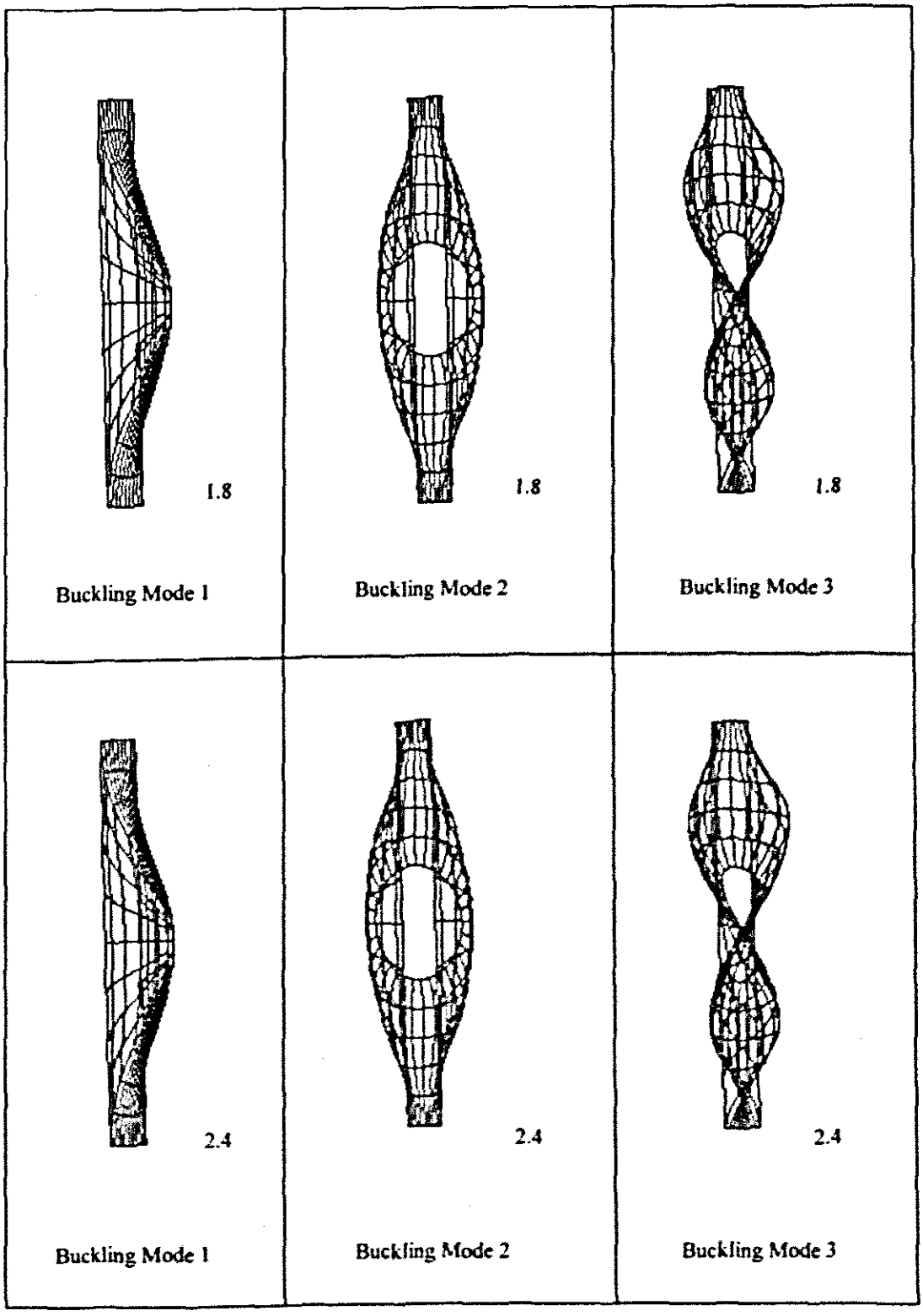

Figure 7.4.3.2 Buckling mode shapes for each of the aspect ratios

The buckling mode shapes in the diagrams below were tilted such that the maximum deformation is visible. The protruding lines are the distortions of the finite element meshes of the plate that was initially flat.

Simply supported (continued)

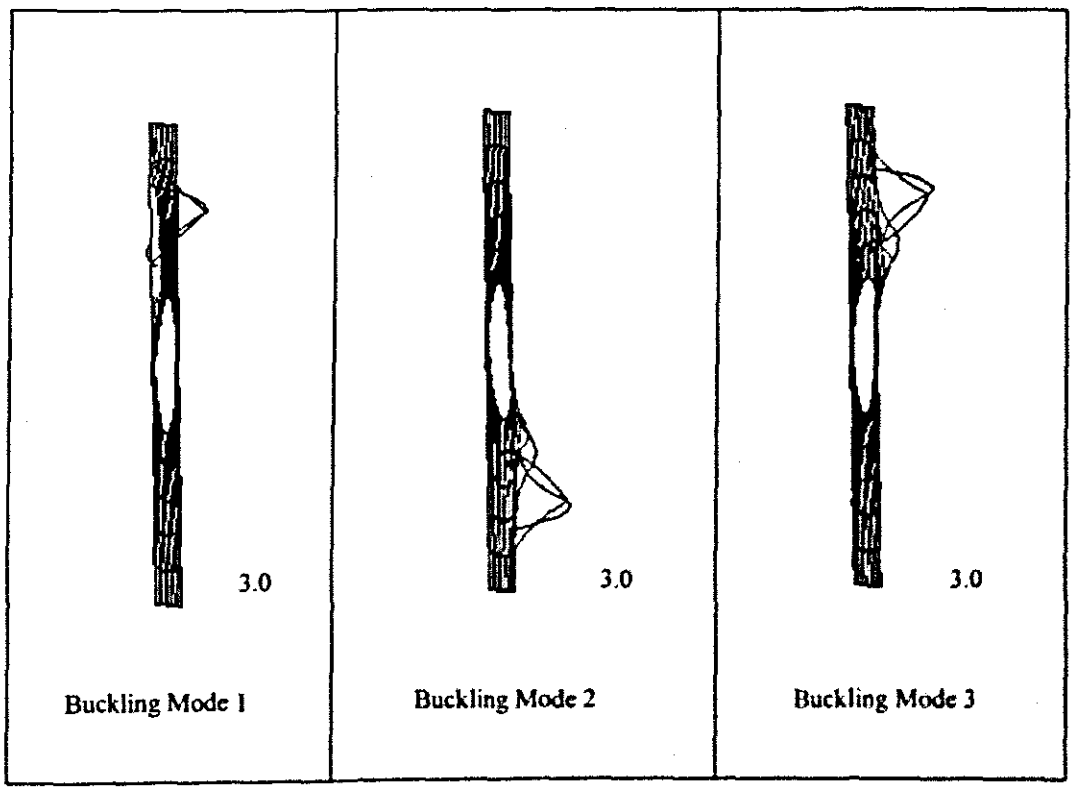

Figure 7.4.3.2 Buckling mode shapes for each of the aspect ratios

Clamped

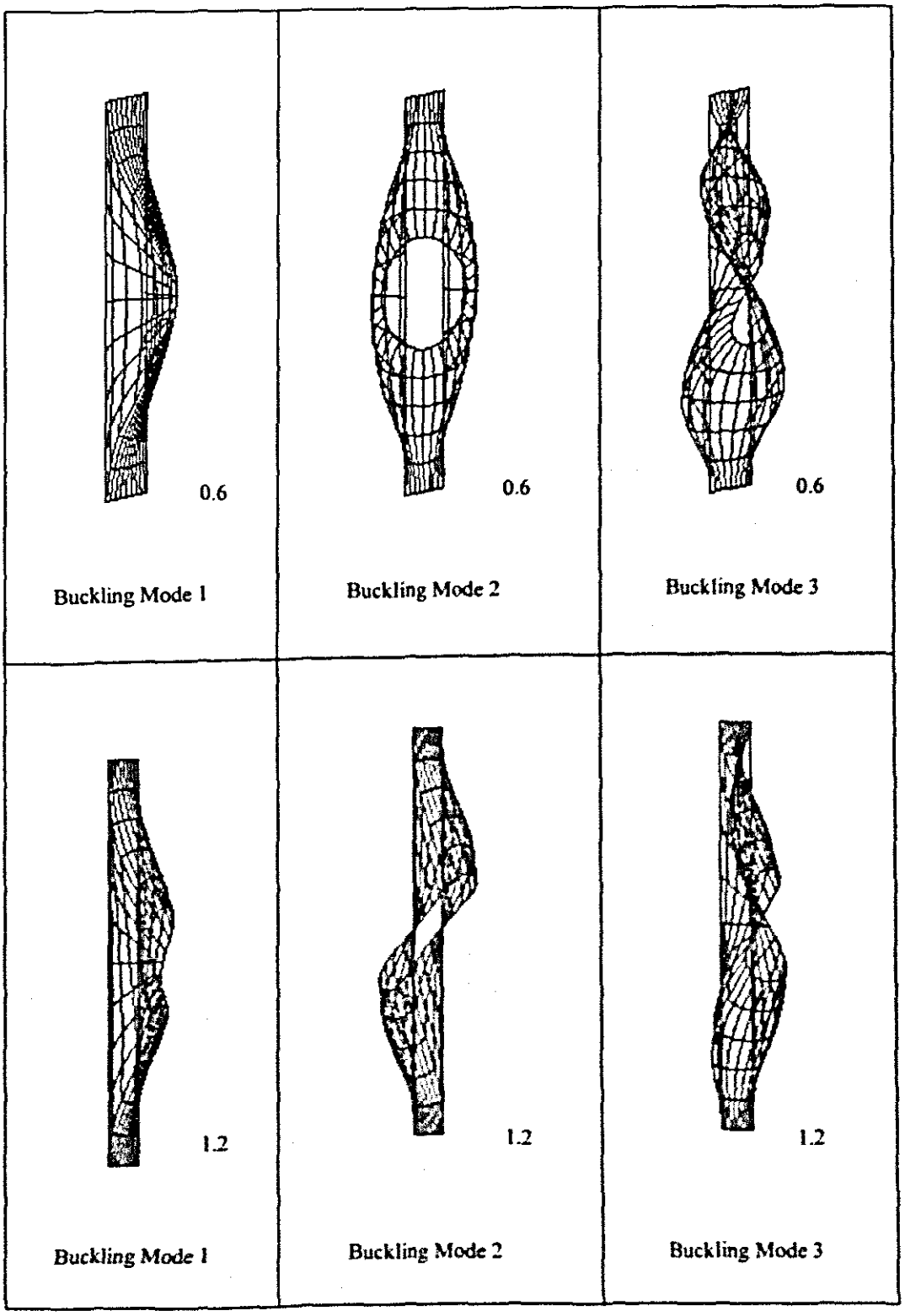

Figure 7.4.3.3 Buckling mode shapes for each of the aspect ratios

Clamped (continued)

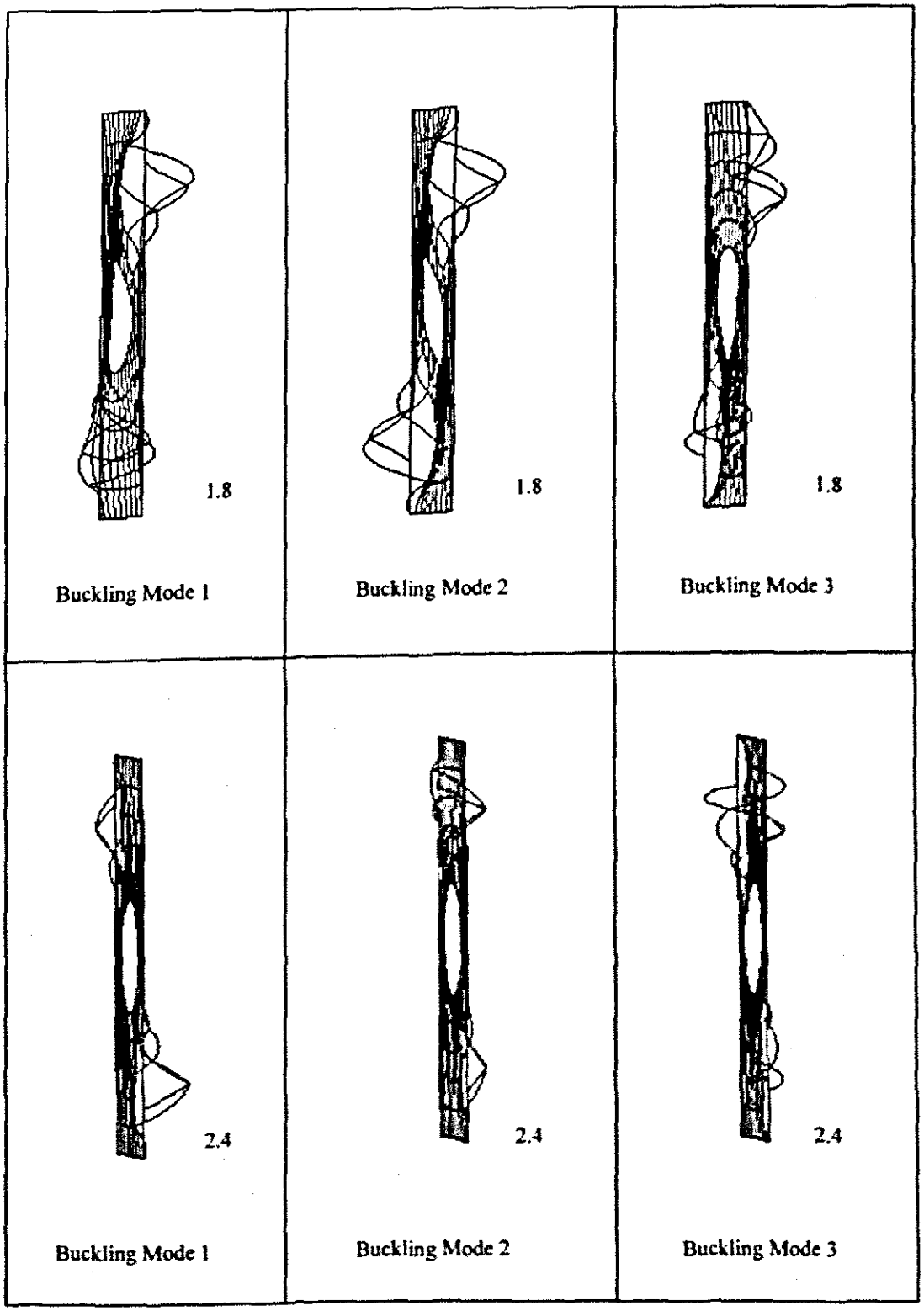

***Figure* 7.4.3.2** Buckling mode shapes for each of the aspect ratios

Clamped (continued)

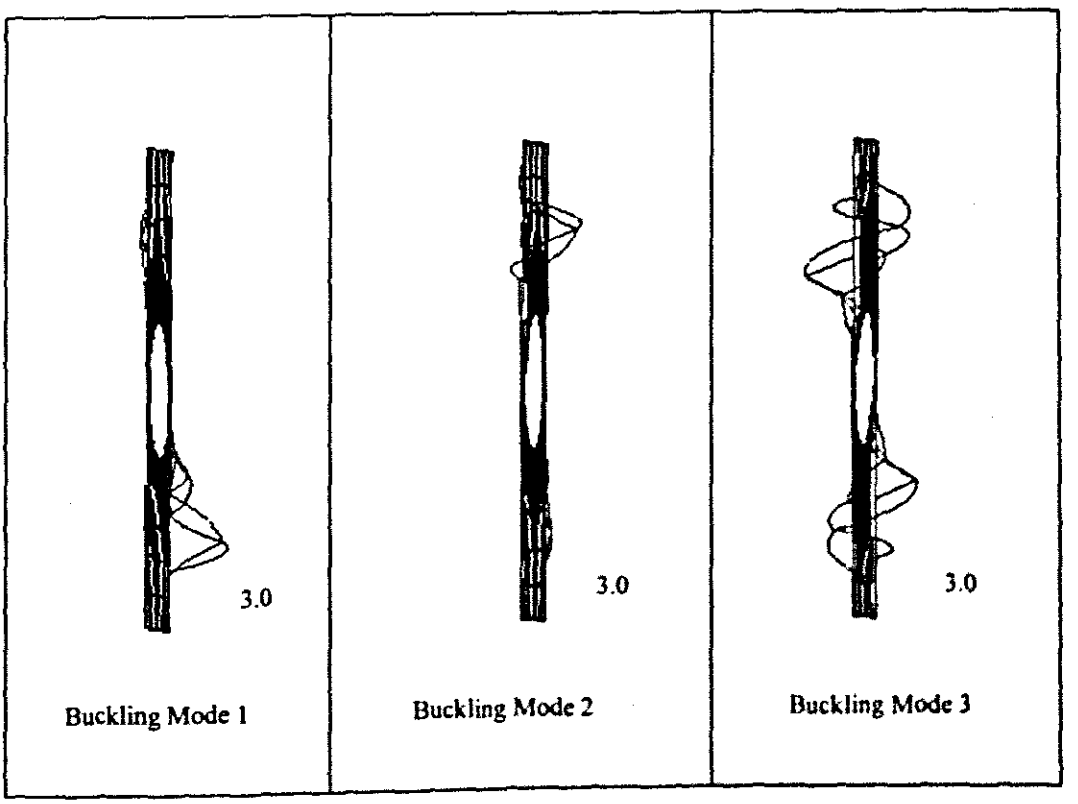

Figure 7.4.3.2 Buckling mode shapes for each of the aspect ratios

7.4.4 The effect of the modulus ratio E_1 / E_2

The influence of the modulus ratio in a laminate with a central hole is the same as the influence on a laminate without a hole. This was also the case in the previous section.

Simply supported

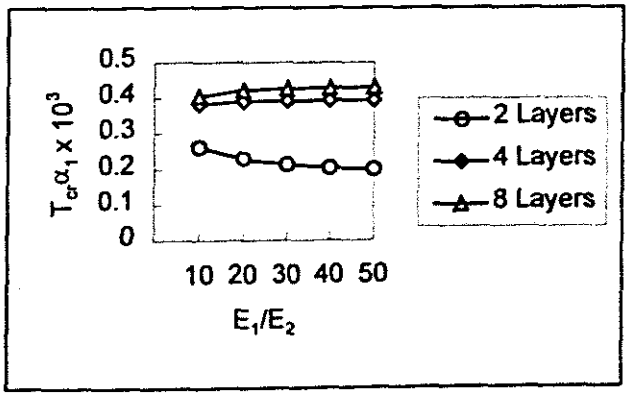

E_1/E_2	2 Layers	4 Layers	8 Layers
10	0.2622	0.3821	0.4040
20	0.2282	0.3897	0.4194
30	0.2132	0.3920	0.4249
40	0.2047	0.3932	0.4277
50	0.1994	0.3938	0.4294

Clamped

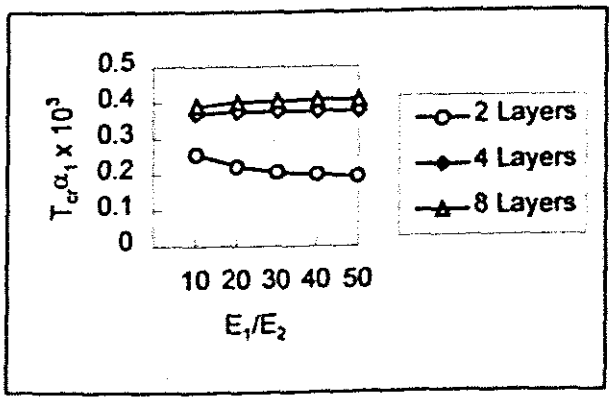

E1/E2	2 Layers	4 Layers	8 Layers
10	0.2556	0.3687	0.3887
20	0.2210	0.3737	0.4004
30	0.2060	0.3751	0.4044
40	0.1977	0.3757	0.4064
50	0.1924	0.3761	0.4078

Figure 7.4.4 Effect of the modulus ratio on the critical buckling temperature of laminates ($a / t = 20$, $\psi = 45^0$)

The elastic moduli E_1 and E_2 affect the material behaviour of a laminate. This is because of the interaction of the material properties of the different layers.

7.4.5 The effect of thermal expansion coefficient ratio α_2/α_1

Figure 7.4.5 shows that, as with other material property configurations, the change in the critical buckling temperature of a laminate is proportional to the change in the expansion coefficient ratio.

Clamped

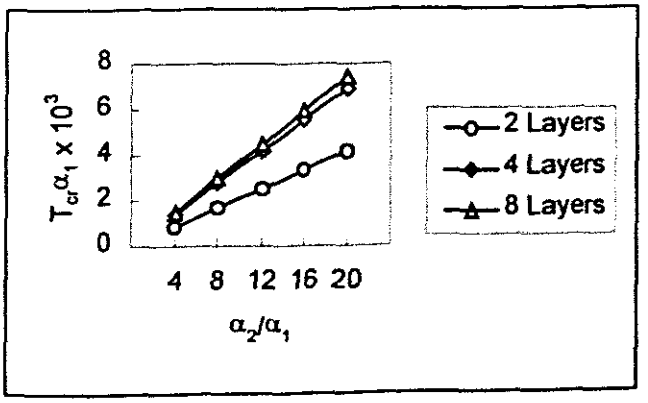

α_2/α_1	2 Layers	4 Layers	8 Layers
4	0.8316	1.3821	1.4836
8	1.6633	2.7642	2.9673
12	2.495	4.1463	4.4509
16	3.3267	5.5284	5.9346
20	4.1583	6.9105	7.4182

Simply Supported

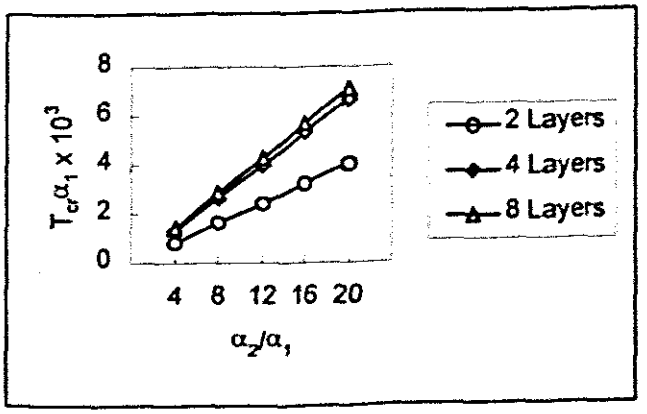

α_2/α_1	2 Layers	4 Layers	8 Layers
4	0.8061	1.3267	1.4179
8	1.6122	2.6534	2.8358
12	2.4183	3.9801	4.2536
16	3.2245	5.3068	5.6715
20	4.0306	6.6335	7.0894

Figure 7.4.5 The effect of thermal expansion coefficient ratio on the critical buckling temperature of laminates ($a / b = 1$, $a / t = 20$, $\psi = 45^\circ$)

For a given lamination geometry, the material properties do not influence the buckling behaviour of laminate under mechanical compressive load as much as under the thermal load. However from the derivations in the previous chapters we know that the thermal load is converted to the equivalent mechanical load. This effectively means that the thermal buckling behaviour of laminate is more of a geometric consideration than a material one, although the former was seen to have some effect as well. The next section compares the different geometric configurations, noting the influence of each of the variable as was done previously.

7.5 A cracked plate with a circular hole

Figure 7.5 shows a plate with a 4mm-diameter hole. It is meshed with the S9R5 finite element. The dimensions are also a = b = 20mm and the diameter is 4mm. The boundary conditions are applied on the outer edges while the hole is a free edge. The crack will be apparent as the plate deforms. In actual fact, the crack is in such a way that the nodes are not connected along a diagonal line, and this will be evident in the deformed meshes of the following page. Similar analyses are performed as in the previous sections.

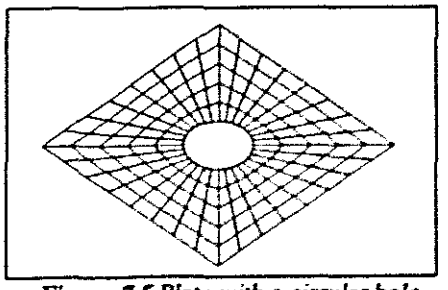

Figure 7.5 Plate with a circular hole

7.5.1 Effects of ply orientation

The two graphs below show the same pattern as in Figure 7.3.1.1, where the critical buckling temperature increases as the number of layers increases. For the clamped boundaries, the effect of ply orientation is not as significant as in the simply supported case.

Clamped

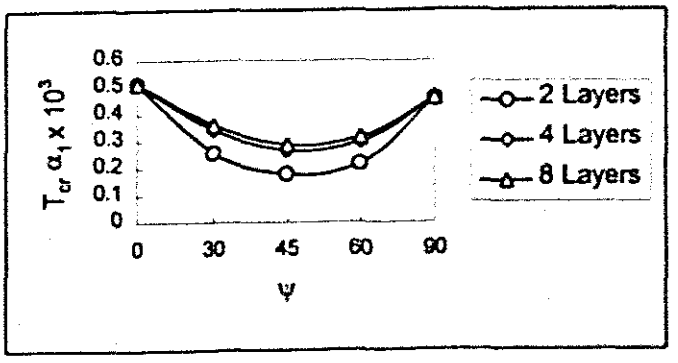

Ψ	2 Layers	4 Layers	8 Layers
0	0.5147	0.5147	0.5147
30	0.2557	0.3413	0.3604
45	0.1786	0.2654	0.2851
60	0.2168	0.2976	0.3161
90	0.4586	0.4586	0.4586

Simply Supported

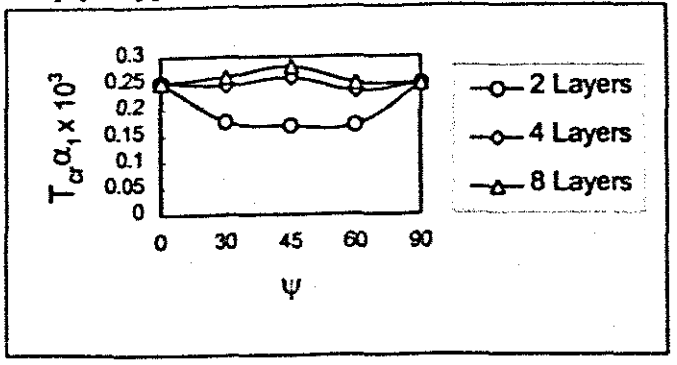

Ψ	2 Layers	4 layers	8 Layers
0	0.2511	0.2511	0.2511
30	0.1769	0.2465	0.2627
45	0.1684	0.2604	0.2819
60	0.1698	0.2352	0.2503
90	0.2491	0.2491	0.2491

Figure 7.5.1.1 Effects of ply orientation on the critical buckling temperature of laminates (a / t = 20, a / b = 1)

Figures 7.5.1.2 and 7.5.1.3 show the different buckling modes for the different lamination angles and boundary conditions. These buckling modes are associated with the eigenvalues that were calculated in ABAQUS. As the angle of orientation is increased, the severity of deformation becomes more significant. Although the nodes along the discontinuous edges are given the same geometric co-ordinates, the deformation of these edges occurs independently of these nodes.

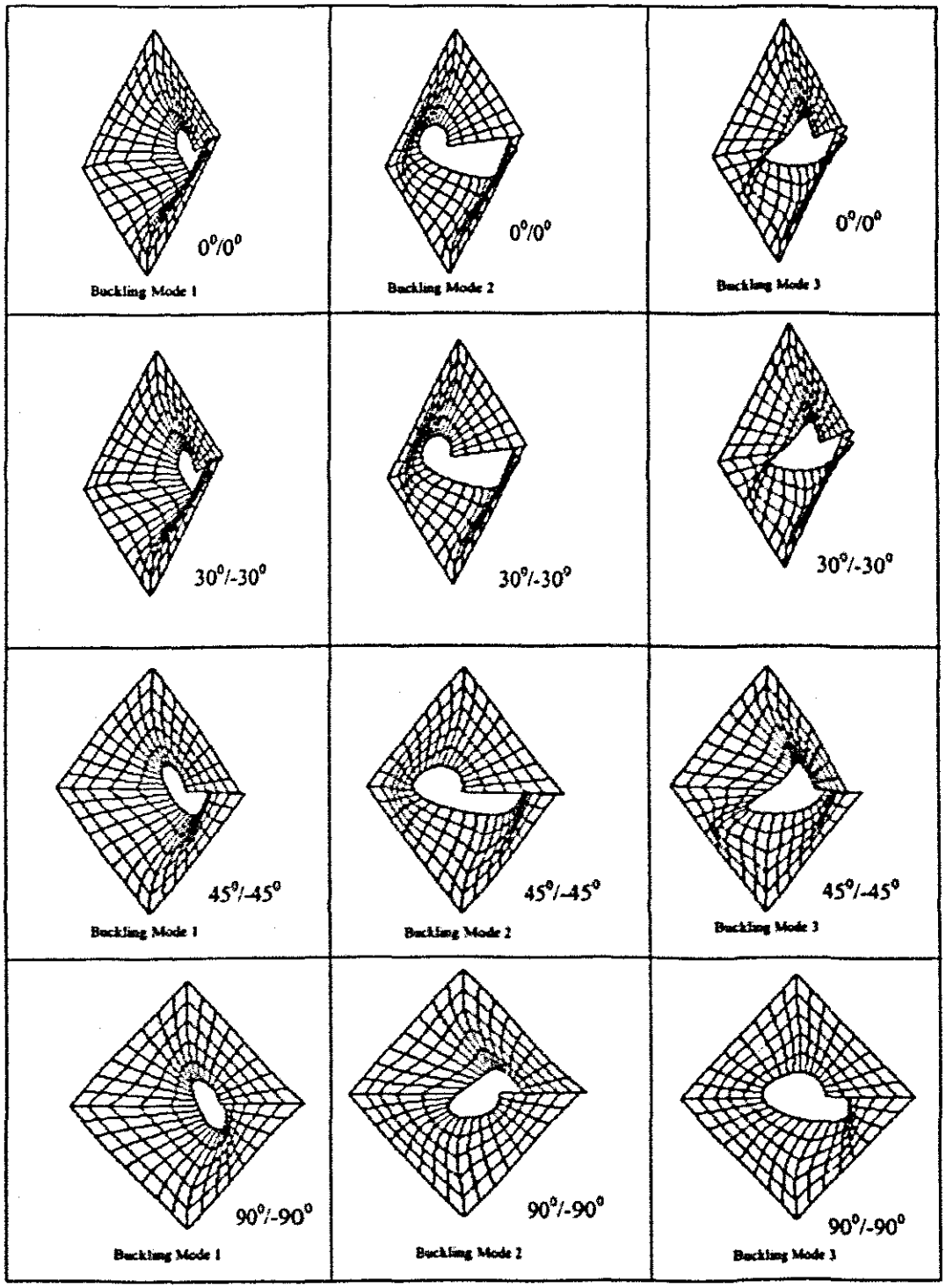

Figure 7.5.1.2 Buckling mode predictions for 2-layered simply supported plate

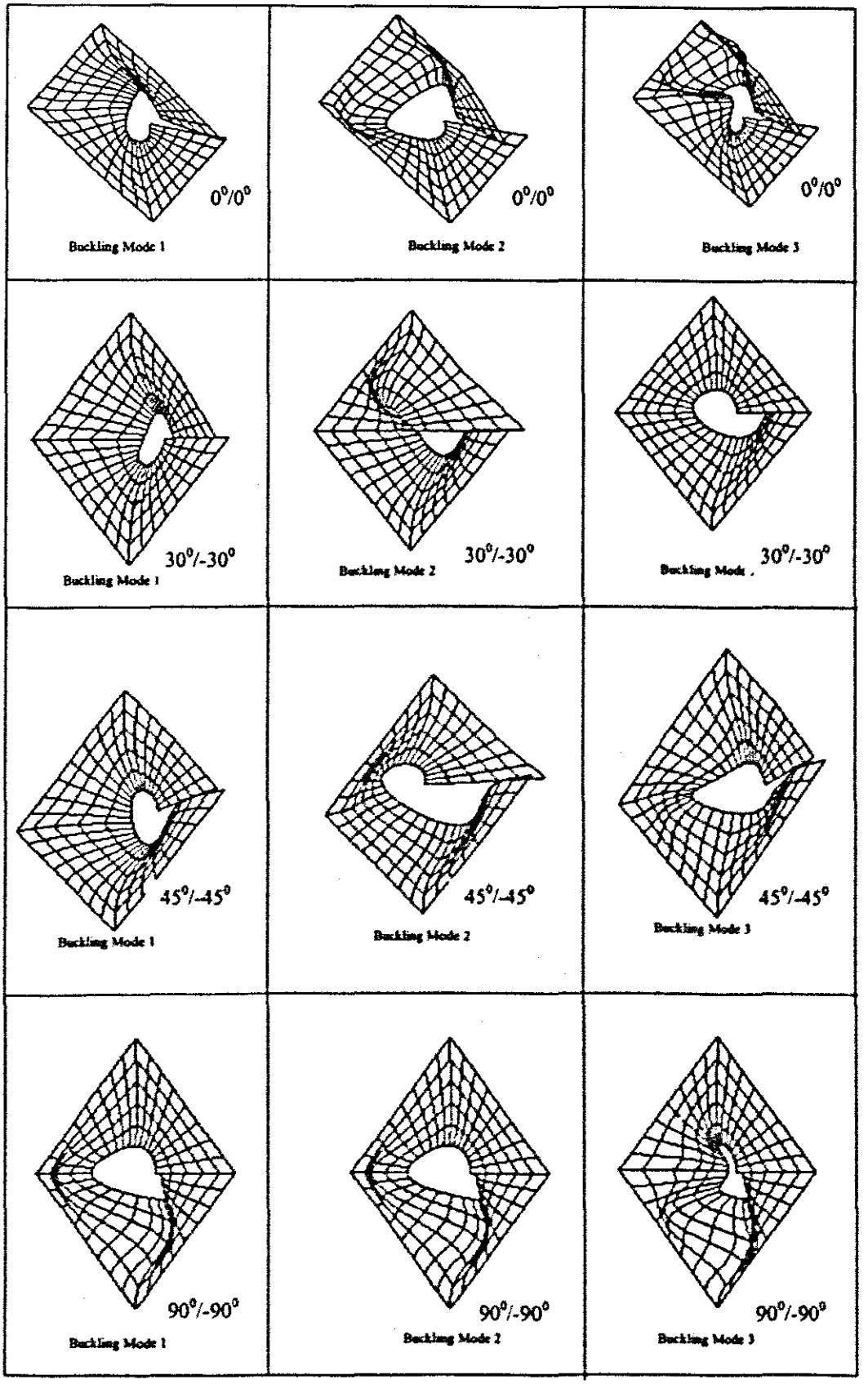

Figure 7.5.1.3 Buckling mode predictions for 2-layered clamped plate

7.5.2 Effects of plate thickness ratio

The graph for the simply supported plate is the same as the graph for clamped edges as shown in Figure 7.5.2, with the clamped case having higher values of the critical buckling temperature than the simply supported laminate. This is to be expected due to the fact that the boundary conditions were applied only on the outer edges. T_{cr} increases with the number of layers but this becomes insignificant for a/t ≥ 50.

Clamped

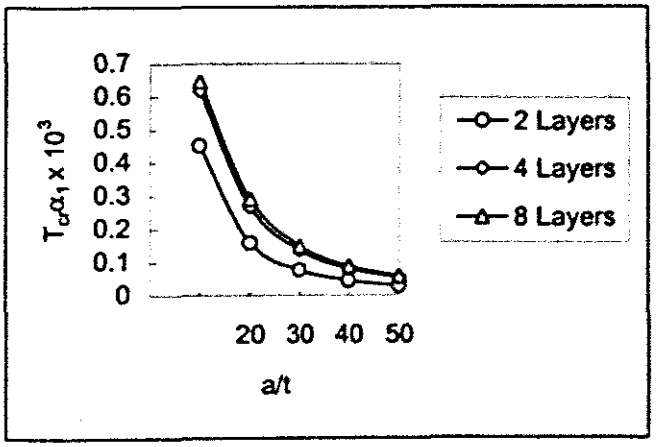

a / t	2 Layers	4 Layers	8 Layers
10	0.4515	0.6174	0.6454
20	0.1584	0.2670	0.2913
30	0.0756	0.1347	0.1486
40	0.0436	0.0796	0.0883
50	0.0282	0.0522	0.0580

Simply Supported

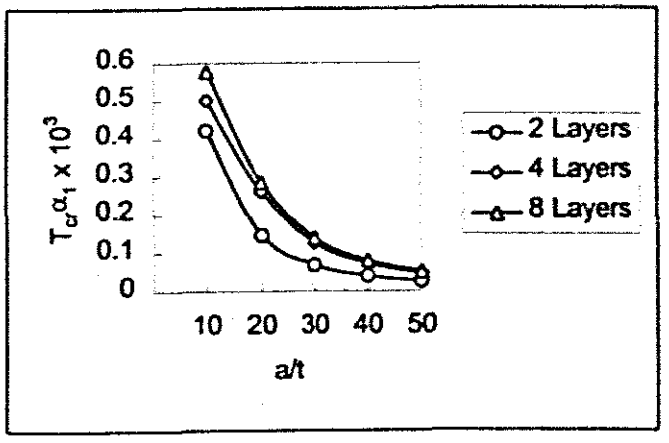

a / t	2 Layers	4 Layers	8 Layers
10	0.4210	0.4997	0.5765
20	0.1459	0.2591	0.2852
30	0.0675	0.1248	0.1386
40	0.0383	0.0718	0.0800
50	0.0246	0.0463	0.0516

Figure 7.5.2 Effect of plate thickness ratio on the critical buckling temperature of laminates (a/b = 1, $\psi = 45^0$)

7.5.3 The effect of the modulus ratio E_1 / E_2

Figure 7.5.3 shows that the effect of the modulus ratio becomes less as the number of layers is increased. For $E_1/E_2 \geq 20$, the graph flattens out for N = 4 and N = 8, while for N = 2 it slopes down gently until E_1/E_2 reaches the value of about 40 and then start to flatten out. A similar trend is observed in both the simply supported and clamped edges.

Clamped

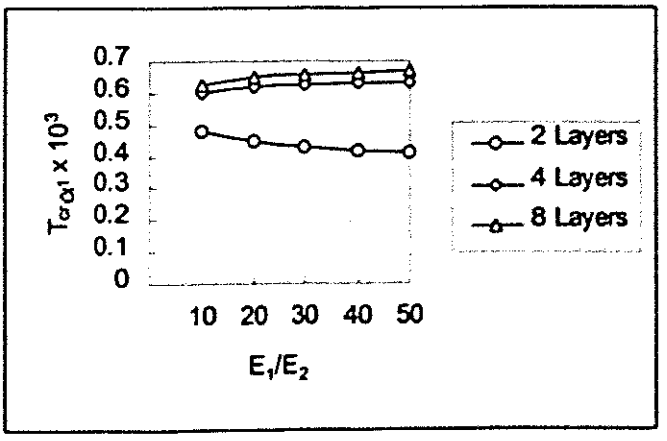

E_1/E_2	2 Layers	4 Layers	8 Layers
10	0.4804	0.6014	0.6231
20	0.4451	0.6200	0.6492
30	0.427	0.6265	0.6588
40	0.4162	0.6298	0.6638
50	0.4092	0.6318	0.6668

Simply Supported

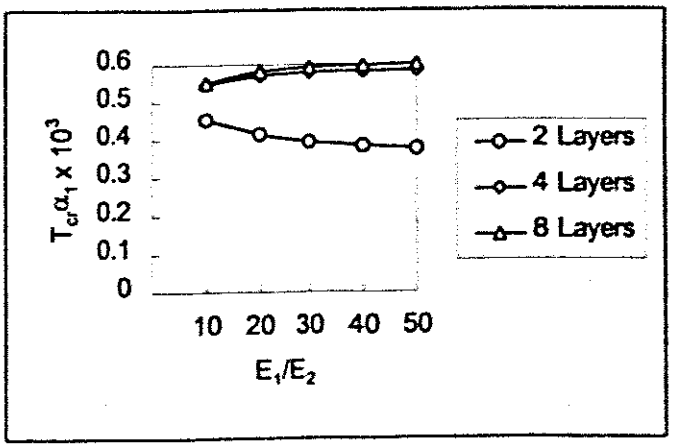

E_1/E_2	2 Layers	4 Layers	8 Layers
10	0.4527	0.5451	0.5518
20	0.4141	0.5694	0.5807
30	0.3946	0.5772	0.5910
40	0.3831	0.5810	0.5962
50	0.3756	0.5833	0.5994

Figure 7.5.3 The effect of the modulus ratio on the critical buckling temperature of laminates ($a / t = 20$, $\psi = 45^\circ$)

7.5.4 The effect of thermal expansion coefficient ratio α_2/α_1

In Figure 7.5.4 the critical buckling temperature is directly proportional to α_2/α_1. In fact the relationship is linear. As the number of layers increases, so does the critical buckling temperature. For N = 4 and N = 8, the slope is steeper as a result of increased interaction as the number of layers in increased.

Simply Supported

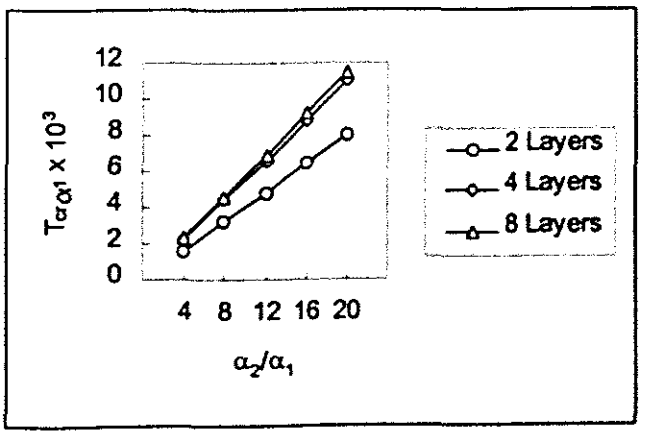

α_2/α_1	2 Layers	4 Layers	8 Layers
4	1.6054	2.1953	2.2948
8	3.2108	4.3907	4.5897
12	4.8162	6.586	6.8845
16	6.4216	8.7814	9.1794
20	8.0270	10.977	11.474

Clamped

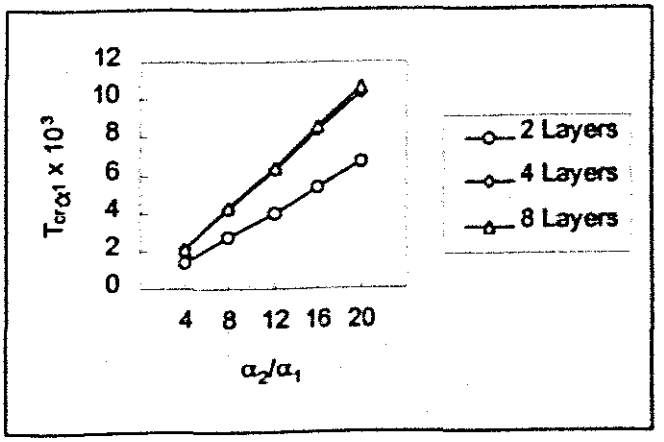

α_2/α_1	2 Layers	4 Layers	8 Layers
4	1.3358	2.0740	2.1313
8	2.6716	4.1480	4.2627
12	4.0074	6.2221	6.3940
16	5.3432	8.2961	8.5254
20	6.6790	10.370	10.657

Figure 7.5.4 The effect of thermal expansion coefficient ratio on the critical buckling temperature of laminates (a / b = 1, a / t = 20 $\psi = 45^0$)

The same conclusions are drawn as in the previous two sections. For different geometric patterns, with all the other variables being the same, the thermal buckling behaviour will follow the same trend, of course the values of the critical buckling temperatures will occur at different points. The only geometric considerations that was treated so far were the plate laminate aspect ratio and the laminate thickness, the following section studies the effect of a central cut-out on a laminated composite plate.

7.6 Effect of a cut-out on critical buckling temperature

Laminates, as any structure, have holes to serve various purposes. An obvious purpose is to accommodate a bolt. Another reason is to provide access from one side of the laminate to the other. This section compares the effects of the cut-outs on the critical buckling temperature of a laminated composite plate with two layers. Unless otherwise stated, the lamination sequence is $45^0/-45^0$, a/t = 20, a/b = 1. Both plates in Figure 7.6.1 and Figure 7.6.2 have the dimension of a = b = 20mm and the plate with a hole has the radius of 2mm.

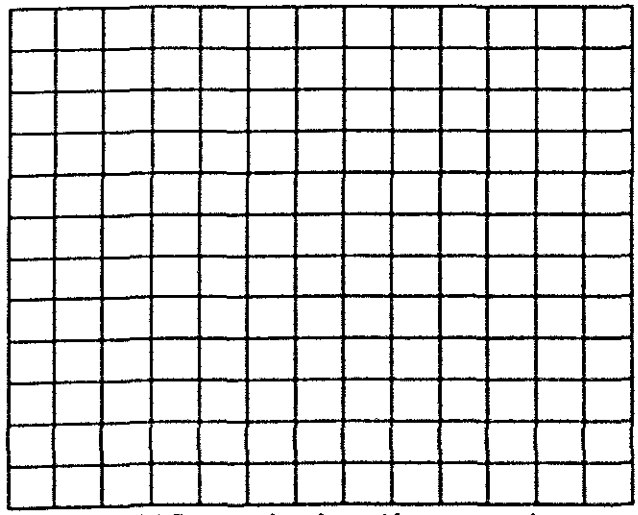

Figure 7.6.1 Rectangular plate without a central cut-out

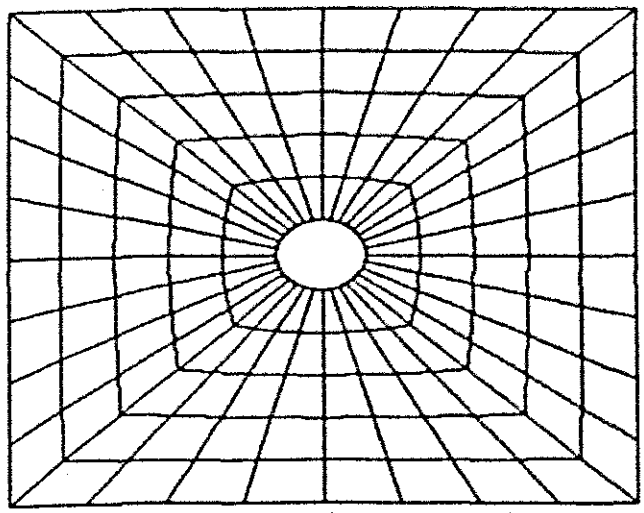

Figure 7.6.2 Rectangular plate with a central cut-out

As can be seen in the two diagrams above, the finite elements do not have the same shape, the obvious reason being the different in geometry. However, each element has midside nodes and another node at the centre. The hole is expected to have a significant influence on the critical buckling temperature, because of the altered integrity of the structure. This is now investigated in the following sections.

7.6.1 Effects of ply orientation

Table 7.6.1 shows that the critical buckling temperature of a laminate containing holes is lower that those without holes, and in both instances this temperature decreases as the lamination angle approaches 45^0/-45^0. This is expected because the presence of a hole reduces the ability of a laminate to carry the same applied load and the coupling stiffness [B] (from Chapter 4) in a two layered laminate is less effective as the laminate becomes a cross-ply. The same conclusion was reached by Wu *et al* [32].

Lamination sequence	Normal plate	Plate with cut-out
$0^0/0^0$	482.23	429.45
30^0/-30^0	391.90	236.13
45^0/-45^0	329.40	173.75

Table 7.6.1 Effect of ply orientation

7.6.2 Effect of thickness ratio

Generally, the thicker the laminate, the more it can carry the loads, and an increase in the thickness ratio effectively makes the laminate thinner. The decreasing values of the critical buckling temperature in Table 6.7.2 attest to this. Once again the presence of a hole reduces the critical buckling temperature. We note from the table that at a/t > 30 the reverse takes place.

Thickness ratio (a/t)	Normal plate	Plate with cut-out
10	494.83	245.39
20	177.570	173.75
30	82.678	84.355
40	47.062	48.533
50	30.249	31.318

Table 7.6.2 Effect of thickness ratio

7.6.3 Effect of aspect ratio

In a layered laminate, an increase in aspect ratio enhances the critical buckling temperature, and this is evident in Table 7.6.3. However, the presence of a hole alters this behaviour and the buckling temperature is actually lower. At a/b =1.8 the critcal buckling temperature could not be calculated for a laminate containing the hole.

Aspect ratio (a/b)	Normal plate	Plate with cut-out
0.6	143.88	128.78
1.2	218.55	211.29
1.8	415.66	XXX
2.4	630.10	154.90
3	865.25	90.671

Figure 7.6.3 Effect of aspect ratio

Figure 7.6.3 shows the predicted buckling mode shapes for each of the aspect ratios of Section 7.6.3. We note in passing that for lower critical buckling temperatures, the hole seems to maintain its shape, and as the temperature is increased, so does the severity of deformation. The buckling mode shapes were rotated to expose the maximum deformation.

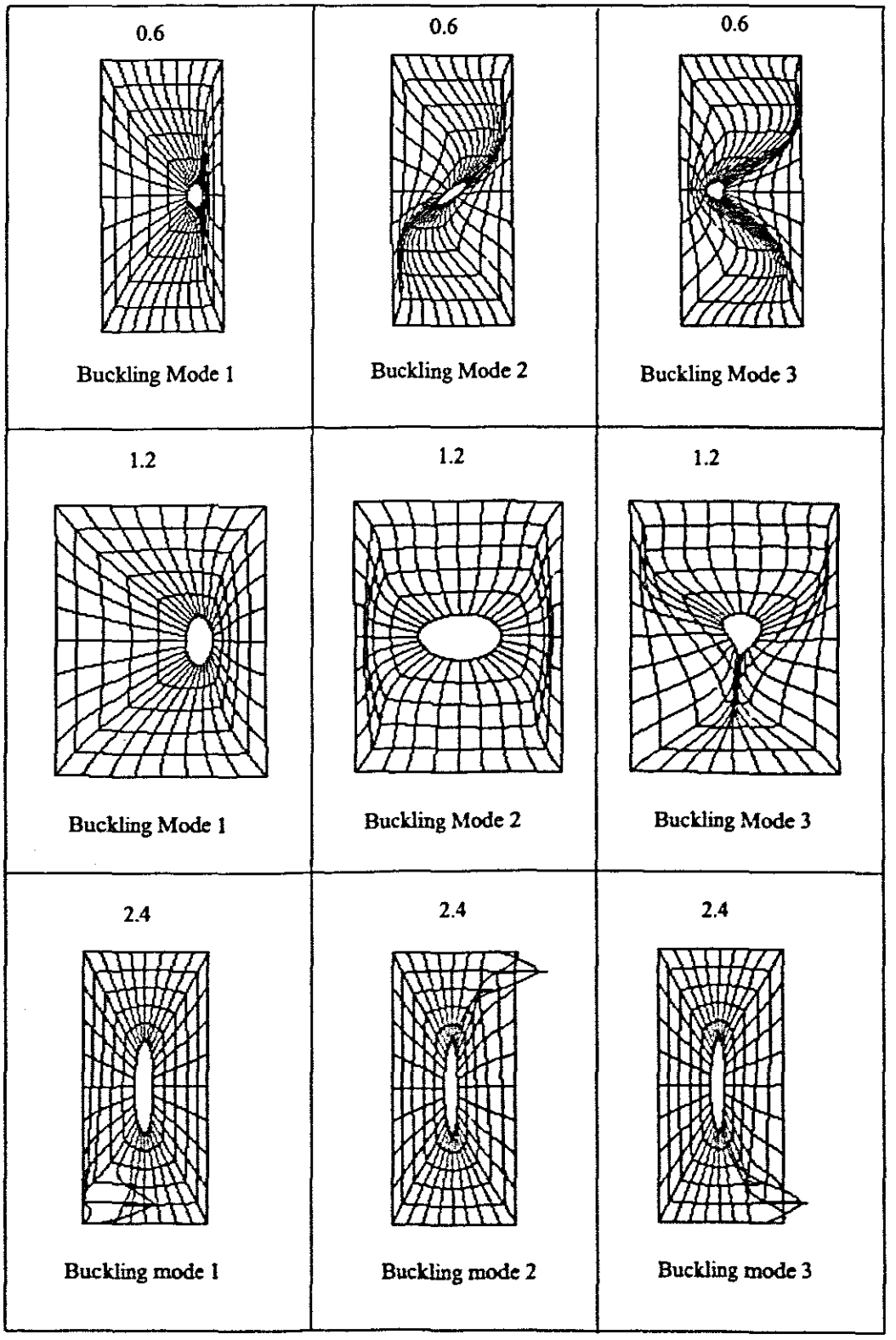

Figure 7.6.3 Buckling mode predictions for each of the aspect ratios

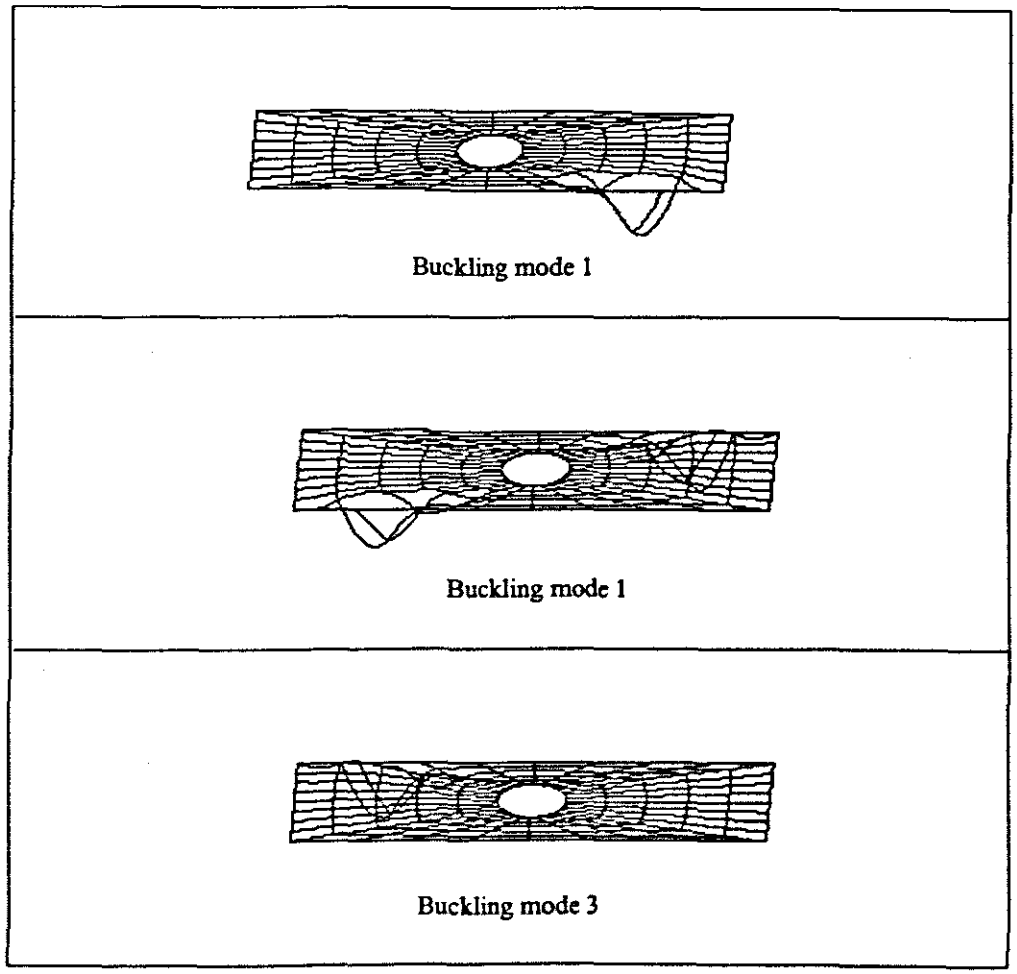

Figure 7.6.3 Buckling mode predictions for each of the aspect ratios (continued)

7.6.4 The effect of the modulus ratio

As expected the critical buckling temperatures for a laminate containing a hole are lower than those without a hole. This is because the removal of a material implies the lowering of material properties. In Ref. [31] the same conclusion was reached.

Modulus ratio (E_1/E_2)	Normal plate $T_{cr}\alpha_1$	Plate with cut-out $T_{cr}\alpha_1$
10	206.25	195.72
20	172.17	169.37
30	158.01	157.61
40	150.29	151.02
50	145.44	146.81

Table 7.6.4 Effect of modulus ratio

7.6.5 The effect of thermal expansion coefficient ratio

The same conclusions can be made as in Section 7.6.5 that because of the presence of a hole, the load carrying capacity of the laminate is compromised.

Expansion coefficient ratio (α_2/α_1)	Normal plate $T_{cr}\alpha_1$	Plate with cut-out $T_{cr}\alpha_1$
4	0.63138	0.61776
8	1.2628	1.2355
12	1.8941	1.8533
16	2.5255	2.4711
20	3.1569	3.0888

Table 7.6.1 Effect of thermal expansion coefficient

7.7 Conclusions

A general background on composites was presented in Chapter 1. The basic components such as the fiber and the matrix that together constitute a composite material were discussed. It was discovered that these fibers and matrix material could be arranged in various ways according to the use for which they are intended. The idea was to combine two distinctly different materials into the one with a superior performance. Also in Chapter 1 the buckling phenomenon was presented as an introduction to the study of buckling in laminated composite plates. However a rather thin cylinder was used to highlight two types of buckling that might occur in structures; collapse at the maximum point in a load versus deflection curve and bifurcation buckling, with the latter being the basis of this project. It was also pointed out that, unlike isotropic plates, laminated plates might fail "several times" before the actual failure, for the failure of layer does not necessarily imply failure of the entire laminate. The main factors that influence the strength of a laminate were introduced. The use of Mindlin plate theory was found to be suitable for the study of laminated composites.

The elastic deformation of an elemental cube, as discussed in Chapter 2, showed that because of rotational equilibrium, the governing equations that describe the motion of a point in a body could be simplified. The non-linear behaviour of the strains in buckling was defined in Chapter 3. Also the stresses that influence the behaviour of a plate under bending load were formulated. For the sake of completion, the differential governing equations of a Mindlin plate were formulated.

In Chapter 4 the macromechanics of lamination were formulated with a view to building up the constitutive model of laminated composite plates. The elastic constants were combined with the stress and moment resultants to form the general governing equations. A closer look at this equation revealed that this equation could be manipulated into special cases according to laminate construction, thereby simplifying the analysis of laminated composites.

Buckling was formulated analytically in Chapter 5 and the resulting equations were found to be more complex, and as a result the Finite Element Method of Chapter 6 was used as a tool to solve the buckling equations. FEM is also used by ABAQUS and the procedures are discussed at end of Chapter 6and the beginning of Chapters 7, and also in Appendix E.

From the results presented throughout Chapter 7, it can be concluded that the presence of coupling between bending and extension in a laminate generally decreases the effective stiffnesses of a laminate, while at the same time it reduces buckling loads or temperatures. Generally, there is no significant increase in the buckling temperature for the laminate with the number of layers N greater than 4 and an increase in lamination angle. This is because the coupling effect decreases with increasing number of plies. However, the thicker the laminate, the higher the thermal buckling load. Any defect or imperfection would reduce the ability of a structure to withstand the applied load, and a hole is one of them. Here we distinguish between a defect that is induced deliberately, such as a hole, and the one that cannot be avoided, such as impurities and voids in a laminate. The latter was also discussed at great length in Section1.3.2. In any case, no real structure is perfect and in order to serve any purpose, the plates may be drilled and machined. This causes the integrity of the laminate to be compromised, as can be seen in the preceding results. For a normal plate (without cut-outs) and the plate with central cut-outs, the increase in the number of layers causes an increase in the buckling temperature, and this applies to all the variables (ply orientation, plate thickness, aspect ratio, modulus ratio and the expansion coefficient ratio). As pointed out in Section 7.2 and Reference [29], the effect of the aspect ratio is greater on the laminate with a central cut-out than is an ordinary plate. As concluded in Reference [31], a central cut-out will have a greater effect when the aspect ratio is small. This would be expected because the geometry is significantly changed by the central cut-out while the width is being reduced.

In the final analysis

- The thicker the laminate is the lower the thermal buckling load.
- The thermal buckling load increases with an increase of the number of layers.
- The thermal buckling load increases with an increase in the aspect ratio
- The thermal buckling load decreases greatly with increasing modulus ratio.
- The thermal buckling load decreases greatly with increasing expansion coefficient ratio.
- The presence of hole reduces the critical buckling load of a laminate

Finally, the types of analysis that were performed during this particular study are by no means the only options available to determine the strength, and consequently, the critical buckling temperature of laminated composite plate. For example, as stated in Chapter 5, the number of boundary conditions that may be imposed on a composite plate, and the combinations thereof, is enormous. Also the lamination sequence, the thickness of each particular layer, as well as any other variable that is of interest to the analyst, can provide endless options as to the behaviour of laminated composite plates. This effectively means that there is a lot of room for future study of the effects that other thermal stress fields and other laminated plates would have on this and other geometries. Consequently, this project had to be limited, not by the number of available options, but by the fact that at a given time, one can only do so much.

References

[1] ABAQUS/Standard User's Manual, Vol. 1 and Vol. 2, Version 5.6.

[2] ABAQUS Theory Manual

[3] Barrett, K.E., Ellis, S., 1988, An Exact Theory of Elastic Plates, Int. J. Solids Structures, **24**, 859- 880.

[4] Bathe, K., 1996, Finite Element Procedures, Prentice-Hall, Englewood, New Jersey.

[5] Boresi, A.P., Sidebottom, O.M., 1952, Advanced Mechanics of Materials, 4th Ed., John Wiley and Sons, New York.

[6] Brush, D.O., Almroth, B.O., 1975, Buckling of Bars, Plates, and Shells, McGraw-Hill, New York, Chap. 3.

[7] Bushnell, D., 1985, Static Collapse: A Survey of Methods and Modes of Behaviour, Finite Elements in Analysis and Design, **1**, 165-205.

[8] Calcote, L.R., 1969, The Analysis of Laminated Composite Structures, Van Nostrand Reinhold Co., New York.

[9] Chandrashekhara, K., 1992, Thermal Buckling of Laminated Plates using a Shear Flexibility Finite Element, Finite Elements in Analysis and Design, Vol. 12, pp. 51-61.

[10] Chawle, K.K., 1987, Composite Materials, Springer-Verlag.

[11] Chen, W.J., Lin, P.D., Chen, L.W., 1991, Thermal Buckling Behaviour of Thick Composite Laminated Plates under Non-uniform Temperature Distribution, Computers and Structures, Vol. 41, No. 4, pp. 637-645.

[12] Cook, R.D., Malkus, D.S., Olesha, M.E., 1989, Concepts and Applications of Finite Element Analysis, 3rd Ed., John Wiley and Sons, Inc.

[13] Dawe, D.J., Roufaeil, O.L., 1982, Buckling of Rectangular Mindlin Plates, Computers and Structures, **15**, No. 4, 461 – 471.

[14] Dym, C.L., Shames, I.H., Solid Mechanics: A Variational Approach, McGraw-Hill, New York.

[15] Halpin, J.C., 1992, Primer on Composite Materials Analysis, 2nd Ed., Technomic Publishing Co., Pennsylvania, USA.

[16] Hinton, E., Owen, D.R.J., 1979, An introduction to Finite Element Computation, Pineridge Press Limited, Swansea, U.K.

[17] Hughes, T.J.R., 1987, The Finite Element Method, Prentice-Hall, Englewood Cliffs, New Jersey.

[18] Jones, R.M., 1975, Mechanics of Composite Materials, McGraw-Hill Kogakusha, Tokyo.

[19] Liew, K.M., Xiang, Y., Kitipornchai, S., 1996, Analytical Buckling Solutions for Mindlin Plates involving Free Edges, Int. J. Mech. Sci., **38**, No. 10, 1127 – 1138.

[20] Marsden, J.E., Hughes, T.J.R., 1983, Mathematical Foundation of Elasticity, Prentice-Hall, Englewood Cliffs, New York.

[21] Mathew, T.C., Singh, G., RAO, G.V., 1992, Thermal Buckling of Cross-Ply Composite Laminates, Computers and Structures, Vol. 42, No. 2, pp. 281-287.

[22] Mindlin, R.D., 1951, Influence of Rotatory Inertia and Shear on Flexural Motions of Isotropic, Elastic Plates, J. Appl. Mech. 31-38.

[23] Reissner. E., 1945, The Effect of Transverse Shear Deformation on the Bending of Elastic Plates, J. Appl. Mech. Vol. 12.

[24] Robinson, J., 1981, Understanding Finite Element Stress Analysis, Robinson and Associates, England.

[25] Simelane, P., Sun B., 1998, Thermal buckling analysis of laminated composite plates, Proceedings of the 2nd SA Conference of Applied Mechanics'98, Vol.2, 925-936, Cape Town.

[26] Simelane, P., Sun, B., 1998, Buckling behaviour of laminated composite plates under thermal loading, Proceedings of the 2nd International Conference on Composite Science and Technology (ICCST/2), 371-376, 9-11 June 1998, Durban.

[27] Sun, B-H.,1993, The Buckling Theory based on the Generalised Variational Principle, Report of the ASME Winter Annual Meeting.

[28] Sun, B., 1995, Design of Low Order, Locking Free and Mesh Distortion Insensitive Finite Element for Mindlin Plates by using Enhanced Assumed Strain Methods, Cerecam Report, University of Cape Town, South Africa.

[29] Timoshenko, S., Woinowsky-Krieger, S., 1959, Theory of Plates and Shells, McGraw-Hill, New York.

[30] Ugural, A.C.., 1981, Stresses in Plates and Shells, McGraw-Hill, USA.

[31] Walker, M., Adali, S., Verijenko, V., 1995, Optimal Design of Laminated Composite Plates with Central Cut-out for Maximum Buckling Load using the FEM, Proc. of the 13th Symposium on Finite Element Methods in South Africa, Vol. 2, pp. 708-718.

[32] Wu, T., Shiau, L., 1995, Application of the Finite Element Method to Postbuckling Analysis of Laminated Plates, AIAA Journal, Vol. 33, No. 12, pp. 2379-2385.

[33] Wung, R.M., Reddy, J.N., 1991, A Transverse Deformation Theory of Laminated Composite Plates, Computers and Structures, Vol. 41, No. 4, pp. 821-833.

[34] Yang, I., Shieh, J., 1988, Generic Thermal Buckling of Initially Stressed Antisymmetric Cross-ply Thick Laminates, Int. J. Solids Structures, Vol. 24, No. 10, pp. 1059-1070.

[35] Zeggane, M., Sridharan, S., 1991, Stability Analysis of Long Laminated Composite Plates using Reissner-Mindlin 'Infinite' Strips, Computers and Structures, Vol. 40, No. 4, pp. 1033 - 1042.

[36] Zienkiewicz, O.C., Taylor, R.L., 1989, The Finite Element Method, 4th ed., McGraw-Hill, London.

[37] Noor, A.K., Peters, J.M., 1992, Postbuckling of Multilayered Composite Plates Subjected to Combined Axial and Thermal Loads, Finite Elements in Analysis and Design, Vol. 11, 91-104.

[38] ABAQUS/Standard Example Problems Manual, Vol. 1 and Vol. 2, Version 5.6.

Appendix A

Transverse Shear in Composite Plates

As the Mindlin plate element is based on first-order transverse shear flexible theory in which the transverse shear strain is assumed to be constant through the thickness of the plate, it is necessary to use shear correction factors. These correction factors are easily shown to be 5/6 for isotropic plates.

For laminated plates the equivalent factors are established by calculating the distribution of transverse shear stress through the thickness of the plate, for the case of unidirectional bending and assuming linear elastic response. The shear strain energy, expressed in terms of section forces and strains, is then equated to the strain energy of this distribution of transverse stresses. This method supplies reasonable estimates of transverse shear stiffness and can be outlined as follows;

Considering a plate in the (x-y) plane, and assuming only bending and shear in the x-direction, without gradients in the y-direction, the membrane forces in the plate are zero: $N_x = N_y = N_{xy}$, and $\partial/\partial y = 0$ for all response variables. In this case equilibrium within the section in the z-direction is:

$$\frac{\partial \sigma_x}{\partial x} + \frac{\partial \tau_{xz}}{\partial z} = 0. \qquad \text{(A1)}$$

Moment equilibrium about the y-axis gives:

$$V_x + \frac{\partial M_x}{\partial x} = 0 \qquad \text{(A2)}$$

where V_x is the transverse shear force per unit width in the plate and M_x is the bending moment per unit width for bending about the y-axis.

For the bending behaviour we assume the strain varies linearly across the section:

$$\varepsilon_{\alpha\beta} = \bar{\varepsilon}_{\alpha\beta} - (z - z_0)\bar{\kappa}_{\alpha\beta}$$

where $\bar{\varepsilon}_{\alpha\beta}$ is the membrane strain of the reference surface and $z = z_0$, and $\bar{\kappa}_{\alpha\beta}$ is the curvature of that surface. If the response of the plate is linearly elastic, any in-plane component of stress at a point through the plate section, $\sigma_{\alpha\beta}$, is given by

$$D_{\alpha\beta\gamma\delta}\left(\bar{\varepsilon}_{\gamma\delta} - (z - z_0)\bar{\kappa}_{\gamma\delta}\right) \qquad \text{(A3)}$$

where the plane stress elastic stiffness, $D_{\alpha\beta\gamma\delta}$, is defined from the elasticity and orientation of the material at the particular layer of the plate. The Greek subscripts take the range (1,2). Integrating through the thickness and inverting the resultant section stiffness provides the 6 x 6 section matrix, [H]:

$$\begin{Bmatrix} \bar{\varepsilon}_{\alpha\beta} \\ \bar{\kappa}_{\alpha\beta} \end{Bmatrix} = [H] \begin{Bmatrix} N_{\alpha\beta} \\ M_{\alpha\beta} \end{Bmatrix}.$$

It has already been assumed that

$$N_x = N_y = N_{xy}.$$

It is also now assumed that

$$M_y = M_{xy} = 0;$$

that is, that it is possible to have no bending in the y-direction without any restraining moments associated with the y-direction. This is clearly not the case for unbalanced composite section, but we nevertheless use it as a simplifying assumption used to obtain the shear correction factor. Thus

$$\begin{Bmatrix} \bar{\varepsilon}_{\alpha\beta} \\ \bar{\kappa}_{\alpha\beta} \end{Bmatrix} = \{H_{i4}\} M_x \tag{A4}$$

where $\{H_{i4}\}$ is the fourth column of [H]. Combining this result with the elastic stiffness at a point through the plate thickness provides the in-plane stress components in terms of M_x as

$$\sigma_x = (B_{x1} - (z - z_0) B_{x2}) M_x \tag{A5}$$

where

$$B_{x1} = D_{xxxx} H_{14} + D_{xxyy} H_{24} + D_{xxxy} H_{34}$$

and

$$B_{x2} = D_{xxxx} H_{44} + D_{xxyy} H_{54} + D_{xxxy} H_{64}.$$

Combining the gradient of this equation in the x-direction with the equilibrium Equations A1 and A2 yields a description of the variation of the transverse shear stress through the thickness of the plate:

$$\frac{\partial \tau_{xz}}{\partial z} = (B_{x1} - (z - z_0) B_{x2}) V_x. \tag{A6}$$

In calculating $\partial\sigma_x/\partial x$ we have assumed that the elasticity and thickness of the composite section do not vary (or vary slowly) with position along the plate.

A laminated composite plate section consists of N layers 1,2,3, ... with different values of $\left(B^1_{x1}, B^1_{x2}\right)$ at layer 1, $\left(B^2_{x1}, B^2_{x2}\right)$ at layer 2, ... $\left(B^N_{x1}, B^N_{x2}\right)$ at layer N. Layer i extends from z_i to z_{i+1} and its thickness is $t_i = z_{i+1} - z_i$. Integrating Equation A6 through the plate, using the boundary conditions $\tau_{xz} = 0$ at $z = 0$, $\tau^i_{xz} = \tau^{i+1}_{xz}$ at $z = z_{i+1}$ and $\tau_{xz} = 0$ at $z = z_{N+1}$, gives the transverse shear stress in layer i as

$$\tau^i_{xz} = \left[B^i_{x1}(z - z_i) - \left(\tfrac{1}{2}\left(z^2 - z_i^{\,2}\right) - z_{x0}(z - z_i)\right)B^i_{x2} + B^i_{x0}\right]V_x \qquad \text{(A7)}$$

where

$$B^i_{x0} = \sum_{j=1}^{i-1} t_j\left[B^j_{x1} - \left(\tfrac{1}{2}\left(z_{j+1} + z_j\right) - z_{x0}\right)B^j_{x2}\right]$$

and

$$z_{x0} = \frac{\sum_{i=1}^{N} t_i\left(\frac{1}{2}(z_{i+1}+z_i)B^i_{x2} - B^i_{x1}\right)}{\sum_{i=1}^{N} t_i B^i_{x2}}.$$

The subscript z_{x0} is used instead of z_0 in this case because the result is associated with pure bending in the x-direction. The variation of τ_{yz} through the plate thickness is obtained using a similar procedure, based on pure bending in the y-direction.

These results provide the estimates of interlaminar shear stresses.
We define the shear flexibility of the plate section by matching the shear strain energy obtained by integrating the elastic strain energy density associated with transverse shear stress distribution obtained above:

$$\frac{1}{2}\begin{bmatrix} V_x & V_y \end{bmatrix}\left[F^s\right]\begin{Bmatrix} V_x \\ V_y \end{Bmatrix} = \frac{1}{2}\sum_{i=1}^{N}\int_{z_i}^{z_{i+1}}\begin{bmatrix} \tau_{xz} & \tau_{yz} \end{bmatrix}\left[F^i\right]\begin{Bmatrix} \tau_{xz} \\ \tau_{yz} \end{Bmatrix} dz$$

where $\left[F^s\right]$ is the shear flexibility of the section and $\left[F^i\right]$ is the continuum transverse shear flexibility within layer i. Here we introduce the assumption that the transverse shear flexibility within a layer is not coupled to the in-plane flexibility. This is usually the case for plate constructions.

Substituting the relations for τ^i_{xz} and τ^i_{yz} into the above equation and integrating defines the shear flexibility of the section as

$$F^s_x = \sum_{i=1}^{N} F^i_x t_i\left[\left(B^i_{x0}\right)^2 + t_i B^i_{x0}\left(B^i_{x1} - (z_i - z_{x0})B^i_{x2}\right) + \tfrac{1}{3}t_i^2\left(B^i_{x1} - (z_i - z_{x0})B^i_{x2}\right)^2 - \tfrac{1}{4}t_i^3 B^i_{x2}\left(B_{x1} - (z_i - z_{x0})B^i_{x2}\right)^2 + \tfrac{1}{20}t_i^4\left(B^i_{x2}\right)^2\right]$$

$$F_y^s = \sum_{i=1}^{N} F_y^i t_i \left[\left(B_{y0}^i\right)^2 + t_i B_{y0}^i \left(B_{y1}^i - \left(z_i - z_{y0}\right) B_{y2}^i\right) + \tfrac{1}{3} t_i^2 \left(B_{y1}^i - \left(z_i - z_{y0}\right) B_{y2}^i\right)^2 \right.$$
$$\left. - \tfrac{1}{4} t_i^3 B_{y2}^i \left(B_{y1} - \left(z_i - z_{y0}\right) B_{y2}^i\right)^2 + \tfrac{1}{20} t_i^4 \left(B_{y2}^i\right)^2 \right]$$

$$F_{xy}^s = \sum_{i=1}^{N} F_{xy}^i t_i \left[B_{x0}^i B_{y0}^i + \tfrac{1}{2} t_i \left[B_{x0}^i \left(B_{y1}^i - \left(z_i - z_{y0}\right) B_{y2}^i\right) + B_{y0}^i \left(B_{x1} - \left(z_i - z_{x0}\right) B_{x2}^i\right) \right] \right.$$
$$+ \tfrac{1}{3} t_i^2 \left(B_{x1}^i - \left(z_i - z_{x0}\right) B_{x2}^i\right)\left(B_{y1}^i - \left(z_i - z_{y0}\right) B_{y2}^i\right)$$
$$- \tfrac{1}{8} t_i^3 \left[B_{x2}^i \left(B_{y1}^i - \left(z_0 - z_{y0}\right) B_{y2}^i\right) + B_{y2}^i \left(B_{x1}^i - \left(z_0 - z_{x0}\right) B_{x2}^i\right) \right]$$
$$\left. + \tfrac{1}{20} t_i^4 B_{x2}^i B_{y2}^i \right]$$

The transverse shear stiffness of the section is then available as $\left[F_{\alpha\beta}^s\right]^{-1}$. We notice that F_{12}^s will be nonzero if any layer is anisotropic or orthotropic in a local system (since then F_{xy}^i will be nonzero).

Appendix B

Stress-Strain Matrix of a Laminated Composite

B.1 Transformation of Stress-Strain Relationships

Using the principal material directions (1,2,3) the stress-strain relations are written as

$$\begin{bmatrix}\sigma_1\\ \sigma_2\\ \sigma_3\\ \sigma_4\\ \sigma_5\\ \sigma_6\end{bmatrix} = \begin{bmatrix}Q_{11} & Q_{12} & Q_{13} & Q_{14} & Q_{15} & Q_{16}\\ Q_{21} & Q_{22} & Q_{23} & Q_{24} & Q_{25} & Q_{26}\\ Q_{31} & Q_{32} & Q_{33} & Q_{34} & Q_{35} & Q_{36}\\ Q_{41} & Q_{42} & Q_{43} & Q_{44} & Q_{45} & Q_{46}\\ Q_{51} & Q_{52} & Q_{53} & Q_{54} & Q_{55} & Q_{56}\\ Q_{61} & Q_{62} & Q_{63} & Q_{64} & Q_{65} & Q_{66}\end{bmatrix}\begin{bmatrix}\varepsilon_1-\alpha_{11}\Delta T\\ \varepsilon_2-\alpha_{22}\Delta T\\ \varepsilon_3-\alpha_{33}\Delta T\\ \gamma_4\\ \gamma_5\\ \gamma_6\end{bmatrix} \qquad \text{(B.1.1)}$$

When each layer (or ply) is taken to be macroscopically homogeneous and orthotropic, the above reduces to

$$\begin{bmatrix}\sigma_1\\ \sigma_2\\ \sigma_3\\ \sigma_4\\ \sigma_5\\ \sigma_6\end{bmatrix} = \begin{bmatrix}Q_{11} & Q_{12} & Q_{13} & 0 & 0 & 0\\ Q_{21} & Q_{22} & Q_{23} & 0 & 0 & 0\\ Q_{31} & Q_{32} & Q_{33} & 0 & 0 & 0\\ 0 & 0 & 0 & Q_{44} & 0 & 0\\ 0 & 0 & 0 & 0 & Q_{55} & 0\\ 0 & 0 & 0 & 0 & 0 & Q_{66}\end{bmatrix}\begin{bmatrix}\varepsilon_1-\alpha_{11}\Delta T\\ \varepsilon_2-\alpha_{22}\Delta T\\ \varepsilon_3-\alpha_{33}\Delta T\\ \gamma_4\\ \gamma_5\\ \gamma_6\end{bmatrix} \qquad \text{(B.1.2)}$$

These relations were defined using the principal material directions (1,2,3). However, for angle-ply laminated plate the principal direction of orthotropy of each individual lamina do not coincide with the geometrical co-ordinate frame. It is therefore necessary to transform the principal-direction quantities into the co-ordinate frame quantities. Because of the highly directional nature of the properties, laminae are used in laminates and the stresses or strains are applied in the plane in directions (x, y) at angle ψ to the principal directions (1,2). The strains in the (x,y) directions are related to the stresses in the (x,y) directions using the measured properties in the (1,2) directions and the transformation matrix [T] On rotation of the co-ordinate system (1,2) to an angle ψ to the (x,y)system, the stresses transform according to

$$\begin{bmatrix}\sigma_x\\ \sigma_y\\ \tau_{yz}\\ \tau_{xz}\\ \tau_{xy}\end{bmatrix} = [T]^{-1}\begin{bmatrix}\sigma_1\\ \sigma_2\\ \tau_{23}\\ \tau_{13}\\ \tau_{12}\end{bmatrix} = [T]^{-1}[Q][R][T][R]^{-1}\begin{bmatrix}\varepsilon_x-\alpha_x\Delta T\\ \varepsilon_y-\alpha_y\Delta T\\ 0\\ 0\\ \gamma_{xy}-\alpha_{xy}\Delta T\end{bmatrix} \tag{B.1.3}$$

where the stress transformation matrix is given by

$$[T] = \begin{bmatrix} \cos^2\psi & \sin^2\psi & 0 & 0 & 0 & 2\cos\psi\sin\psi \\ \sin^2\psi & \cos^2\psi & 0 & 0 & 0 & -2\cos\psi\sin\psi \\ 0 & 0 & 1 & 0 & 0 & 0 \\ 0 & 0 & 0 & \cos\psi & \sin\psi & 0 \\ 0 & 0 & 0 & \sin\psi & \cos\psi & 0 \\ -\cos\psi\sin\psi & \cos\psi\sin\psi & 0 & 0 & 0 & \cos^2\psi-\sin^2\psi \end{bmatrix} \tag{B.1.4}$$

and $[T]^{-1}$ is the inverse. The strain transforms according to the Reiter's matrix [8]:

$$[R] = \begin{bmatrix}1&0&0&0&0&0\\0&1&0&0&0&0\\0&0&0&0&0&0\\0&0&0&0&0&0\\0&0&0&0&0&0\\0&0&0&0&0&2\end{bmatrix} \qquad [R]^{-1} = \begin{bmatrix}1&0&0&0&0&0\\0&1&0&0&0&0\\0&0&0&0&0&0\\0&0&0&0&0&0\\0&0&0&0&0&0\\0&0&0&0&0&\frac{1}{2}\end{bmatrix} \tag{B.1.5}$$

After multiplying out Equation (B.1.3), we obtain;

$$\begin{bmatrix}\sigma_x\\ \sigma_y\\ \sigma_z\\ \tau_{yz}\\ \tau_{xz}\\ \tau_{xy}\end{bmatrix} = \begin{bmatrix}\bar{Q}_{11}&\bar{Q}_{12}&0&0&0&\bar{Q}_{16}\\ \bar{Q}_{12}&\bar{Q}_{22}&0&0&0&\bar{Q}_{26}\\ \bar{Q}_{13}&\bar{Q}_{23}&\bar{Q}_{33}&0&0&\bar{Q}_{36}\\ 0&0&0&\bar{Q}_{44}&\bar{Q}_{45}&0\\ 0&0&0&\bar{Q}_{45}&\bar{Q}_{55}&0\\ \bar{Q}_{16}&\bar{Q}_{26}&0&0&0&\bar{Q}_{66}\end{bmatrix}\begin{bmatrix}\varepsilon_x\\ \varepsilon_y\\ \varepsilon_z\\ \gamma_{yz}\\ \gamma_{xz}\\ \frac{1}{2}\gamma_{xy}\end{bmatrix} + \begin{bmatrix}\bar{Q}_{11}&\bar{Q}_{12}&0&0&0&\bar{Q}_{16}\\ \bar{Q}_{12}&\bar{Q}_{22}&0&0&0&\bar{Q}_{26}\\ \bar{Q}_{13}&\bar{Q}_{23}&\bar{Q}_{33}&0&0&\bar{Q}_{36}\\ 0&0&0&\bar{Q}_{44}&\bar{Q}_{45}&0\\ 0&0&0&\bar{Q}_{45}&\bar{Q}_{55}&0\\ \bar{Q}_{16}&\bar{Q}_{26}&0&0&0&\bar{Q}_{66}\end{bmatrix}\begin{bmatrix}z\kappa_x\\ z\kappa_y\\ 0\\ 0\\ 0\\ z\kappa_{xy}\end{bmatrix}$$
$$- \begin{bmatrix}\bar{Q}_{t11}&\bar{Q}_{t12}&0&0&0&\bar{Q}_{t13}\\ \bar{Q}_{t12}&\bar{Q}_{t22}&0&0&0&\bar{Q}_{t23}\\ \bar{Q}_{13}&\bar{Q}_{23}&0&0&0&\bar{Q}_{33}\\ 0&0&0&0&0&0\\ 0&0&0&0&0&0\\ \bar{Q}_{t13}&\bar{Q}_{t23}&0&0&0&\bar{Q}_{t33}\end{bmatrix}\begin{bmatrix}\alpha_x\\ \alpha_y\\ \alpha_z\\ \alpha_{yz}\\ \alpha_{xz}\\ 2\alpha_{xy}\end{bmatrix}\Delta T \tag{B.1.6}$$

where, with subscript "$_t$" denoting thermal effects;

$\bar{Q}_{11} = Q_{11}\cos^4\psi + Q_{22}\sin^4\psi + (2Q_{12} + 4Q_{66})\cos^2\psi\sin^2\psi$
$\bar{Q}_{12} = Q_{12}(\cos^4\psi + \sin^4\psi) + (Q_{11} + Q_{22} - 4Q_{66})\cos^2\psi\sin^2\psi$
$\bar{Q}_{22} = Q_{11}\sin^4\psi + Q_{22}\cos^4\psi + (2Q_{12} + 4Q_{66})\cos^2\psi\sin^2\psi$
$\bar{Q}_{16} = (Q_{11} - Q_{12} - 2Q_{66})\cos^3\psi\sin\psi - (Q_{22} - Q_{12} - 2Q_{66})\cos\psi\sin^3\psi$
$\bar{Q}_{26} = (Q_{11} - Q_{12} - 2Q_{66})\cos\psi\sin^3\psi - (Q_{22} - Q_{12} - 2Q_{66})\cos^3\psi\sin\psi$
$\bar{Q}_{66} = (Q_{11} + Q_{22} - 2Q_{12} - 2Q_{66})\cos^2\psi\sin^2\psi + Q_{66}(\cos^4\psi + \sin^4\psi)$
$\bar{Q}_{t11} = Q_{11}\cos^4\psi + Q_{22}\sin^4\psi + 2Q_{12}\cos^2\psi\sin^2\psi$
$\bar{Q}_{t12} = Q_{12}\cos^4\psi + Q_{12}\sin^4\psi + (Q_{11} + Q_{22})\sin^2\psi\cos^2\psi$
$\bar{Q}_{t13} = (Q_{21} - Q_{11})\cos^3\psi\sin\psi + (Q_{22} - Q_{12})\sin^3\psi\cos\psi$
$\bar{Q}_{t21} = Q_{12}(\sin^4\psi + \cos^4\psi) + (Q_{11} + Q_{22})\sin^2\psi\cos^2\psi$
$\bar{Q}_{t22} = Q_{11}\sin^4\psi + Q_{22}\cos^4\psi + 2Q_{12}\sin^2\psi\cos^2\psi$
$\bar{Q}_{t23} = (Q_{12} - Q_{11})\sin^3\psi\cos\psi + (Q_{22} - Q_{12})\cos^3\psi\sin\psi$
$\bar{Q}_{t31} = (Q_{11} - Q_{12})\cos^3\psi\sin\psi + (Q_{12} + Q_{22})\sin^3\psi\cos\psi$
$\bar{Q}_{t32} = (Q_{11} - Q_{12})\sin^3\psi\cos\psi - (Q_{12} + Q_{22})\cos^3\psi\sin\psi$
$\bar{Q}_{t33} = [(Q_{12} - Q_{11}) - (Q_{22} - Q_{12})]\sin^2\psi\cos^2\psi$
$\bar{Q}_{44} = Q_{44}\cos^2\psi + Q_{55}\sin^2\psi$
$\bar{Q}_{45} = (Q_{44} + Q_{55})\cos^2\psi\sin^2\psi$
$\bar{Q}_{55} = Q_{44}\sin^2\psi + Q_{55}\cos^2\psi$

With $\sigma_z = \sigma_3$, the normal stress σ_z transforms according to

$$\sigma_z = Q_{13}(\varepsilon_1 - \alpha_{11}\Delta T) + Q_{23}(\varepsilon_2 - \alpha_{22}\Delta T) + Q_{33}(\varepsilon_3 - \alpha_{33}\Delta T)$$

with

$\bar{Q}_{13} = Q_{13}\cos^2\psi + Q_{23}\sin^2\psi$
$\bar{Q}_{23} = Q_{13}\sin^2\psi + Q_{23}\cos^2\psi$
$\bar{Q}_{33} = Q_{33}$
$\bar{Q}_{36} = (Q_{13} - Q_{23})\sin\psi\cos\psi$

The bar over the $\left[\bar{Q}_{ij}\right]$ matrix denotes that we are dealing with the transformed reduced stiffnesses instead of the reduced stiffnesses $\left[Q_{ij}\right]$.

B.2 Formulation of Laminated Stiffness Matrix

The system of stress resultants and moment resultants in Chapter 3 is statically equivalent to actual stress distribution through the thickness of the composite laminate. These stress resultants having the dimensions of force per unit length are positive in the same directions as the corresponding stress components. These resultants give the total force per unit length acting at the midplane. In addition to that, there are moments applied at the midplane, which are equivalent to the moments produced by the stresses with respect to the midplane.

To obtain the constitutive model of a laminated composite, we substitute the transformed stress matrix into the stress resultants and sum over the N plies. Thus

$$\begin{bmatrix} N_x \\ N_y \\ N_{xy} \end{bmatrix} = \sum_{k=1}^{N} \left(\begin{bmatrix} \bar{Q}_{11} & \bar{Q}_{12} & \bar{Q}_{16} \\ \bar{Q}_{16} & \bar{Q}_{22} & \bar{Q}_{26} \\ \bar{Q}_{16} & \bar{Q}_{26} & \bar{Q}_{66} \end{bmatrix} \begin{bmatrix} \varepsilon_x \\ \varepsilon_y \\ \gamma_{xy} \end{bmatrix} + \begin{bmatrix} \bar{Q}_{11} & \bar{Q}_{12} & \bar{Q}_{16} \\ \bar{Q}_{16} & \bar{Q}_{22} & \bar{Q}_{26} \\ \bar{Q}_{16} & \bar{Q}_{26} & \bar{Q}_{66} \end{bmatrix} \begin{bmatrix} \kappa_x \\ \kappa_y \\ \kappa_{xy} \end{bmatrix} - \begin{bmatrix} \bar{Q}_{t11} & \bar{Q}_{t12} & \bar{Q}_{t16} \\ \bar{Q}_{t16} & \bar{Q}_{t22} & \bar{Q}_{t26} \\ \bar{Q}_{t16} & \bar{Q}_{t26} & \bar{Q}_{t66} \end{bmatrix} \begin{bmatrix} \alpha_x \\ \alpha_y \\ 2\alpha_{xy} \end{bmatrix} \right) \int_{h_{k-1}}^{h_k} dz \tag{B.2.1}$$

where $\begin{bmatrix} N_x & N_y & N_{xy} \end{bmatrix}^T$ is the stress resultant in x, y, and xy. These equations may be written as

$$\begin{bmatrix} N_x \\ N_y \\ N_{xy} \end{bmatrix} = \begin{bmatrix} A_{11} & A_{12} & A_{16} \\ A_{12} & A_{22} & A_{26} \\ A_{16} & A_{26} & A_{66} \end{bmatrix} \begin{bmatrix} \varepsilon_x \\ \varepsilon_y \\ \frac{1}{2}\gamma_{xy} \end{bmatrix} + \begin{bmatrix} B_{11} & B_{12} & B_{16} \\ B_{12} & B_{22} & B_{26} \\ B_{16} & B_{26} & B_{66} \end{bmatrix} \begin{bmatrix} \kappa_x \\ \kappa_y \\ \kappa_{xy} \end{bmatrix} - \begin{bmatrix} N_{tx} \\ N_{ty} \\ N_{txy} \end{bmatrix} \tag{B.2.2}$$

$$A_{ij} = \sum_{k=1}^{N} \left(\bar{Q}_{ij}\right)_k \left(h_k - h_{k-1}\right) \qquad B_{ij} = \frac{1}{2} \sum_{k=1}^{N} \left(\bar{Q}_{ij}\right)_k \left(h_k^2 - h_{k-1}^2\right)$$

Typically

$$N_x = \sum_{k=1}^{N} \left[\left(\bar{Q}_{11}\varepsilon_x + \bar{Q}_{12}\varepsilon_y + \bar{Q}_{16}\gamma_{xy}\right) \int_{h_{k-1}}^{h_k} dz + \left(\bar{Q}_{11}\kappa_x + \bar{Q}_{12}\kappa_y + \bar{Q}_{16}\kappa_{xy}\right) \int_{h_{k-1}}^{h_k} z dz \right]$$

$$= \sum_{k=1}^{n} \left[\left(\bar{Q}_{11}\varepsilon_x + \bar{Q}_{12}\varepsilon_y + \bar{Q}_{16}\gamma_{xy}\right)\left(h_k - h_{k-1}\right) + \left(\bar{Q}_{11}\kappa_x + \bar{Q}_{12}\kappa_y + \bar{Q}_{16}\kappa_{xy}\right)\left(h_k^2 - h_{k-1}^2\right) \right]$$

such that the first part of the first term is A_{11} and the first part of the second term is B_{11}.

The moment resultants are given by

$$\begin{bmatrix} M_x \\ M_y \\ M_{xy} \end{bmatrix} = \begin{bmatrix} B_{11} & B_{12} & B_{16} \\ B_{12} & B_{22} & B_{26} \\ B_{16} & B_{26} & B_{66} \end{bmatrix} \begin{bmatrix} \varepsilon_x \\ \varepsilon_y \\ \gamma_{xy} \end{bmatrix} + \begin{bmatrix} D_{11} & D_{12} & D_{16} \\ D_{12} & D_{22} & D_{26} \\ D_{16} & D_{26} & D_{66} \end{bmatrix} \begin{bmatrix} \kappa_x \\ \kappa_y \\ \kappa_{xy} \end{bmatrix} - \begin{bmatrix} M_{tx} \\ M_{ty} \\ M_{txy} \end{bmatrix} \tag{B.2.3}$$

where

$$D_{ij} = \tfrac{1}{3}\sum_{k=1}^{N}\left(\bar{Q}_{ij}\right)_k \left(h_k^3 - h_{k-1}^3\right)$$

and the shear force resultant are given as

$$\begin{bmatrix} V_y \\ V_x \end{bmatrix} = \sum_{k=1}^{N}\begin{bmatrix} \bar{Q}_{44} & \bar{Q}_{45} \\ \bar{Q}_{45} & \bar{Q}_{55} \end{bmatrix}\begin{bmatrix} \bar{\gamma}_{yz} \\ \bar{\gamma}_{xz} \end{bmatrix}\int_{h_{k-1}}^{h_k} dz$$

$$= \begin{bmatrix} A_{44} & A_{45} \\ A_{45} & A_{55} \end{bmatrix}\begin{bmatrix} \bar{\gamma}_{xz} \\ \bar{\gamma}_{yz} \end{bmatrix} \tag{B.2.4}$$

where extensional stiffness A_{ij}, flexural-extensional coupling stiffness B_{ij}, and flexural stiffness D_{ij} of the plate are as defined previously. Thermal stress resultants, $[N_t]$, and thermal moment resultants, $[M_t]$, are defined as

$$\begin{bmatrix} N_{tx} \\ N_{ty} \\ N_{txy} \end{bmatrix} = \begin{bmatrix} A_{t11} & A_{t12} & A_{t13} \\ A_{t12} & A_{t22} & A_{t23} \\ A_{t13} & A_{t23} & A_{t33} \end{bmatrix} \begin{bmatrix} \alpha_x \\ \alpha_y \\ 2\alpha_{xy} \end{bmatrix} \Delta T \tag{B.2.5}$$

$$\begin{bmatrix} M_{tx} \\ M_{ty} \\ M_{txy} \end{bmatrix} = \begin{bmatrix} B_{t11} & B_{t12} & B_{t13} \\ B_{t12} & B_{t22} & B_{t23} \\ B_{t13} & B_{t23} & B_{t33} \end{bmatrix} \begin{bmatrix} \alpha_x \\ \alpha_y \\ 2\alpha_{xy} \end{bmatrix} \Delta T \tag{B.2.6}$$

where

$$\left[A_{tij}\right] = \sum_{k=1}^{N}\left[\bar{Q}_{tij}\right]\int_{h_{k-1}}^{h_k} dz \qquad \left[B_{tij}\right] = \sum_{k=1}^{N}\left[\bar{Q}_{tij}\right]\int_{h_{k-1}}^{h_k} z\,dz$$

These are combined into

$$\begin{bmatrix} N_x \\ N_y \\ N_{xy} \\ M_x \\ M_y \\ M_{xy} \\ V_y \\ V_x \end{bmatrix} = \begin{bmatrix} A_{11} & A_{12} & A_{16} & B_{11} & B_{12} & B_{16} & 0 & 0 \\ A_{12} & A_{22} & A_{26} & B_{12} & B_{22} & B_{26} & 0 & 0 \\ A_{16} & A_{26} & A_{66} & B_{16} & B_{26} & B_{66} & 0 & 0 \\ B_{11} & B_{12} & B_{16} & D_{11} & D_{12} & D_{16} & 0 & 0 \\ B_{12} & B_{22} & B_{26} & D_{12} & D_{22} & D_{26} & 0 & 0 \\ B_{16} & B_{26} & B_{66} & D_{16} & D_{26} & D_{66} & 0 & 0 \\ 0 & 0 & 0 & 0 & 0 & 0 & A_{44} & A_{45} \\ 0 & 0 & 0 & 0 & 0 & 0 & A_{45} & A_{55} \end{bmatrix} x \begin{bmatrix} \varepsilon_x \\ \varepsilon_y \\ \gamma_{xy} \\ \kappa_x \\ \kappa_y \\ \kappa_{xy} \\ \bar{\gamma}_{yz} \\ \bar{\gamma}_{xz} \end{bmatrix} - \begin{bmatrix} N_{tx} \\ N_{ty} \\ N_{txy} \\ M_{tx} \\ M_{ty} \\ M_{txy} \\ 0 \\ 0 \end{bmatrix} \quad \text{(B.2.7)}$$

B.3 Analytical Evaluation of the Stiffness Matrix

An examination of the above expression reveals a complex situation in laminated composites, where the stress resultants, for example

$$N_x = A_{11}\varepsilon_x + A_{12}\varepsilon_y + A_{16}\gamma_{xy} + B_{11}\kappa_x + B_{12}\kappa_y + B_{16}\kappa_{xy} \quad \text{(B.3.1)}$$

is a function of midplane tensile strain ε_x and ε_y, the midplane shear (γ_{xy}), the bending curvatures (κ_x and κ_y), and twisting (κ_{xy}). In a laminated plate, there is coupling between

- tensile and shear due to A_{16} and A_{26}
- tensile and bending
- tensile and twisting

B_{16} and B_{26} bring about tension-twisting coupling and D_{16} and D_{26}, in a similar expression for M_x represent flexture-twisting coupling

Equations (B.2.7) can be used to obtain the partially or fully inverted form of the constitutive equation. After solving for [ε] and substituting, the combination of the resulting equations leads to the partially inverted form of the constitutive equation

$$\begin{bmatrix} \varepsilon \\ \hline M \end{bmatrix} = \begin{bmatrix} A^* & B^* \\ \hline C^* & D^* \end{bmatrix} \begin{bmatrix} N \\ \hline K \end{bmatrix} \quad \text{(B.3.2)}$$

From this form, we can solve for [κ], substitute into the equation involving [ε] and obtain the fully inverted form:

$$\begin{bmatrix} \varepsilon \\ \hline \kappa \end{bmatrix} = \begin{bmatrix} A' & B' \\ \hline B' & D' \end{bmatrix} \begin{bmatrix} N \\ \hline M \end{bmatrix} \quad \text{(B.3.3)}$$

Each of the combined form of the constitutive equations involves obtaining the elastic properties of the lamina (form the $\overline{Q}_i$ values for each lamina) and the ply stacking sequence (z coordinate).

The governing equations of the anisotropic composite plate are determined using equation (B.3.3). In expanded form, this equation becomes

$$[M] = [C^*][N] + [D^*][\kappa]$$

$$[\varepsilon] = [A^*][N] + [B^*][\kappa] \qquad \text{(B.3.4)}$$

where we note that

$$[A^*] = [A]^{-1} = [a]$$

$$[B^*] = -[A]^{-1}[B] = [b]$$

$$[C^*] = [B][A]^{-1} = -[B^*]^T = [c]$$

$$[D^*] = [D] - [b][A]^{-1}[B] = [d]$$

A system of two determinative equations is needed to reduce the two equations (B.3.4) to the final two governing differential equations. The first is the equilibrium equation, given by

$$M_{x,xx} + M_{y,yy} + 2M_{xy,xy} = -q \qquad \text{(B.3.5)}$$

where M are the moment resultants and q is the lateral force. Substituting Equation (B.3.4) into this equation, based on Kirchhoff's thin plate theory, results in the first governing equation

$$\begin{aligned}&(c_{11}N_x + c_{21}N_y + c_{31}N_{xy})_{,xx} + (c_{12}N_x + c_{22}N_y + c_{32}N_{xy})_{,yy} \\ &+ d_{11}w_{,xxxx} + 2(d_{12} + 2d_{33})w_{,xxyy} + 4d_{13}w_{,xxxy} \\ &+ 4d_{23}w_{,xyyy}\, 2(c_{13}N_x + c_{23}N_y + c_{33}N_{xy})_{,xy} + d_{22}w_{,yyyy} = -q\end{aligned} \qquad \text{(B.3.6)}$$

The second equation is the compatibility equation for the in-plane strain components at the reference surface of the plate

$$\varepsilon_{1,yy} + \varepsilon_{2,xx} - \gamma_{12,xy} = 0 \qquad \text{(B.3.7)}$$

When Equation (B.3.6) is substituted into this equation, the second governing equation is given by

$$\begin{aligned}&(a_{11}N_x + a_{12}N_y + a_{13}N_{xy})_{,yy} + (a_{12}N_x + a_{22}N_y + a_{23}N_{xy})_{,xx} - (a_{13}N_x + a_{23}N_y + a_{33}N_{xy})_{,xy} + \\ &b_{21}w_{,xxxx} + (2b_{23} - b_{31})w_{,xxxy} + (b_{11} + b_{22} + 2b_{33})w_{,xxyy} + (2b_{13} - b_{32})w_{,xyyy} + b_{12}w_{,yyyy} = 0\end{aligned} \qquad \text{(B.3.8)}$$

The derivation of equations (B.3.6) and (B.3.7) is called the classical theory of laminated plates because a generalisation of the classical small deflection theory of plates to account for the orthotropic characteristics of the various laminae composing the plate was made, and the complexity of the governing equations practically defies solution by exact methods.

Appendix E

ABAQUS Input Files

E.1 Introduction

ABAQUS/Standard is a general purpose finite element program and the following input files are examples of the analysis that were conducted in this study. Some of the concepts are explained throughout the main text while a thorough treatment is found in the ABAQUS/Standard User's Manuals [1] and ABAQUS Theory Manual [2], as well as in the ABAQUS/Standard Example Problems Manuals [38] . We note here that the basic structure of these input files stays the same while the variables are changed according to the analysis as contained in the report.

Thermal buckling is a linear perturbation step and all loads are defined as change in load to the reference state. ABAQUS uses the sparse solver for the analysis. The temperature values are given as values at the centroid and gradient. The middle surface of the shell is the reference surface and the Simpson integration is used.

The analysis in ABAQUS is generally carried out as follows

Buckling load estimate = ("Dead loads") + Eigenvalue × ("Live" loads)

where

"Dead" load = Total loads before x Buckle step
"Live" loads = Incremental load x Buckle step

E.2 Plate Section Properties

The plate section response is defined by

$$\{\mathbf{N}\} = y(T)[\mathbf{D}]:\{\mathbf{E}\} - \{\mathbf{N}^{th}\} \tag{E.2.1}$$

where

- $\{\mathbf{N}\}$ are the forces and moments on the plate section (membrane forces per unit length, bending moment per unit length)
- $\{\mathbf{E}\}$ are the generalized plate strains in the shell (middle surface strains and curvatures)
- $[\mathbf{D}]$ is the section stiffness matrix
- $y(T)$ is the scaling modulus, which can be used to introduce temperature (T) dependence of the cross-section, and
- $\{\mathbf{N}^{th}\}$ are the plate forces and moments caused by thermal strains.

These thermal forces and moments in the plate are generalized according to the formula

$$\{N^{th}\} = (\alpha(T)(T - T^0) - \alpha(T_I)(T_I - T^0))\{F\} \quad \text{(E.2.2)}$$

where

$\alpha(T)$ is a scaling factor (the "thermal expansion coefficient")

T_I is the initial (stress-free) temperature at this point in the plate, defined by the initial nodal temperature

$\{F\}$ are the generalized stresses caused by a fully constrained unit temperature rise as input by the user.

E.3 Thermal Expansion Coefficient

Thermal expansion coefficients are interpreted as total expansion coefficients from a reference temperature, so that they generate thermal strains according to the following formula:

$$\varepsilon^{th} = \alpha(T, f_\beta)(T - T^0) - \alpha(T^I, f_\beta^I)(T^I - T^0) \quad \text{(E.3.1)}$$

where

ε^{th} = is the total thermal strain at a material point,

$\alpha(T, f_\beta)$ = is the thermal expansion coefficient

T = is the current temperature

T^I = is the initial temperature

f_β = are the current values of the predefined field variables

f_β^I = are the initial values of the predefined field variables

T^o = is the reference temperature for the coefficient of thermal expansion, in this case zero

E.4 Isotropic Square Plate (with 16 Elements)

```
*HEADING
ISOTROPIC SQUARE PLATE - ELASTIC BUCKLING
A STUDY BY P.S. SIMELANE
*NODE
101
109,10.
901,0.,10.
909,10.,10.
*NGEN,NSET=XSYM
101,901,100
*NGEN,NSET=XEDG
109,909,100
*NFILL,NSET=ALL
XSYM,XEDG,8,1
*NGEN,NSET=YSYM
101,109
*NGEN,NSET=YEDG
901,909
*NSET,NSET=RIGHT
109,209,309,409,509,609,709,809,909
*NSET,NSET=LEFT
101,201,301,401,501,601,701,801,901
*NSET,NSET=BOTTOM
101,102,103,104,105,106,107,108,109
*NSET,NSET=TOP
901,902,903,904,905,906,907,908,909
*ELEMENT,TYPE=S9R5,ELSET=ONE
1,101,103,303,301,102,203,302,201,202
*ELGEN,ELSET=ONE
1,4,2,1,4,200,4
*MATERIAL,NAME=PLATE
*ELASTIC
1.E9,.3
*EXPANSION
1.E-6
*SHELL SECTION,MATERIAL=PLATE,ELSET=ONE
0.1,3
**********
*STEP
*BUCKLE
3,
*TEMPERATURE
ALL,100.
**********
*BOUNDARY
**SIMPLY SUPPORTED EDGES
LEFT,1
LEFT,3
LEFT,4
RIGHT,1
RIGHT,3
RIGHT,4
TOP,2
TOP,3
TOP,5
BOTTOM,2
BOTTOM,3
BOTTOM,5
*MODAL FILE
```

```
*PRINT,RESIDUAL=NO
*EL PRINT,ELSET=ONE,SUMMARY=NO,POSITION=CENTROID
S
*EL FILE,ELSET=ONE,POSITION=CENTROID
S
*NODE FILE
U,RF,CF
*RESTART,WRITE,FREQUENCY=999
*END STEP
```

E.5 Laminated Square Plate (16 Elements)

```
*HEADING
SQUARE LAMINATED PLATE - ELASTIC BUCKLING
*NODE
101
109,10.
901,0.,10.
909,10.,10.
*NGEN,NSET=XSYM
101,901,100
*NGEN,NSET=XEDG
109,909,100
*NFILL,NSET=ALL
XSYM,XEDG,8,1
*NGEN,NSET=YSYM
101,109
*NGEN,NSET=YEDG
901,909
*NSET,NSET=RIGHT
109,209,309,409,509,609,709,809,909
*NSET,NSET=LEFT
101,201,301,401,501,601,701,801,901
*NSET,NSET=BOTTOM
101,102,103,104,105,106,107,108,109
*NSET,NSET=TOP
901,902,903,904,905,906,907,908,909
*ELEMENT,TYPE=S9R5,ELSET=ONE
1,101,103,303,301,102,203,302,201,202
*ELGEN,ELSET=PLATE
1,4,2,1,4,200,4
*SHELL SECTION,ELSET=PLATE,COMPOSITE,ORIENTATION=SECORI
0.25,3,LAMINA,0.
**CENTER LINE
0.25,3,LAMINA,0.
*MATERIAL,NAME=LAMINA
*ELASTIC,TYPE=LAMINA
181.0E9,10.3E9,0.28,7.17E9,7.17E9,6.21E9
*EXPANSION
0.02E-6,22.5E-6
*ORIENTATION,NAME=SECORI,SYSTEM=RECTANGULAR
1.,1.,0.,-1.,1.,1.
3,0.
**********
*STEP
*BUCKLE
3,
*TEMPERATURE
ALL, 1000.
**********
*BOUNDARY
```

```
**SIMPLY SUPPORTED EDGES
LEFT,1
LEFT,3
LEFT,5
RIGHT,1
RIGHT,3
RIGHT,5
TOP,2
TOP,3
TOP,4
BOTTOM,2
BOTTOM,3
BOTTOM,4
********
*MODAL FILE
*RESTART,WRITE,FREQUENCY=1
*END STEP
```

E.6 Square Plate with a Circular Hole (160 elements)

```
*HEADING
BUCKLING OF COMPOSITE HOLE WITH A CIRCULAR HOLE
*NODE
1001,10.,-10.
1017,10.,10.
1033,-10.,10.
1049,-10.,-10.
1065,10.,-10.
*NGEN,NSET=OUTSIDE
1001,1017
1001,1017
1017,1033
1033,1049
1049,1065
**
**DEFINE A HOLE
**
*NODE
1,2.,-2.
17,2.,2.
33,-2.,2.
49,-2.,-2.
65,2.,-2.
*NGEN,LINE=C,NSET=HOLE
1,17
17,33
33,49
49,65
*NFILL,NSET=ALL
HOLE,OUTSIDE,10,100
*NSET,NSET=RIGHT,GENERATE
1001,1017
*NSET,NSET=TOP,GENERATE
1017,1033
*NSET,NSET=LEFT,GENERATE
1033,1049
*NSET,NSET=BOTTOM,GENERATE
1049,1065
*ELEMENT,TYPE=S9R5
1,1,201,203,3,101,202,103,2,102
*ELGEN,ELSET=PLATE
```

```
1,5,200,100,32,2,1
*ELEMENT,TYPE=S9R5
32,63,263,201,1,163,264,101,64,164
*ELGEN,ELSET=PLATE
32,5,200,100
*SHELL SECTION,ELSET=PLATE,COMPOSITE,ORIENTATION=SECORI
0.25,3,LAMINA,0.
**CENTRE LINE
0.25,3,LAMINA,0.
*TRANSVERSE SHEAR STIFFNESS
2.9875E9,2.5875E9
*MATERIAL,NAME=LAMINA
*ELASTIC,TYPE=LAMINA
181.0E9,10.3E9,0.28,7.17E9,7.17E9,6.21E9
*EXPANSION
0.02E-6,22.5E-6
*ORIENTATION,NAME=SECORI,SYSTEM=RECTANGULAR
1.,1.,0.,-1.,1.,1.
3,0.
**********************
*STEP
*BUCKLE
5,
*TEMPERATURE
ALL,1000.
**
*BOUNDARY
**SIMPLY SUPPORTED
LEFT,1
LEFT,3
LEFT,5
RIGHT,1
RIGHT,3
RIGHT,5
TOP,2
TOP,3
TOP,4
BOTTOM,2
BOTTOM,3
BOTTOM,4
**
*MODAL FILE
*RESTART,WRITE,FREQUENCY=1
*END STEP
```

E.7 Square Laminated Plate – (156 elements)

```
*NODE
101
125,10.
2701,0.,10.
2725,10.,10.
*NGEN,NSET=LEFT
101,2701,100
*NGEN,NSET=RIGHT
125,2725,100
*NFILL,NSET=ALL
LEFT,RIGHT,24,1
*NGEN,NSET=BOTTOM
101,125
*NGEN,NSET=TOP
```

```
2701,2725
*ELEMENT,TYPE=S9R5,ELSET=ONE
1,101,103,303,301,102,203,302,201,202
*ELGEN,ELSET=PLATE
1,12,2,1,13,200,12
*SHELL SECTION,ELSET=PLATE,COMPOSITE,ORIENTATION=SECORI
0.25,3,LAMINA,45.
**CENTER LINE
0.25,3,LAMINA,-45.
*TRANSVERSE SHEAR STIFFNESS
2.9875E9,2.5875E9
*MATERIAL,NAME=LAMINA
*ELASTIC,TYPE=LAMINA
181.0E9,10.3E9,0.28,7.17E9,7.17E9,6.21E9
*EXPANSION
0.02E-6,22.5E-6
*ORIENTATION,NAME=SECORI,SYSTEM=RECTANGULAR
1.,1.,0.,-1.,1.,1.
3,0.
**********************
*STEP
*BUCKLE
3,
*TEMPERATURE
ALL,1000.
************
*BOUNDARY
**SIMPLY SUPPORTED EDGES
LEFT,1
LEFT,3
LEFT,5
RIGHT,1
RIGHT,3
RIGHT,5
TOP,2
TOP,3
TOP,4
BOTTOM,2
BOTTOM,3
BOTTOM,4
********
*MODAL FILE
*RESTART,WRITE,FREQUENCY=1
*END STEP
```